

# REPORT DOCUMENTATION PAGE

Form Approved  
OMB No. 074-0188

Public reporting burden for this collection of information is estimated to average 1 hour per response, including the time for reviewing instructions, searching existing data sources, gathering and maintaining the data needed, and completing and reviewing this collection of information. Send comments regarding this burden estimate or any other aspect of this collection of information, including suggestions for reducing this burden to Washington Headquarters Services, Directorate for Information Operations and Reports, 1215 Jefferson Davis Highway, Suite 1204, Arlington, VA 22202-4302, and to the Office of Management and Budget, Paperwork Reduction Project (0704-0188), Washington, DC 20503

1. AGENCY USE ONLY (Leave blank)	2. REPORT DATE August 2003	3. REPORT TYPE AND DATES COVERED Annual (1 Aug 2002 - 31 Jul 2003)
4. TITLE AND SUBTITLE Biochemical Markers for Exposure to Low Doses of Organophosphorus Insecticides		5. FUNDING NUMBERS DAMD17-01-1-0776
6. AUTHOR(S) Oksana Lockridge, Ph.D.		20040130 144
7. PERFORMING ORGANIZATION NAME(S) AND ADDRESS(ES) Nebraska University Medical Center Omaha, Nebraska 68198-6810		8. PERFORMING ORGANIZATION REPORT NUMBER
E-Mail: olockrid@unmc.edu		
9. SPONSORING / MONITORING AGENCY NAME(S) AND ADDRESS(ES) U.S. Army Medical Research and Materiel Command Fort Detrick, Maryland 21702-5012		10. SPONSORING / MONITORING AGENCY REPORT NUMBER
11. SUPPLEMENTARY NOTES		
12a. DISTRIBUTION / AVAILABILITY STATEMENT Approved for Public Release; Distribution Unlimited		12b. DISTRIBUTION CODE
13. ABSTRACT (Maximum 200 Words) Though acetylcholinesterase is the primary target of organophosphorus toxicants, our finding that acetylcholinesterase knockout mice are supersensitive to the lethal effects of VX, DFP, chlorpyrifos oxon, and iso-OMPA demonstrates that other important targets exist. The goal of this work is to identify non-acetylcholinesterase targets of organophosphorus toxicants. Using mass spectrometry we have identified platelet activating factor acetyl hydrolase as a sensitive target of organophosphorus insecticides in mouse brain extracts. Two additional biomarkers may be fatty acid amide hydrolase and acylpeptide hydrolase. Studies in living mice to test the involvement of these proteins in low level toxicity are beginning. This work is expected to identify new biological markers for low dose exposure to organophosphorus toxicants and to explain the neurologic symptoms of some of our Gulf War veterans.		
14. SUBJECT TERMS Gulf War Illness, insecticide, nerve agent, acetylcholinesterase, low dose, biochemical markers, organophosphorus toxicant		15. NUMBER OF PAGES 89
		16. PRICE CODE
17. SECURITY CLASSIFICATION OF REPORT Unclassified	18. SECURITY CLASSIFICATION OF THIS PAGE Unclassified	19. SECURITY CLASSIFICATION OF ABSTRACT Unclassified
		20. LIMITATION OF ABSTRACT Unlimited

NSN 7540-01-280-5500

Standard Form 298 (Rev. 2-89)  
Prescribed by ANSI Std. Z39-18  
298-102

AD \_\_\_\_\_

Award Number: DAMD17-01-1-0776

TITLE: Biochemical Markers for Exposure to Low Doses of Organophosphorus Insecticides

PRINCIPAL INVESTIGATOR: Oksana Lockridge, Ph.D.

CONTRACTING ORGANIZATION: University of Nebraska Medical Center  
Omaha, Nebraska 68198-6810

REPORT DATE: August 2003

TYPE OF REPORT: Annual

PREPARED FOR: U.S. Army Medical Research and Materiel Command  
Fort Detrick, Maryland 21702-5012

DISTRIBUTION STATEMENT: Approved for Public Release;  
Distribution Unlimited

The views, opinions and/or findings contained in this report are those of the author(s) and should not be construed as an official Department of the Army position, policy or decision unless so designated by other documentation.

## Table of Contents

<b>Cover.....</b>	<b>1</b>
<b>SF 298.....</b>	<b>2</b>
<b>Table of Contents.....</b>	<b>3</b>
<b>Abbreviations.....</b>	<b>4</b>
<b>Introduction.....</b>	<b>5</b>
<b>Body.....</b>	<b>5</b>
<b>Key Research Accomplishments.....</b>	<b>52</b>
<b>Reportable Outcomes.....</b>	<b>52</b>
<b>Conclusions.....</b>	<b>52</b>
<b>References.....</b>	<b>53</b>
<b>Appendices.....</b>	<b>55</b>

## Abbreviations

AChE	acetylcholinesterase enzyme
APH	acylpeptide hydrolase
BChE	butyrylcholinesterase enzyme
BSA	bovine serum albumin
CHO	Chinese Hamster Ovary Cells
CPO	chlorpyrifos oxon
DFP	diisopropylfluorophosphate
DTNB	dithiobisnitrobenzoic acid; color reagent for activity assay
FAAH	fatty acid amide hydrolase
FP-biotin	biotinylated organophosphate where the leaving group is the fluoride ion and the marker is biotin; 10-(fluoroethoxyphosphinyl)-N-(biotinamidopentyl) decanamide
IC <sub>50</sub>	the concentration of inhibitor necessary to obtain 50% inhibition
iso-OMPA	tetraisopropyl pyrophosphoramide; inhibitor for BChE
OP	organophosphorus toxicant
PVDF	polyvinylidene difluoride; membrane for binding proteins
QNB	3H-quinuclidinyl benzilate, ligand for muscarinic receptors
SDS	sodium dodecyl sulfate
VX	O-ethyl S-[2-(diisopropylamino)ethyl] methylphosphonothioate; nerve agent

## Introduction

The purpose of this work is to identify proteins that react with low doses of organophosphorus agents (OP). There is overwhelming evidence that acute toxicity of OP is due to inhibition of acetylcholinesterase (AChE). However, we have found that the AChE knockout mouse, which has zero AChE, is supersensitive to low doses of OP. The AChE-/ mouse dies at doses of OP that are not lethal to wild-type mice (Duysen et al., 2001). This demonstrates that non-AChE targets are involved in OP toxicity. Our goal is to identify new biological markers of exposure to organophosphorus agents.

Our strategy uses biotinylated OP to label proteins, which are then visualized with streptavidin conjugated to a fluorophore. Labeled proteins are identified by mass spectrometry.

Since some cases of Gulf War Illness may have been caused by exposure to low doses of OP, our studies may lead to an explanation for the neurologic symptoms in some of our Gulf War veterans.

## Relation to Statement of Work

In this second year of the project we have made progress on Tasks 3, 4, and 5. Work on Task 6 is beginning.

## Task 3

Human and mouse brains will be extracted and treated with biotinylated OP. The biotinylated proteins will be purified with avidin-Sepharose, and separated by gel electrophoresis. The number and size of proteins that reacted with biotinylated OP will be visualized on blots by treating with avidin conjugated to an indicator.

Progress on Task 3 is described in the following section. All work to date has been with mouse brain extracts.

**Abstract.** Mouse brains were extracted and treated with FP-biotin. The proteins were separated by gel electrophoresis and transferred to a membrane. Biotinylated proteins were visualized by hybridization with streptavidin conjugated to a fluorophore. About 55 FP-biotin labeled proteins were identified in the 100,000xg supernatant of mouse brain. This number is up from the 32 proteins described in our 2002 report. The higher number of biotinylated proteins is due to increased resolution of bands during electrophoresis. To prepare proteins for identification by mass spectrometry, we developed techniques to purify FP-biotin-labeled proteins. Purification was achieved by binding to avidin-agarose followed by gel electrophoresis.

**Introduction.** The purpose of this work is to identify proteins that react with organophosphorus agents (OP). We are especially interested in proteins that react with OP at doses that do not significantly inhibit acetylcholinesterase (AChE). It is generally agreed that the acute toxicity of OP is due to inhibition of AChE, however little is known about low dose effects. Biomarkers for low dose exposure to OP are needed. The techniques developed in this report are intended to identify new biomarkers.

## Methods

**Preparation of sub-cellular fractions from mouse brain, and protein quantitation.** Mouse brain was separated into its sub-cellular fractions by centrifugation, essentially as described by Gray and Whittaker (1962). Brain tissue was homogenized by two 1-minute disruptions with a Potter-Elvehjem homogenizer (Teflon pestle with glass vessel) rotating at 840 rpm (in 10-volumes of ice cold 50 mM TrisCl buffer, pH 8.0, containing 0.32 M sucrose, to prevent disruption of organelles). The suspension was centrifuged at 1000xg for 10 minutes at 4°C to pellet nuclei, mitochondria, plasma membranes and unbroken cells. The supernatant was re-centrifuged at 17,000xg for 55 minutes at 4°C to pellet myelin, synaptosomes and mitochondria. That supernatant was re-centrifuged at 100,000xg for 60 minutes at 4°C to separate microsomes (pellet) from soluble proteins (supernatant).

Protein in the supernatant fraction was estimated by absorbance at 280 nm, using  $A_{280} = 1.0$  for 1 mg protein/ ml. The 100,000xg supernatant was divided into 0.4 ml aliquots and stored at -70°C, along with the other sub-cellular fractions.

**Labeling proteins with FP-biotin.** Mouse brain supernatant (0.1 ml of 1.25 mg protein/ml) was reacted with 2-40  $\mu$ M FP-biotin in 50 mM TrisCl buffer, pH 8.0, containing 5 mM EDTA and 2.4% methanol at 25°C for up to 450 minutes. Reaction was stopped by addition of 1/5 volume of 10% SDS, 30% glycerol, 0.6 M dithiothreitol, and 0.012% bromophenol blue in 0.2 M TrisCl buffer, pH 6.8; followed by heating at 80°C for 5 minutes.

**Visualization of FP-biotin labeled proteins.** For determination of the number and size of proteins labeled by FP-biotin, proteins were subjected to SDS gel electrophoresis, the proteins transferred to a PVDF membrane, and the protein bands visualized with a fluorescent probe. The details of the procedure follow.

A 10-20% gradient SDS-PAGE with 4% stacking gel was poured in a Hoefer gel apparatus. The dimensions of the sandwich were 16x18x0.075 cm, with 20 wells. Twenty-four to thirty micrograms of protein were loaded per lane. Electrophoresis was for 4000 volt-hours in the cold room (4°C), with stirring. The bottom tank contained 4.5 L of 60 mM TrisCl buffer, pH 8.1, plus 0.1% SDS. The top tank buffer contained 0.6 L of 25 mM Tris, 192 mM glycine buffer, pH 8.2, plus 0.1% SDS.

Proteins were transferred from the gel to PVDF membrane (Immun-Blot from BioRad) electrophoretically in a tank using plate electrodes (TransBlot from BioRad), at 0.5 amps, for 1 hour, in 3 L of 25 mM Tris/192 mM glycine buffer, pH 8.2, in the cold room (4°C), with stirring. The membrane was blocked with 3% gelatin (BioRad) in 20 mM TrisCl buffer, pH 7.5, containing 0.5 M NaCl for 1 hour at room temperature. The 3% gelatin solution had been prepared by heating the gelatin in buffer in a microwave oven for several seconds. The blocked membrane was washed twice with 20 mM TrisCl buffer, pH 7.5, containing 0.5 M NaCl and 0.05% Tween-20, for 20 minutes.

Biotinylated proteins were labeled with 9.5 nM Streptavidin-Alexa 680 fluorophore in 20 mM TrisCl buffer, pH 7.5, containing 0.5 M NaCl and 1% gelatin, for 2 hours, at room temperature, protected from light. Shorter reaction times resulted in less labeling. The membrane was washed twice with 20 mM TrisCl buffer, pH 7.5, containing 0.5 M NaCl and 0.05% Tween-20, and twice with 20 mM TrisCl buffer, pH 7.5, containing 0.5 M NaCl, for 20 minutes each. This is essentially the BioRad protocol (BioRad Lit 171 Rev D).

Membranes were scanned with the Odyssey Infrared Imaging System (LI-COR, Lincoln, NE) at 42 microns per pixel. The Odyssey employs an infrared laser to excite a fluorescent probe which is attached to the target protein, and then collects the emitted light. The emitted light intensity is directly proportional to the amount of probe. Both the laser and the detector are mounted on a moving carriage positioned directly below the membrane. The membrane can be scanned in step sizes as small as 21 microns, providing resolution comparable to x-ray film. Data are collected using a 16-bit dynamic range, and can be transferred directly to the Kodak 1D analysis program. The fluorophore is stable in the laser, making it possible to scan the membrane repeatedly, while using different intensity settings to optimize data collection for both strong and weak signals. The membrane is kept wet during scanning.

The intensity of the signal from each labeled protein was determined using a Gaussian deconvolution routine from the Kodak 1D Image Analysis program, v 3.5.3 (Kodak).

**Isolation of FP-biotin labeled protein.** To prepare OP-labeled proteins for mass spectrometry, FP-biotin labeled proteins were purified on avidin-agarose beads and separated by SDS polyacrylamide gel electrophoresis. The following method was modified from Kidd et al. (2001). Protein (6.3 mg in 4.5 ml of 50 mM TrisCl, pH 8.0, containing 5 mM EDTA) was reacted with 10 µM FP-biotin for 5 hours at 25°C. The reaction mixture was passed over a 3.5 x 32 cm Sephadex G-25 gel filtration column (Pharmacia) to separate unreacted FP-biotin from protein. The protein eluent was heated in the presence of 0.5% SDS at 85°C for 3 minutes to enhance accessibility of the biotin label. The protein was diluted 2.5-fold with the starting buffer, to yield 0.2% SDS, and incubated with 200 µl of avidin-agarose beads (catalog # A-9207 Sigma-Aldrich.com, 1.9 mg avidin/ml of beads) overnight at room temperature, with continuous mixing. Beads were washed three times with the TrisCl/EDTA buffer, containing 0.2% SDS. Fifty µl of 6x SDS PAGE loading buffer (0.2 M TrisCl, pH 6.8, 10% SDS, 30% glycerol, 0.6

M dithiothreitol and 0.012% bromophenol blue) were added to the 200  $\mu$ l of beads, and the mixture was heated at 85°C for 3 minutes. This step released the biotinylated proteins from the avidin beads. Equal amounts of the bead mixture were loaded directly into two dry wells of a 10-20% gradient SDS PAGE (10-well format, 1.5 mm thick) and run for 4000 volt-hours in the cold room. The gel was stained with Coomassie blue G250 (Bio-Safe from BioRad), and destained with water. Coomassie G250 is reportedly 2-8 fold more sensitive than Coomassie R250 (BioRad specifications). In order to minimize contamination from keratin, the staining dish had been cleaned with sulfuric acid, and the water was Milli-Q purified. For the same reason, gloves were worn for all operations involving the gel.

## Results

**Improved resolution of the screening procedure.** When the SDS PAGE electrophoresis was run for 3600-4000 volt-hours rather than 3000 volt-hours, as had been the case previously, more bands could be resolved from some of the clusters. This required a re-numbering of the bands. In that process, some minor bands and shoulders from major bands, which had been ignored in the original numbering, were included. In the end, 55 bands were identified (see Figure 3.1). This is up from 32 bands shown in the 2002 report. Minor bands which were previously ignored are now numbered. The old band numbers are translated into the new band numbers in Table 3.1.

**Table 3.1 Band Number Translation**

Band numbers									
old		new		old		new		old	
1	1	6	12	10	23	16	34	-	45
-	2	-	13	11	24	17	35	-	46
-	3	7	14	-	25	18	36	25	47
-	4	8	15	-	26	-	37	-	48
2	5	-	16	-	27	19	38	26	49
-	6	9	17	-	28	20	39	27	50
3	7	-	18	12	29	21	40	28	51
4	8	-	19	-	30	22	41	29	52
5	9	-	20	13	31	23	42	30	53
-	10	-	21	14	32	-	43	31	54
-	11	-	22	15	33	24	44	32	55

A series of experiments similar to that in Figure 3.1, using a range of FP-biotin concentrations, showed that a reaction time of 300 minutes with 10  $\mu$ M FP-biotin gave maximum labeling. Use of lower concentrations of FP-biotin required longer reaction times to achieve maximum labeling. It was estimated that the

proteins capable of reacting with FP-biotin had a concentration of 1  $\mu$ M, so that 10  $\mu$ M FP-biotin was a 10-fold excess. Figure 3.1 shows that 55 biotinylated bands could be resolved. Three out of 55 bands were endogenous biotinylated proteins. The endogenous biotinylated proteins were bands 1, 14, and 15.

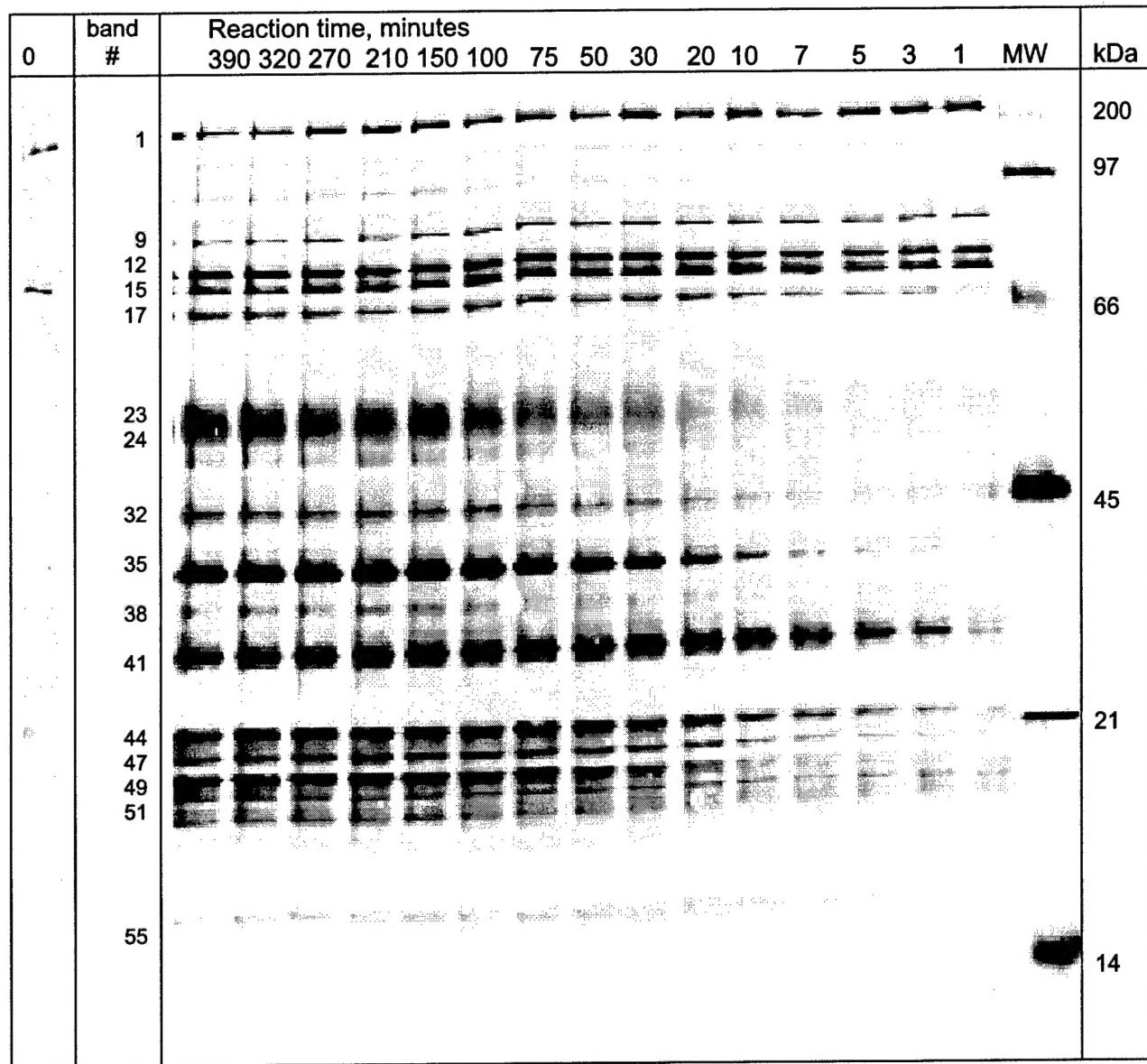
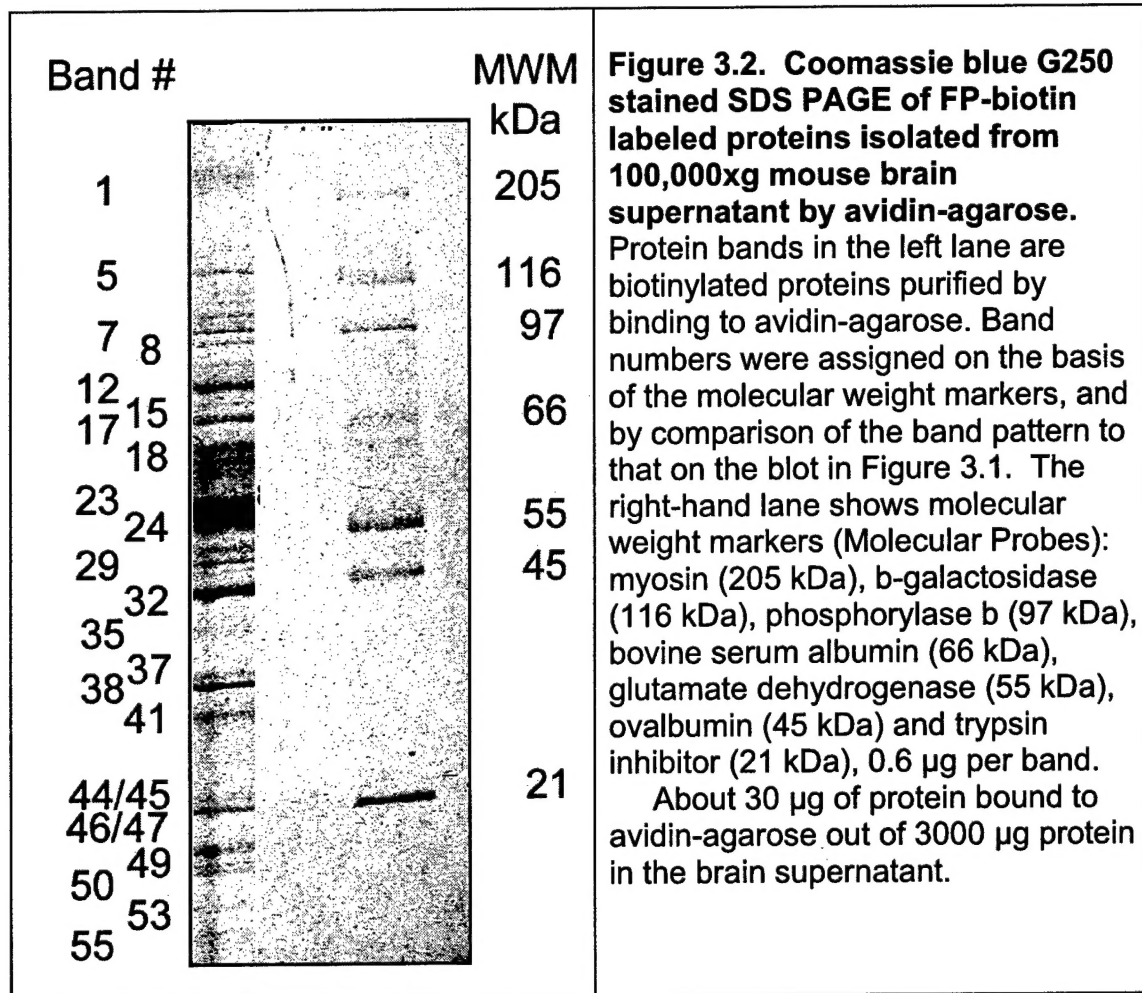


**Figure 3.1. SDS-PAGE showing the time course for the reaction of FP-biotin with proteins extracted from mouse brain.** The 10  $\mu$ M FP-biotin was reacted with 1.25 mg protein/ml of mouse brain supernatant in 50 mM TrisCl buffer, pH 8.0, containing 5 mM EDTA and 2.4% methanol, at 25°C, for selected times. The numbers above each lane indicate the reaction times in minutes. 30  $\mu$ g protein was loaded per lane. Biotinylated molecular weight markers were from BioRad. Endogenous biotinylated proteins are in bands 1, 14, and 15. A total of 55 biotinylated protein bands are visible.

**Isolation of FP-biotin labeled proteins.** To prepare FP-biotin labeled proteins for identification by mass spectrometry, FP-biotin labeled proteins were purified by binding to avidin-agarose and separated by electrophoresis on SDS polyacrylamide gel. Twenty-two bands could be seen on a Coomassie G250 stained, SDS PAGE gel, of biotin labeled proteins extracted from the 100,000xg mouse brain supernatant and purified on avidin-agarose (Figure 3.2). Numbers were assigned to the bands based on the band positions relative to the molecular weight markers, and by comparison of the band pattern to the blot in Figure 3.1.



There were 22 Coomassie stained bands in Figure 3.2. The 22 bands in Figure 3.2 corresponded to bands 1, 5, 7, 8, 12, 15, 17, 18, 23, 24, 29, 32, 35, 37, 38, 41, 44+45, 46+47, 49, 50, 53, and 55 in Figure 3.1.

To determine whether all the Coomassie stained protein bands were biotinylated, the same avidin-agarose purified protein sample was transferred to PVDF membrane and stained with streptavidin Alexafluor. Figure 3.3 compares the staining patterns and shows that every Coomassie stained band has a

corresponding fluorescent band. The pattern of staining is different in panels A and B of Figure 3.3, indicating that the fluorescent signal from binding to streptavidin Alexafluor does not correlate with the quantity of protein revealed by staining with Coomassie blue.

The pattern of fluorescent bands in Figure 3.3 for the avidin-agarose purified proteins is similar to the pattern of fluorescent bands in Figure 3.1 where proteins had not been purified on avidin-agarose before gel electrophoresis. This means that all biotinylated proteins bound with similar affinity to the avidin-agarose beads and that no protein was selectively excluded.

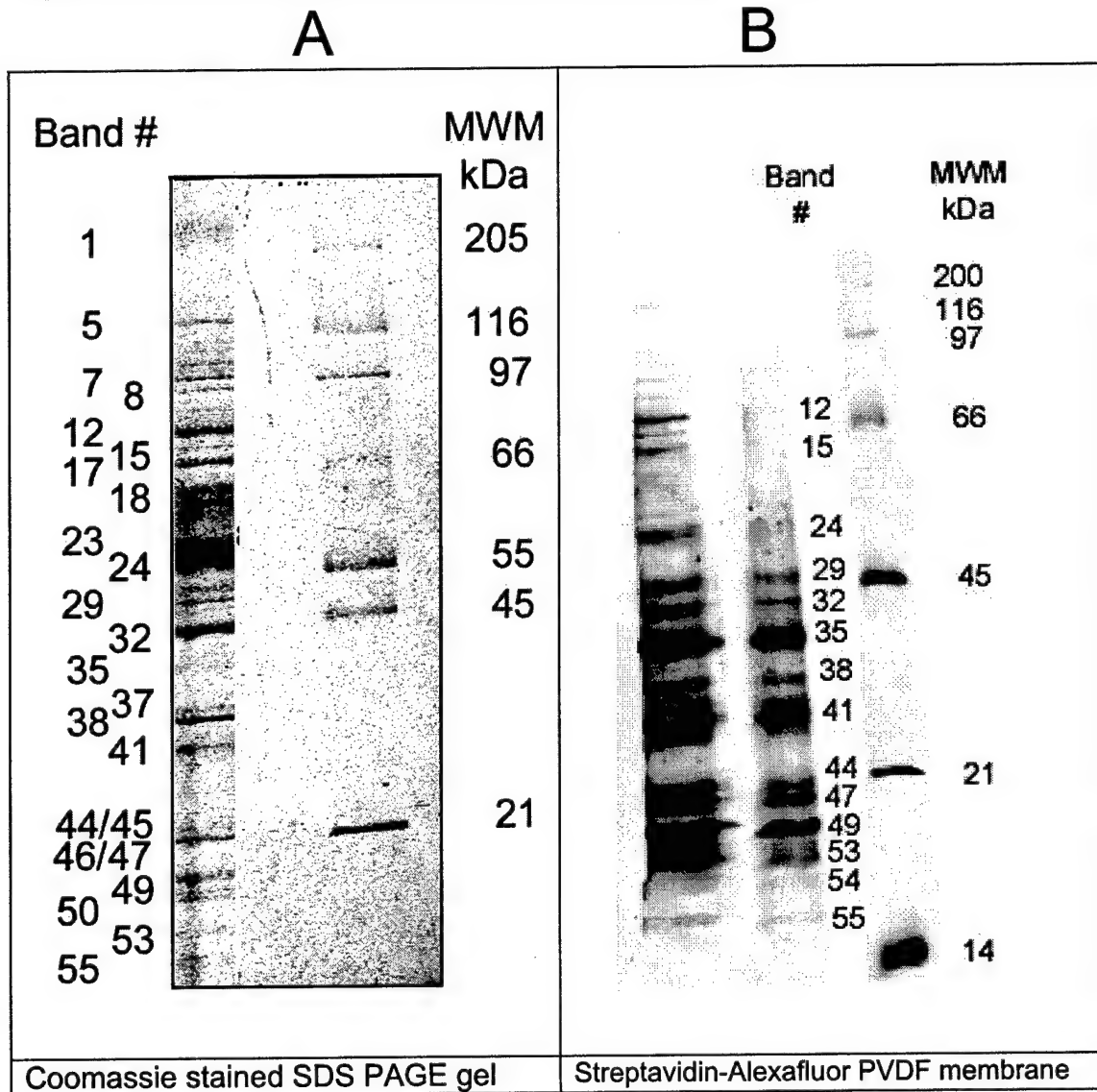


**Figure 3.3. Comparison of Coomassie blue staining and fluorescent signal intensity.** The same sample of avidin-agarose purified FP-biotin labeled protein was loaded into three lanes of an SDS PAGE gel. One lane was stained with Coomassie blue in panel A, while protein in two other lanes was transferred to PVDF membrane and stained with avidin-Alexafluor in panel B.

## Discussion

**Number of proteins that react with FP-biotin.** Soluble mouse brain extract had 55 biotinylated bands after reaction with FP-biotin. Of these, 3 were endogenous biotinylated proteins and 52 were produced by reaction with FP-biotin. Liu et al (1999) found 12 protein bands in the soluble fraction of rat brain after labeling with FP-biotin. The lower number of bands found by Liu et al. (1999) is explained by shorter reaction time (30 min rather than 2 h), lower concentration of FP-biotin (2  $\mu$ M rather than 10  $\mu$ M), use of a lower resolution gel, and detection with chemiluminescence rather than with fluorescence.

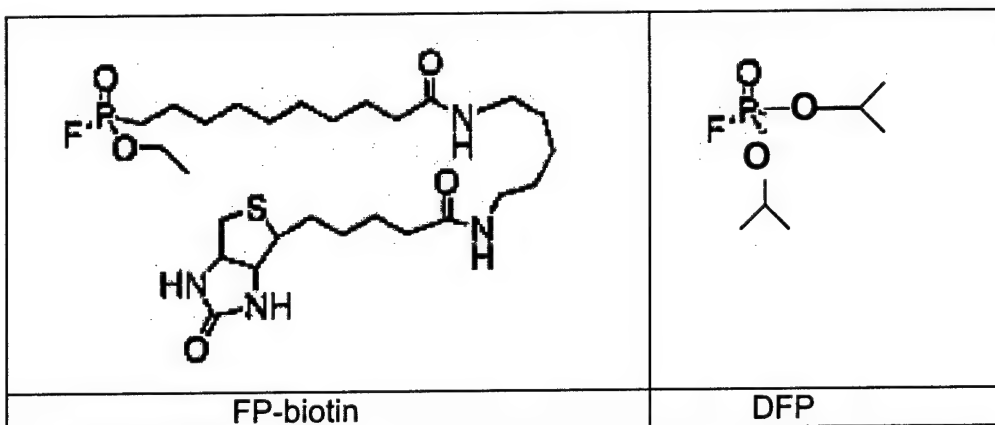


**Figure 3.4. Structures of FP-biotin and DFP.**

FP-biotin is similar in structure to DFP, with the difference that biotin on a 17 atom spacer is substituted for one of the isopropyl groups of DFP and ethanol is substituted for the other isopropyl group (Figure 3.4). FP-biotin reacts with serine hydrolases, for example BChE and AChE, and with serine proteases, for example trypsin (Liu et al., 1999) to make an irreversible covalent bond with the active site serine. Similarly, DFP makes a covalent bond with serine hydrolases and serine proteases by binding to the active site serine. The same mechanism of action of these two compounds allows one to assume that DFP and FP-biotin will label overlapping sets of proteins.

Keshavarz-Shokri et al. (1999) separated 9 bands on gel electrophoresis after labeling chicken brain proteins with 3H-DFP; the sizes were 30 to 155 kDa. Carrington and Abou-Donia (1985) saw 8 DFP-labeled bands in chicken brain ranging in size from 32 to 160 kDa. Richards and Lees (2002) resolved 24 protein spots by 2D-gel electrophoresis of brain proteins labeled with tritiated DFP. Thus, the 52 bands observed in our experiments are a reasonable representation of OP-reactive proteins in the brain. The sizes ranged from 16 to 110 kDa.

## Task 4

The protein bands isolated in task 3 will be partially sequenced. The partial sequences will be used to search the Human and Mouse Genome Databases, for the purpose of obtaining the complete amino acid sequences and identifying the proteins.

**Abstract.** Procedures for purification of FP-biotin labeled proteins have been perfected, and a protocol for digestion of the isolated proteins has been adopted. These procedures have allowed preliminary identification of 26 OP-labeled proteins by mass spectrometry. The 26 proteins are from the 100,000xg supernatant fraction of mouse brain.

**Introduction.** Samples were prepared at the University of Nebraska Medical Center and sent for mass spectral analysis to the laboratory of our collaborator, Dr. Charles Thompson, at the University of Montana. Purified tryptic peptides were fragmented on a Micromass Q-TOF mass spectrometer. The mass and sequence information for each peptide were analyzed with ProteinLynx or MASCOT software to identify the protein.

### Methods

**Protein digestion protocol.** The proteins isolated from SDS PAGE (Task 3, Figure 3.2) were digested with trypsin to prepare them for identification by mass spectral analysis. The procedure we used was established in Dr. Thompson's laboratory at the University of Montana. Gloves were worn throughout these procedures, all solutions were made with Milli-Q purified water, and all glassware, plasticware, and tools were rinsed with Milli-Q purified water in order to minimize keratin contamination. Each band from one lane of the SDS PAGE was excised, placed into a separate 1.5 ml microfuge tube, and chopped into bits. The amount of gel excised was kept to a minimum. The gel bits were destained by washing with 200  $\mu$ l of 25 mM ammonium bicarbonate (Aldrich) in 50% acetonitrile (synthesis grade, from Fisher). After three washes, the gel bits were colorless and had shrunken considerably. Residual liquid was removed and the gel bits dried by evaporation in a Speedvac (Jouan). Protein in each sample was then reduced by incubating the gel bits with 10 mM dithiothreitol (molecular biology grade, from Sigma) in 200  $\mu$ l of 100 mM ammonium bicarbonate for 1 hour at 56°C. The gel pieces were then centrifuged, excess solution was removed, and the protein was alkylated with 55 mM iodoacetamide (Sigma) in 120  $\mu$ l of 100 mM ammonium bicarbonate for 1 hour at room temperature in the dark. The gel bits were again centrifuged, excess solution

was removed, and the bits were washed with 200  $\mu$ l of 25 mM ammonium bicarbonate in 50% acetonitrile (three times). Residual liquid was again removed and the gel bits dried by evaporation in the Speedvac. The proteins were digested with trypsin, 12.5 ng/ $\mu$ l of sequencing grade trypsin (Promega) in 25 mM ammonium bicarbonate. Ninety  $\mu$ l of the trypsin solution were added to the dry gel bits and incubated at 4°C for 20 minutes, to allow the gel to re-swell. Then 60  $\mu$ l of 25 mM ammonium bicarbonate were layered over each sample and the samples were incubated at 37°C overnight (about 17 hours). Peptides were extracted by incubating each reaction mixture with 200  $\mu$ l of 0.1% trifluoroacetic acid (sequencing grade from Beckman) in 60% acetonitrile for one hour at room temperature. Extraction was repeated three times and the extracts for each sample were pooled. The pooled extracts were evaporated to dryness in the Speedvac, and the dry samples were stored at -20°C until analyzed.

**Mass spectral analysis.** Each tryptic peptide digest was resuspended in 40  $\mu$ l of 5% acetonitrile/0.05% trifluoroacetic acid/95% water. A 10- $\mu$ L aliquot of the digest was injected into a CapLC (capillary liquid chromatography system from Waters Corp) using 5% acetonitrile/0.05% trifluoroacetic acid (auxiliary solvent) at a flow rate of 20  $\mu$ L per minute. Peptides were concentrated on a C<sub>18</sub> PepMap<sup>TM</sup> Nano-Precolumn<sup>TM</sup> (5 mm  $\times$  0.3 mm id, 5  $\mu$ m particle size) for 3 minutes, and then eluted onto a C<sub>18</sub> PepMap<sup>TM</sup> capillary column (15 cm  $\times$  75  $\mu$ m id, 3  $\mu$ m particle size both from LC Packings), using a flow rate of 200-300 nL per minute. Peptides were partially resolved using gradient elution. The solvents were 2% acetonitrile/0.1% formic acid (solvent A), and 90% acetonitrile/10% iso-propanol/0.2% formic acid (solvent B). The solvent gradient increased from 5% B to 50% B over 22 minutes, then to 80% B over 1 minute, and remained at 80% B for 4 minutes. The column was then flushed with 95% B for 3 minutes and equilibrated at 5% B for 3 minutes before the next sample injection.

Peptides were delivered to the Z-spray source (nano-sprayer) of a Micromass Q-TOF (tandem quadrupole/time-of-flight mass spectrometer from Waters Corp.) through a 75- $\mu$ m id capillary, which connected to the CapLC column. In order to ionize the peptides, 3300 volts were applied to the capillary, 30 volts to the sample cone, and zero volts to the extraction cone. Mass spectra for the ionized peptides were acquired throughout the chromatographic run, and collision induced dissociation spectra were acquired on the most abundant peptide ions (having a charge state of 2+, 3+, or 4+). The collision induced dissociation spectrum is unique for each peptide, and is based on the amino acid sequence of that peptide. For this reason, identification of proteins using collision induced dissociation data is superior to identification by only the peptide mass fingerprint of the protein. The collision cell was pressurized with 1.5 psi ultra-pure Argon (99.999%), and collision voltages were dependent on the mass-to-charge ratio and the charge state of the parent ion. The time of flight measurements were calibrated daily using fragment ions from collision induced dissociation of [Glu<sup>1</sup>]-fibrinopeptide B. Each sample was post-processed using this calibration and Mass Measure (Micromass). The calibration was adjusted to the exact mass of the autolytic tryptic fragment at 421.76, found in each sample.

The mass and sequence information for each detected peptide was submitted either to ProteinLynx Global Server 1.1 (a proprietary software package, from Micromass), or to MASCOT (a public access package provided by Matrix Science at <http://www.matrix-science.com/cgi/index.pl?page=../home.html>). Data were compared to all mammalian entries (ProteinLynx) or just mouse entries (MASCOT) in the NCBI nr database (National Center for Biotechnology Information). Search criteria for ProteinLynx were set to a mass accuracy of 0.25 Da, and one missed cleavage by trypsin was allowed. Search criteria for MASCOT were set to a mass accuracy of  $\pm 0.1$  Da, one missed cleavage, variable modification of methionine (oxidation) and cysteine (carbidamethylation), and peptide charge +2 and +3. Both software packages calculated a score for each identified protein based on the match between the experimental peptide mass and the theoretical peptide mass, as well as between the experimental collision induced dissociation spectra and the theoretical fragment ions from each peptide. Results were essentially the same from both packages.

## Results

**Identification of the proteins labeled by FP-biotin.** The 22 FP-biotin labeled bands from the SDS PAGE shown in Figure 3.2 were excised, destained, reduced, alkylated, digested with trypsin, and the peptides extracted as described in the Methods section. The dried peptides were sent to Dr Thompson's laboratory for tandem-ms/ms mass spectral analysis. Peptide mass and sequence information from each band was compared to the NCBI nr database using either MASCOT or ProteinLynx software. Out of the 22 bands, proteins could be identified in 15 (see Table 4.1). To be included in the list, a protein needed to be matched to at least 2 peptides, which accounted for at least 3% of the total sequence, and have a protein score greater than 34. Both programs evaluated the sequence and peptide mass information before assigning a reliability score to the protein identity. Scores greater than 34 (MASCOT) or 50 (ProteinLynx) indicated that the identity of the protein was well established.

A total of 26 proteins were identified in the 15 bands. Seven bands (17, 18, 41, 44/45, 46/47, 50 & 53) indicated the presence of two or more proteins. Fourteen were hydrolases: puromycin-sensitive aminopeptidase, prolylendopeptidase, RIKEN D030038c16 which is related to prolylendopeptidase, protein phosphatase 2, dihydropyrimidase-like 2, dihydropyrimidase-like 3, dihydropyrimidase-like 5, acyl-CoA hydrolase, esterase 10, tyrosine 3-monoxygenase/tryptophan 5-monoxygenase activation protein, platelet-activating factor acetylhydrolase alpha 2, platelet-activating factor acetylhydrolase alpha 1, lysophospholipase 1, and lysophospholipase 2. Only 5 of these hydrolases contained the serine nucleophile consensus sequence (GXSXG). Table 4.1 shows that the 5 hydrolases with the GXSXG consensus sequence were prolylendopeptidase, dihydropyrimidinase-like 5, esterase 10,

lysophospholipase 1 and lysophospholipase 2. A sixth protein with the GXSXG sequence was heat shock protein 8.

Four of the proteins were dehydrogenases: formyltetrahydrofolate dehydrogenase, D-3-phosphoglycerate dehydrogenase, glyceraldehyde-3-phosphate dehydrogenase, and lactate dehydrogenase. Two proteins were heat shock proteins, and 3 were forms of tubulin. The remaining 3 proteins were serum albumin precursor, RIKEN 4931406N15, and peroxiredoxin.

The molecular weights of the identified proteins matched the molecular weights of the bands excised from the SDS gel. This supports the assigned identities.

**Table 4.1 Analysis of the Mass Spectral Data for Proteins from Mouse Brain Supernatant (100,000xg)<sup>1</sup>**

Band information		Protein Identification Information				
Band #	MW from SDS PAGE kDa	protein score >50=good	Number of Peptides found	% Total Protein found	GXSXG sequence	Protein name (mouse proteins only) MW kDa
1	200	-	no data	-		
5	110	-	no data	-		
6	100	174	4	4	no	Puromycin-sensitive aminopeptidase MW 103
7	95	426	10	15	no	Formyltetrahydrofolate dehydrogenase MW 97
8	90	352	5	10	no	Heat shock protein 90-Beta MW 84
12	85	827	16	26	yes	Prolylendopeptidase MW 81
15	80	-	no data	-		
17	75	372	10	22	no	RIKEN D030028o16 MW 73 BLAST shows a slight relationship to prolylendopeptidase and protease II
		270	5	9	no	Serum albumin precursor MW 67
		173	4	6	no	RIKEN 4931406N15 MW 70 BLAST shows conserved domains from phosphomannomutase and phosphoglucomutase
		154	3	6	yes	Heat shock protein 8 MW 71
		70	2	3	no	Protein phosphatase 2 MW 65
18	65	62	2	3	no	Dihydropyrimidinase-like 2 MW 61
		59	2	3	no	Dihydropyrimidinase-like 3 MW 62
		43	3	4	yes	Dihydropyrimidinase-like 5 MW 61 dihydropyrimidase is also called 5,6-dihydro-pyrimidine amido hydrolase
		195	3	7	no	D-3-phosphoglycerate dehydrogenase MW 51
24	55	5320	15	50	no	Tubulin MW 50
29	50	-	no data	-		
32	45	-	no data	-		
35	40	296	6	21	no	Acyl-CoA hydrolase MW 38
38	35	275	5	23	no	Glyceraldehyde-3-phosphate

		dehydrogenase MW 36				
37	35	-	no data	-		
41	30	576	11	43	no	Tubulin alpha-1 MW 50
		423	9	33	no	Tubulin beta-5 MW 50
		337	8	27	no	Lactate dehydrogenase 1 MW 36
		261	7	34	yes	Esterase 10 MW 35
44/45	25	286	5	16	no	Tubulin alpha-1 MW 50
		65	2	12	no	Platelet-activating factor acetylhydrolase alpha-2 MW 25
46/47	22	354	7	36	no	Tyrosine 3-monoxygenase/tryptophan 5-monoxygenase activation protein MW 28 a protein phosphatase
		273	4	56	no	Platelet-activating factor acetylhydrolase alpha-1 MW 26
49	20	-	no data	-		
50	20	206	4	20	yes	Lysophospholipase 1 MW 25
		160	5	25	yes	Lysophospholipase 2 MW 25
53	20	245	5	31	no	Peroxiredoxin 1 MW 22
		101	3	12	no	Platelet-activating factor acylhydrolase alpha-1 MW 26

1 Data were analyzed using software from either MASCOT (all entries except bands 23 and 24) or ProteinLynx (entries 23 and 24).

Tubulin alpha-1 was found in two bands, in bands 41 and 44/45. Platelet-activating factor acetylhydrolase alpha-1 was also found in two bands, in bands 46/47 and 53. All other proteins were found in a single band. The 28 entries above represent 26 different proteins. The computer databank number of each protein listed in Table 4.1 is given in Table 4.2.

**Table 4.2 . Databank numbers for the proteins identified in Table 4.1**

Protein name (mouse proteins only) MW kDa	Databank #
Puromycin-sensitive aminopeptidase MW 103	gi 6679491
Formyltetrahydrofolate dehydrogenase MW 97	gi 27532959
Heat shock protein 90-Beta MW 84	gi 123681
Prolylendopeptidase MW 81	gi 6755152
RIKEN D030028o16 MW 73	gi 22122431
Serum albumin precursor MW 67	gi 5915682
RIKEN 4931406N15 MW 70	gi 28076969
Heat shock protein 8 MW 71	gi 13242237
Protein phosphatase 2 MW 65	gi 8394027
Dihydropyrimidinase-like 2 MW 61	gi 6753676
Dihydropyrimidinase-like 3 MW 62	gi 6681219
Dihydropyrimidinase-like 5 MW 61	gi 12746424
D-3-phosphoglycerate dehydrogenase MW 51	gi 3122875
Tubulin MW 50	gi 20455323
Brain acyl-CoA hydrolase MW 38	gi 19923052
Glyceraldehyde-3-phosphate dehydrogenase MW 36	gi 6679937

Tubulin alpha-1 MW 50	gi 6755901
Tubulin beta-5 MW 50	gi 7106439
Lactate dehydrogenase 1 MW 36	gi 6754524
Esterase 10 MW 35	gi 12846304
Tubulin alpha-1 MW 50	gi 6755901
Platelet-activating factor acetylhydrolase alpha-2 MW 25	gi 6679199
Tyrosine 3-monooxygenase/tryptophan 5-monooxygenase activation protein MW 28	gi 6756039
Platelet-activating factor acetylhydrolase alpha-1 MW 26	gi 6679201
Lysophospholipase 1 MW 25	gi 6678760
Lysophospholipase 2 MW 25	gi 7242156
Peroxiredoxin 1 MW 22	gi 6754976
Platelet-activating factor acylhydrolase alpha-1 MW 26	gi 6679201

## Discussion

The 26 proteins identified by mass spectrometry were an unexpected mixture of peptidases, hydrolases, dehydrogenases, lipases, phosphatases, heat shock protein, tubulin, and others. Only 6 proteins had the conserved GXSXG sequence characteristic of serine esterases and serine proteases (Derewenda and Derewenda, 1991). Acetylcholinesterase was not in the set. This was not a surprise because the mouse brain supernatant did not have AChE activity.

Every protein in Table 4.1 was tagged with FP-biotin. The most likely amino acid residues to form a covalent bond with an OP are serine, tyrosine, and histidine. Serine has been documented as the site of OP attachment in enzymes that have the conserved GXSXG motif. Serine is also the site of OP attachment in enzymes with a trypsin-like catalytic triad. Platelet-activating factor acetylhydrolase alpha-1 does not have the GXSXG sequence but it does have a trypsin-like triad of Ser 47, His 195 and Asp 192 (Ho et al., 1997). Tyrosine has been documented as the site of attachment of sarin and soman in human albumin (Black et al., 1999). Tyrosine has also been shown to be the site of attachment of DFP to papain (Chaiken and Smith, 1969). Histidine as well as serine are the sites of attachment of DFP to rabbit liver carboxylesterase (Korza and Ozols, 1988).

The work in Task 4 shows that the methods for searching for new biomarkers of OP toxicity have been mastered by us. We are ready to ask the physiologically important question posed in Task 6, to find proteins labeled by OP exposure in living animals.

## Task 5

The reactivity with insecticides of the new biochemical markers will be compared to the reactivity of AChE and BChE with the same insecticides. The set of proteins identified in task 3, as well as AChE and BChE, will be ranked for reactivity with chlorpyrifos oxon, dichlorvos, diazinon-O-analog, and malathion-O-analog. This will be accomplished by measuring second order rate constants for individual proteins in brain extracts.

**Abstract.** Subcellular fractions of mouse brain (the 100,000xg supernatant and the 17,000xg pellet) were screened for reaction with chlorpyrifos-oxon, dichlorvos, diazoxon (diazinon-O-analog), and malaoxon (malathion-O-analog), using an FP-biotin screening protocol. The screening protocol allowed proteins to react with OP and then the unreacted proteins were visualized by binding FP-biotin. Signal intensity after hybridization of blots with streptavidin-Alexafluor was reduced for OP reactive proteins. Only seven of the 55 protein bands from the 100,000xg supernatant, and seven of the 52 protein bands from the 17,000xg pellet showed significant sensitivity to these OP. Each OP reacted with a somewhat different set of proteins. IC<sub>50</sub> values were determined for each of the sensitive proteins. The identity of 8 OP-reactive proteins was determined by mass spectrometry. They were prolylendopeptidase, D-3-phosphoglycerate dehydrogenase, esterase 10, platelet-activating factor acetylhydrolase alpha-2, tyrosine 3-monoxygenase/tryptophan 5-monoxygenase activation protein, platelet-activating factor acetylhydrolase alpha-1, lysophospholipase 1, and lysophospholipase 2. Comparison of IC<sub>50</sub> values for AChE and IC<sub>50</sub> values for these OP-reactive proteins suggested that only platelet-activating factor acetylhydrolase alpha-2 reacted more readily with OP than AChE.

**Introduction.** The goal of these studies is to identify proteins that react with OP insecticides at doses that do not have a significant effect on AChE activity. Proteins that are more reactive toward OP than AChE do exist. Richards et al. (2000) have shown that acylpeptide hydrolase reacts with selected OP more readily than does AChE; while Quistad et. al. (2001, 2002) have made similar observations with fatty acid amide hydrolase. Other highly reactive OP targets most probably exist. In this section, methods for OP reactivity screening and identification of OP reactive proteins have been applied to subcellular fractions from mouse brain (100,000xg supernatant and 17,000xg pellet). Four OP were tested: chlorpyrifos-oxon, diazoxon, dichlorvos, and malaoxon. Fifty-five FP-biotin reactive bands were found in the 100,000xg supernatant; 22 of these were extracted with avidin-agarose and submitted to mass spectral analysis; 15 yielded information on the proteins associated with the bands. Six proteins

showed significant reactivity toward the test OP. One protein, platelet-activating factor acetylhydrolase alpha-2, was more reactive toward dichlorvos than was AChE. Fifty-two FP-biotin reactive bands were found in the 17,000xg pellet; 7 of these showed significant reactivity toward the test OP.

## Methods

**The screening method.** The  $IC_{50}$  screening method, which was described in the annual report for the year 2002, was used to determine the OP reactivity of proteins in the 100,000xg supernatant and 17,000xg pellet fractions from mouse brain. In brief, that method involved incubating aliquots of the mouse brain fraction (1.3 mg protein/ml) with various concentrations of the OP (0.05 to 300  $\mu$ M) in 50 mM TrisCl buffer, pH 8.0 containing 5 mM EDTA and 2.4% methanol (94  $\mu$ l total volume) for 30 minutes at 25°C. Reactions were stopped by gel filtration through Performa SR spin columns, equilibrated in the reaction buffer. Six  $\mu$ l of 170  $\mu$ M FP-biotin were immediately added to each column eluent, to yield 10  $\mu$ M FP-biotin, and incubation was continued for 300 minutes, to completely react all remaining FP-biotin reactive protein. Reactions were completely stopped by adding 20  $\mu$ l of 6x-SDS PAGE loading buffer (0.2 M TrisCl pH 6.8 containing 10% SDS, 30% glycerol, 0.6 M dithiothreitol and 0.012% bromophenol blue) and heating to 85°C for 5 minutes. Aliquots (30  $\mu$ g protein) from each reaction mixture were separated on a 10-20% gradient SDS PAGE by electrophoresis at a constant voltage of 250 volts for 14 hours (4000 volt-hours). Biotinylated proteins were electrophoretically transferred to PVDF membrane, and reacted with 9.5 nM Streptavidin-Alexa 680 (Molecular Probes, Inc., Eugene, OR). The Streptavidin-Alexa 680 served to place a fluorescent tag on the biotinylated proteins. Fluorescent signals were collected with an Odyssey flat plate scanner (Li-COR, Lincoln, NE), and signal intensity was integrated with Kodak 1D software, where applicable.  $IC_{50}$  values (defined as the concentration of OP at which 50% of the protein had been reacted) were estimated. Due to difficulties in accurately integrating the fluorescence intensities for bands with weak signals,  $IC_{50}$  values were sometimes assigned by visual inspection of the fluorescence pattern.

**Mass spectral analysis.** Isolation of FP-biotin labeled proteins is described in Task 3. Preparation of tryptic peptides and analysis of these peptides by mass spectrometry are described in Task 4.

**Human AChE.** Recombinant human AChE was secreted from Chinese Hamster Ovary cells into serum-free culture medium. The AChE was purified by chromatography on procainamide-Sepharose affinity column. The resulting AChE was free of albumin.

## Results

**Screening for organophosphate reactivity in the 100,000xg mouse brain supernatant.** Four OP were used to assess reactivity of the mouse brain 100,000xg supernatant fraction: chlorpyrifos-oxon, dichlorvos, diazoxon, and malaoxon. Only a few of the 55 FP-biotin reactive proteins were also reactive toward these OP. Three bands were found to disappear upon reaction with chlorpyrifos-oxon (0.05 to 304  $\mu$ M). Figure 5.1 shows that the three bands that reacted with chlorpyrifos oxon had band numbers 12, 41, and 44/45. Their molecular weights were 85, 30 and 25 kDa.

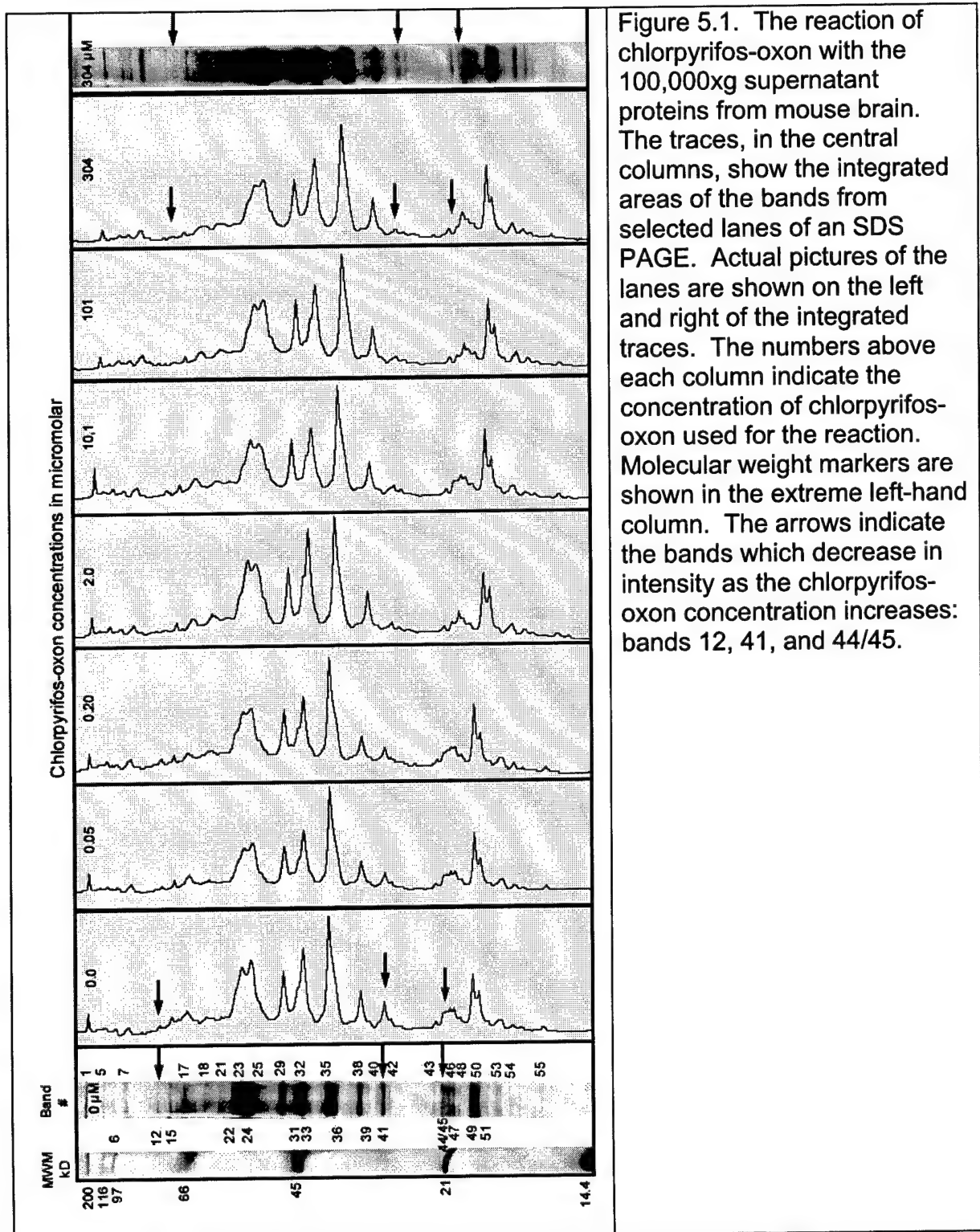
Figure 5.2 shows four bands that reacted with dichlorvos (0.64 to 382  $\mu$ M). Their band numbers were 12, 32, 44/45 and 50. Their molecular weights were 85, 45, 25, 20 kDa. Figure 5.3 shows the four bands that reacted with diazoxon (0.11 to 510  $\mu$ M) as having band numbers 9, 12, 41, and 47. Their molecular weights were 89, 85, 30, and 22 kDa. Figure 5.4 shows that one band reacted with malaoxon (0.11 to 510  $\mu$ M). The band number was 9 and its molecular weight was 89 kDa. These results show that each OP reacted with sets of proteins that only partially overlapped.

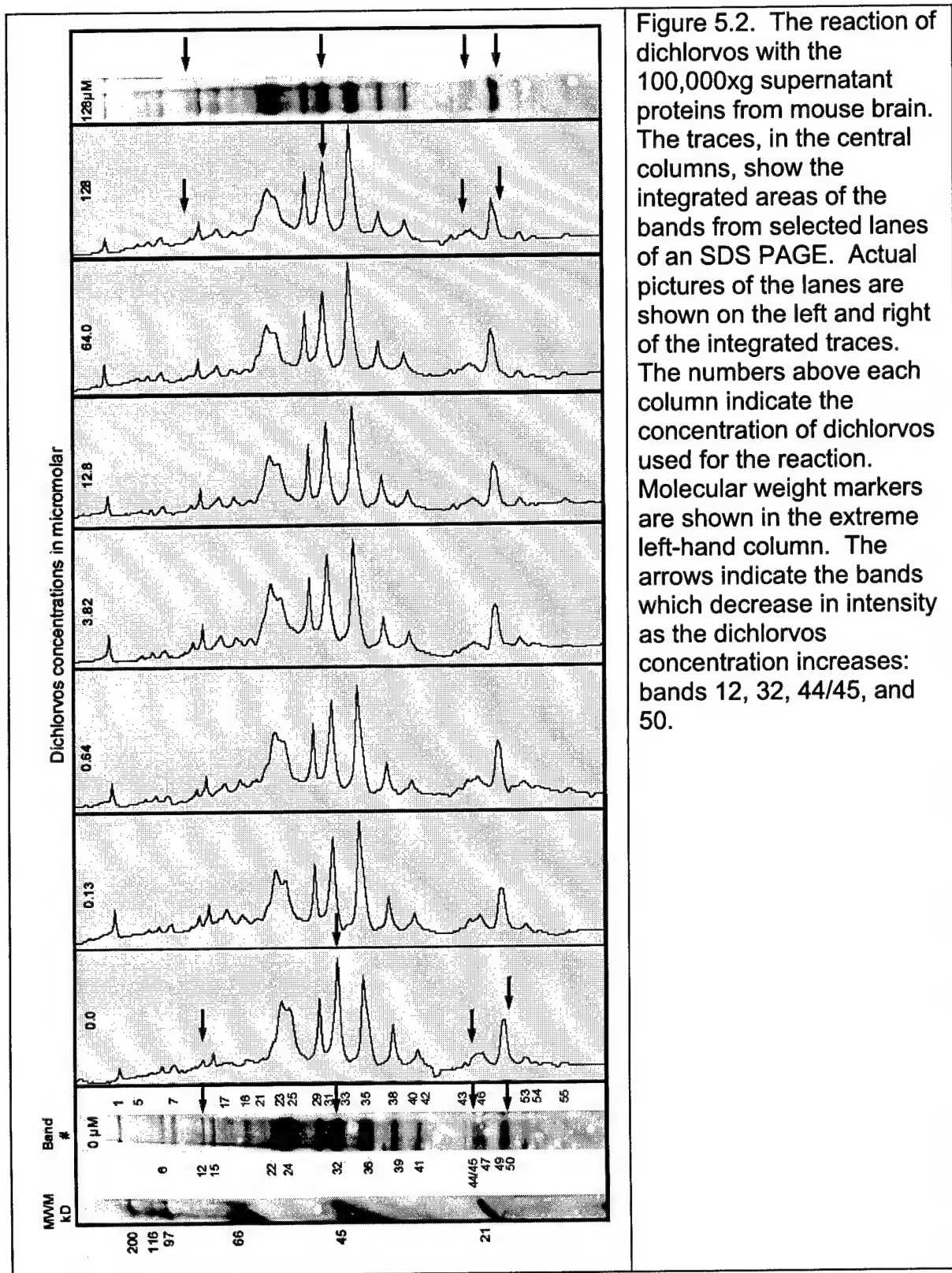
The OP-reactive bands were typically present at low level. For such weak signals, determination of  $IC_{50}$  values (concentration of OP that causes 50% inhibition) was complicated by heterogeneity in the Western blot process. In some cases, a plot of the "integrated signal intensity" versus "OP concentration" was sufficiently well-behaved to allow determination of the  $IC_{50}$  (see Figure 5.5a & b). However, in many cases the  $IC_{50}$  was best determined by visual inspection of the signal pattern (see Figures 5.1 to 5.4).

Estimated  $IC_{50}$  values, for all bands currently considered reliable, are presented in Table 5.1.

$IC_{50}$  values are critically dependent upon the conditions of measurement. Temperature and pH are normal variables which must be controlled in order to make comparisons meaningful, but the time for which the inhibitor is allowed to react is also critical.  $IC_{50}$  values for mouse AChE, taken from the literature (see Table 5.1), were determined under a variety of conditions and therefore serve only as approximate reference values. Determination of  $IC_{50}$  values for the reaction of AChE with the test OP, under the screening conditions is currently underway. Still, most of the OP reactive bands in mouse brain supernatant appear to be substantially less reactive than mouse AChE. At this time, only the reaction of bands 44/45 with dichlorvos appears to be substantially faster than that for AChE. However, the reaction of diazoxon with band 9 is rapid, and there is no literature value for mouse AChE with which to compare, so this band remains of interest. Band 41 is quite reactive with chlorpyrifos-oxon, and also could be of interest. In addition, there are missing  $IC_{50}$  values for the reaction of band 9 with chlorpyrifos-oxon and dichlorvos. Band 9 was not always seen in the Western blot, which accounts for the missing data. Since band 9 was reactive toward diazoxon and malaoxon, this band is of interest. Screening experiments with chlorpyrifos-oxon and dichlorvos are being repeated.

**AChE control.** Sensitivity of AChE to reaction with OP varies from species to species (see literature values in Table 5.1). Direct comparison of mouse AChE reactivity to the reactivity of the other OP sensitive bands, in the screening assay format, would be the best way to determine the relative sensitivity of alternate OP targets and AChE. However, AChE is not present in the mouse brain supernatant at sufficiently high concentration to be visible on blots. We added purified human red blood cell AChE (gift from Dr. Terrone Rosenberry, Mayo, Jacksonville, FL) to the reaction of OP with mouse brain supernatant, as an approximate internal control, but that AChE gave several bands which obscured the 70-80 kDa region. Purified, recombinant wild type AChE made in CHO K1 cells gave the same result. Since OP reactive bands 9 and 12 are in the 70-80 kDa region, the human AChE control could not be used. Currently, the reactivity of the test OP toward mouse brain AChE is being evaluated by standard solution assay methods, as a substitute for an internal AChE control in the screening assay.





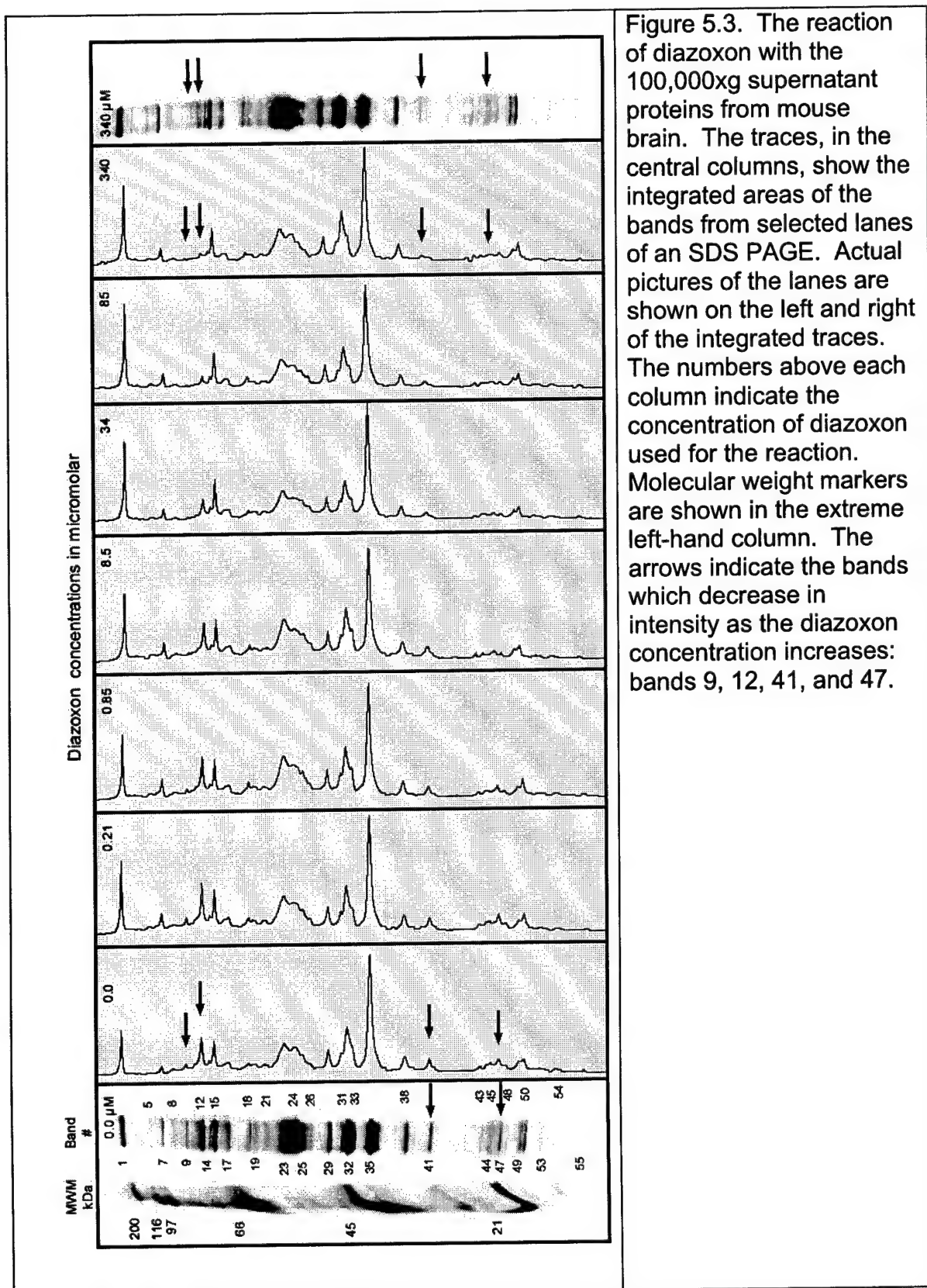
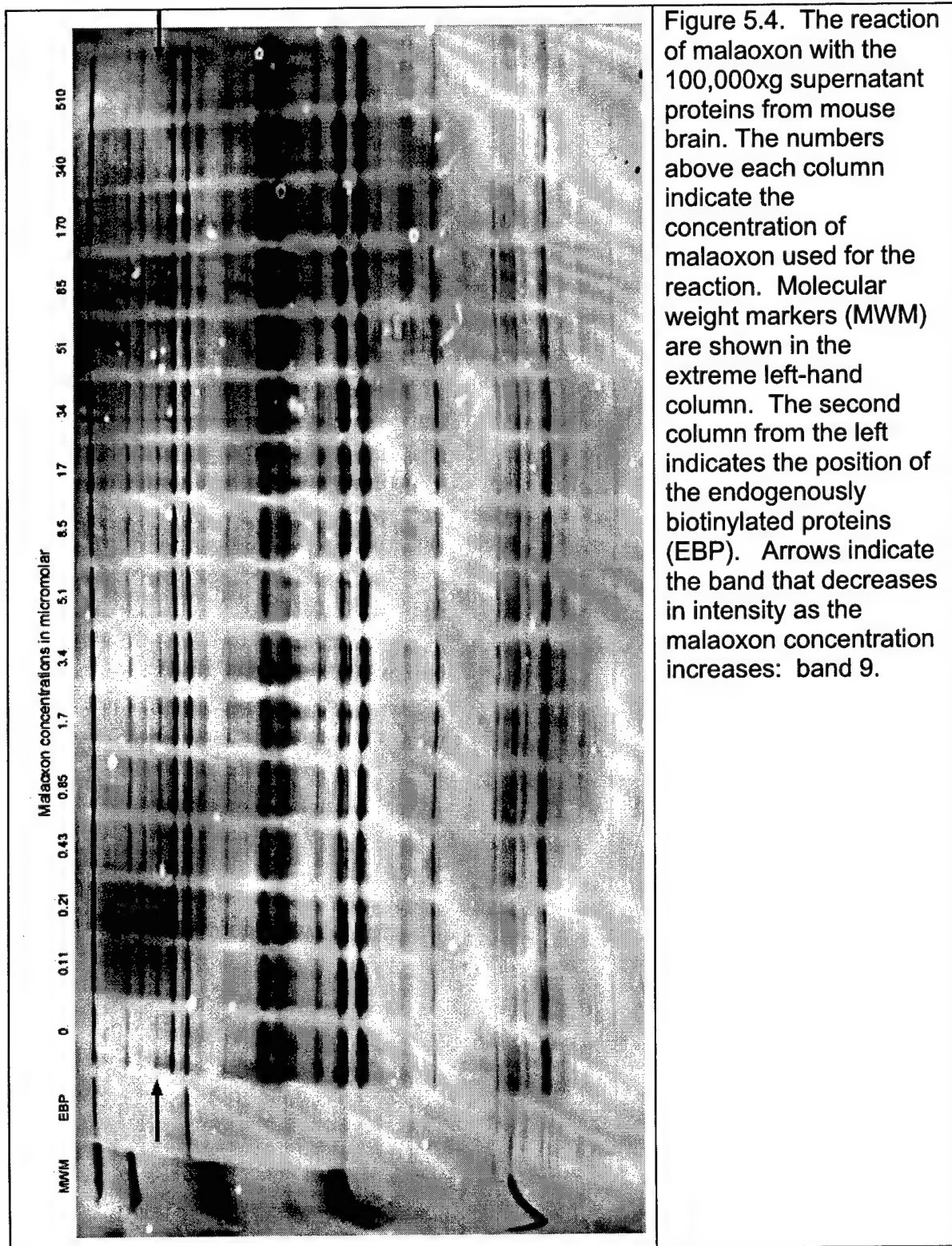


Figure 5.3. The reaction of diazoxon with the 100,000xg supernatant proteins from mouse brain. The traces, in the central columns, show the integrated areas of the bands from selected lanes of an SDS PAGE. Actual pictures of the lanes are shown on the left and right of the integrated traces. The numbers above each column indicate the concentration of diazoxon used for the reaction. Molecular weight markers are shown in the extreme left-hand column. The arrows indicate the bands which decrease in intensity as the diazoxon concentration increases: bands 9, 12, 41, and 47.



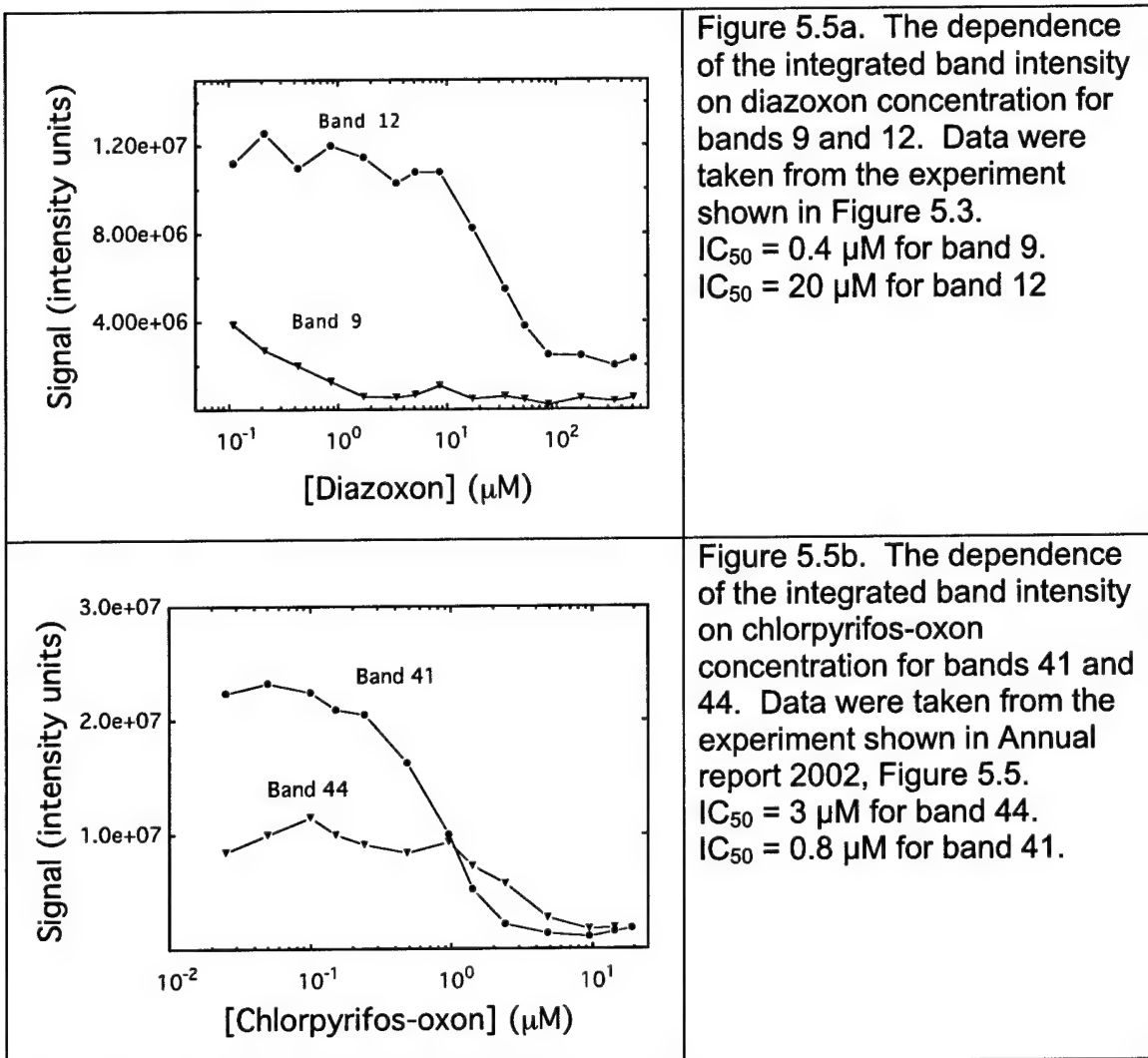
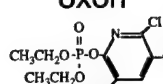
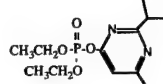
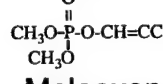
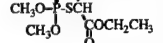


Table 5.1 IC<sub>50</sub> Values

Mouse Brain 100,000xg Supernatant  
 IC<sub>50</sub> (nM) 30 min, pH 8.0, 25°C  
 experimental values

OP	band 9	band 12	bands 23/24	band 41	band 44/45	band 47	band 50
Chlorpyrifos oxon	??	>100,000	-	800	3000	-	-
							
Diazoxon	400	20,000	-	30,000	-	10,000	-
							
Dichlorvos	??	10,000	20,000	-	2000	-	50,000
							
Malaoxon	170,000	-	-	-	-	-	-
							

Mouse Brain 17,000xg Pellet  
 IC<sub>50</sub> (nM) 30 min, pH 8.0, 25°C  
 experimental values

OP	band 8	band 15	band 17	band 19	band 34	band 40	band 43
Chlorpyrifos oxon	1000	300	200	1000	2000	??	20,000
Diazoxon	-	60,000	-	-	-	10,000	1000
Dichlorvos	20,000	-	-	-	-	-	-
Malaoxon	-	10,000	-	-	-	-	-

Literature References  
 IC<sub>50</sub> (nM)

	human 30 min, pH 7-7.6, 25-37°C	mouse 15 min, pH 8-9, 25-37°C		pig 20 min, pH 7.4, 37°C	
OP	AChE	AChE	FAAH	AChE	APH
Chlorpyrifos oxon	2 <sup>5</sup>	19 <sup>1</sup> , 9 <sup>5</sup>	56 <sup>1</sup>	-	-
Diazoxon	60 <sup>6</sup>	-	9300 <sup>1</sup>	269 <sup>3</sup>	1386 <sup>3</sup>
Dichlorvos	200 <sup>7</sup>	5100 <sup>2</sup>	1800 <sup>2</sup>	788 <sup>3</sup>	118 <sup>3</sup>
Malaoxon	300 <sup>8</sup>	159 <sup>4</sup>	-	296 <sup>3</sup>	1,000,000 <sup>3</sup>

IC<sub>50</sub> values for some of the literature values were calculated from reported second-order rate constants using the equation: IC<sub>50</sub> = (ln2)/kt.<sup>9</sup> Where k is the second-order rate constant and t is the inhibition time in minutes.

- 1 Quistad et. al. [2001]
- 2 Quistad et. al. [2002]
- 3 Richards et. al. [2000]
- 4 Johnson and Wallace [1987]
- 5 Amitai et. al. [1998]
- 6 Schopfer unpublished
- 7 Skrinjaric-Spoljar et al. [1973]
- 8 Rodriguez et. al. [1997]
- 9 Main [1979]

?? indicates that an  $IC_{50}$  value is not yet available, but the protein in the band reacts rapidly with OP

**Identity of the proteins which react with the test battery of OP.** Proteins were identified by mass spectroscopy as described in task 4. Six of the 7 OP reactive bands in Table 5.1 yielded identifiable proteins, 5 of which were hydrolases. Band 12 was prolylendopeptidase 81 kDa; band 23/24 was D-3-phosphoglycerate dehydrogenase 51 kDa and tubulin 50 kDa; band 41 contained esterase 10 with a molecular weight of 35 kDa (and three other proteins); band 44/45 was platelet-activating factor acetylhydrolase alpha 2 with a molecular weight of 25 kDa; band 47/46 contained platelet-activating factor acetylhydrolase alpha 1 with a molecular weight of 26 kDa and tyrosine 3-monooxygenase/tryptophan 5-monooxygenase activation protein (a protein phosphatase) 28 kDa; band 50 gave lysophospholipase 1 and 2 with molecular weights of 25 kDa. The remaining OP-reactive band (band 9) can be tentatively assigned to acylpeptide hydrolase (APH). This assignment is based on the molecular weight of acylpeptide hydrolase (MW= 80 kDa), the position of band 9 in the blot pattern, and the fact that acylpeptide hydrolase already has been shown to be highly reactive toward the type of OP tested in these experiments (Richards et. al., 2000).

Band 47/46 showed greater reactivity with dichlorvos ( $IC_{50}$ =2000 nM) than did AChE ( $IC_{50}$ =5100 nM). No literature information on the reaction of dichlorvos with either of the enzymes in this band (platelet-activating factor acetylhydrolase alpha 1 and tyrosine 3-monooxygenase/tryptophan 5-monooxygenase activation protein) could be found.

Band 41 was relatively reactive toward chlorpyrifos-oxon ( $IC_{50}$ =800 nM). Of the 4 proteins which were identified in this sample, esterase 10 is the most likely to be a target for chlorpyrifos-oxon.

Band 9 remains of interest. It shows a relative reactivity with diazoxon and malaoxon which is similar to that of acylpeptide hydrolase (APH) (Table 5.1). This supports the suggestion that band 9 is APH. If so, then band 9 would be expected to show greater reactivity with dichlorvos than does AChE (refer to the  $IC_{50}$  values for pig APH and pig AChE in Table 5.1).

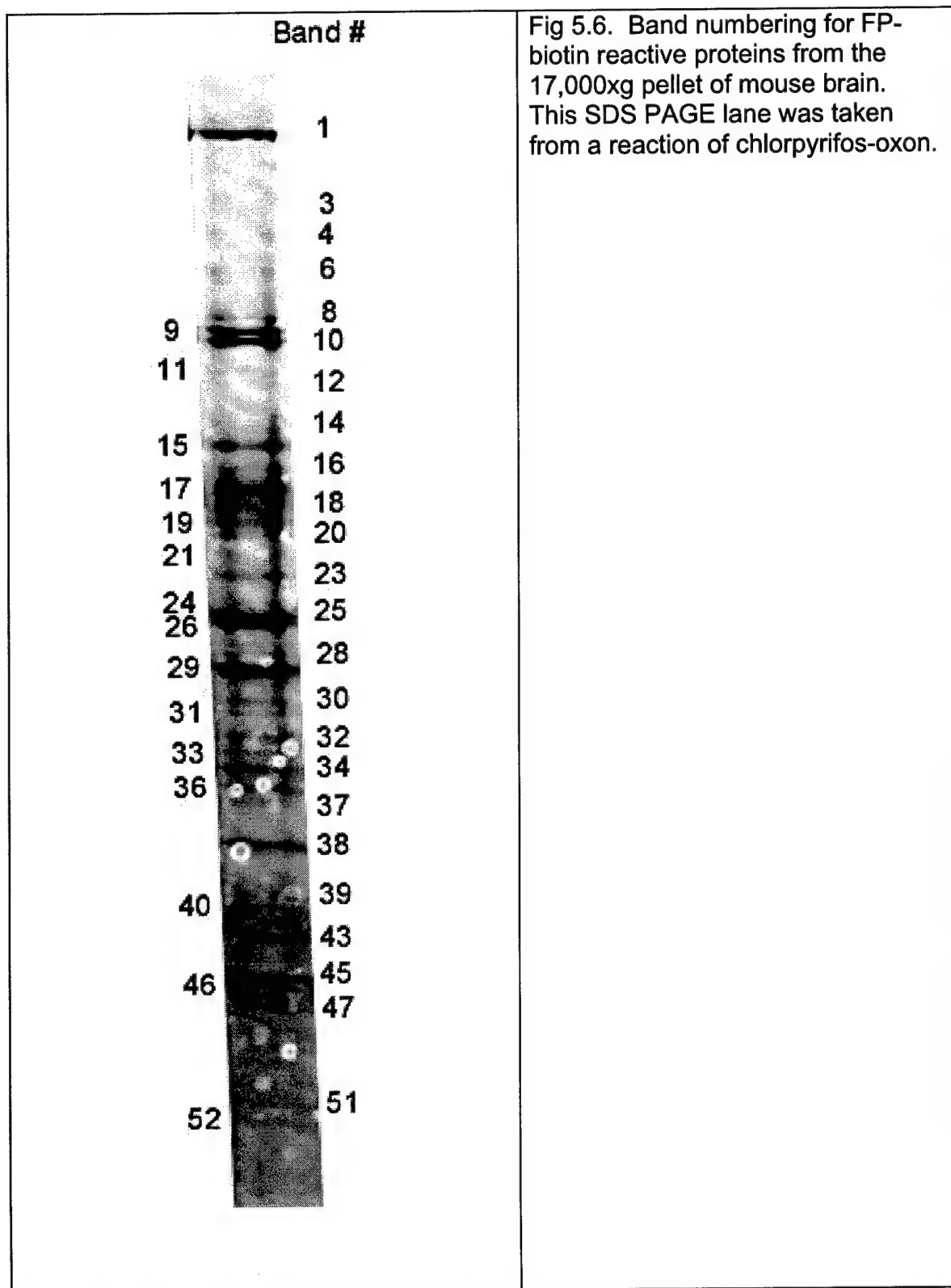
**Screening for organophosphate reactivity in 17,000xg mouse brain pellet.**

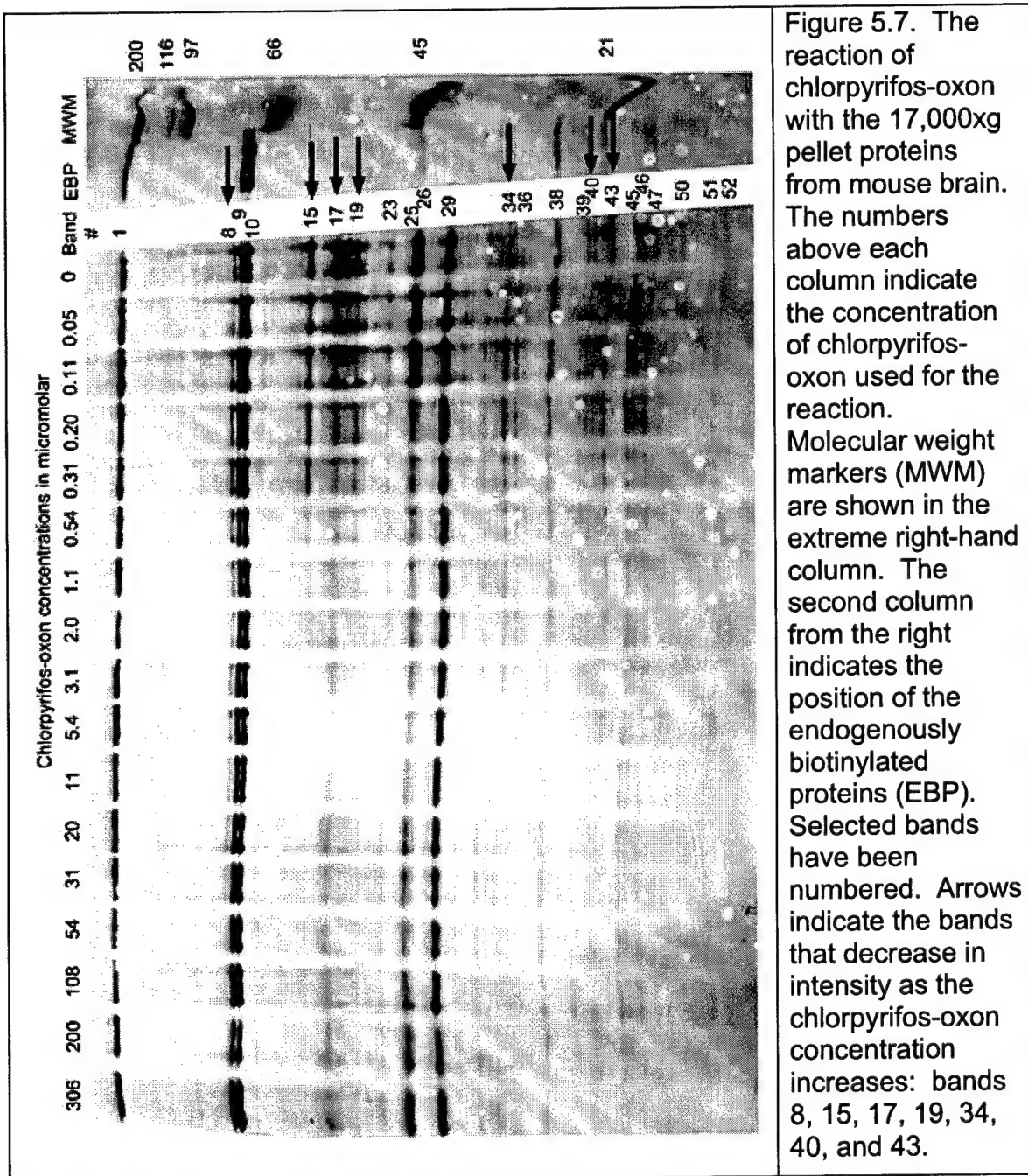
The screening has been extended to the 17,000xg pellet from mouse brain (the synaptosomal fraction). Fifty-two FP-biotin reactive proteins were found in the synaptosomal fraction (Figure 5.6). As with the 100,000xg supernatant, minor bands and shoulders from major bands were included in the numbering. The proteins in this fraction would be expected to be mostly membrane bound, therefore representing a different selection of targets than were available in the 100,000xg supernatant.

The same four OP used on the 100,000x g supernatant were tested with the 17,000xg pellet (Table 5.1): chlorpyrifos oxon, diazoxon, dichlorvos, and malaoxon. Bands which were sensitive to these OP were all present at low levels, therefore IC<sub>50</sub> values were evaluated by visual inspection of the banding patterns (see Figure 5.7 for an example). Seven bands were found to disappear with chlorpyrifos-oxon (8, 15, 17, 19, 34, 40, and 43). Band 8 is heat shock protein 90-Beta 84 kDa. Band 15 has not been identified. Band 17 is a mixture of 4 proteins (see Table 4.1 in task 4). Bands 19, 34, 40 and 43 have not been identified.

The most reactive were bands 15 and 17 (IC<sub>50</sub> values of 200 to 300 nM with chlorpyrifos-oxon). These values are about 10-fold higher than those found in the literature for mouse AChE (9-19 nM), indicating that the proteins in bands 15 and 17 are less reactive than AChE with chlorpyrifos oxon.

The other three OP (diazoxon, dichlorvos, and malaoxon) reacted with a few of the bands in the chlorpyrifos-oxon set, but with no other bands. Diazoxon reacted with bands 15, 40, and 43. Dichlorvos reacted with band 8. Malaoxon reacted with band 15. Dichlorvos and malaoxon were less reactive with those bands than with AChE (Table 5.1). Diazoxon has no literature value for reaction with mouse AChE so a comparison cannot be made at this time.





## Discussion

Methods for screening complex mixtures of proteins for reaction with OP have been refined by us and are currently in routine use. Thus far, they have been applied to the reactions of chlorpyrifos-oxon, diazoxon, dichlorvos, and malaoxon with mouse brain supernatant (100,000xg) and synaptosomal (17,000xg pellet) fractions. In addition, mass spectral methods for identification of the reactive proteins are now operational, and the 100,000xg supernatant has been checked for OP reactive proteins.

Initial experiments suggest that only the reaction of dichlorvos with platelet-activating factor acetylhydrolase alpha-2 occurs more readily than with AChE. However, there are gaps in the reference reactivities for AChE and there are missing IC<sub>50</sub> values for band 9 from the 100,000xg supernatant. These deficiencies are being addressed. Control reactions for mouse AChE reacting with all four OP, under the experimental conditions for screening, are currently underway. These data will improve the AChE reference base and allow for more accurate comparison between the reactivity of the new targets and AChE. Screening of the 100,000xg supernatant with chlorpyrifos-oxon and dichlorvos is being repeated in order to obtain IC<sub>50</sub> values for band 9; and the mass spectral identification of band 9 is also underway.

Band 9 from the 100,000xg supernatant is particularly interesting because it migrates at the position expected for acylpeptide hydrolase, an enzyme which has already been shown to react with some OP more readily than does AChE (Richards et. al., 2000; and see Table 5.1). It is expected that when all of the data and controls are in hand, band 9 will show better reactivity than AChE with some of the test OP.

Fatty acid amide hydrolase is an interesting candidate, which should appear in the synaptosomal fraction. It is a membrane bound enzyme which has been shown to react with some of the test OP more readily than does AChE (Quistad et. al., 2001 and 2002).

## Task 6

The toxicological relevance of the biochemical markers identified in task 3 will be determined. Mice will be treated with the dose of insecticide determined in Task 2, that is, a dose that is not toxic to wild-type mice, but is toxic to AChE deficient mice.

6.1. Toxicity will be measured and recorded.

6.2. Brain will be extracted. The amount of biochemical marker that is phosphorylated by insecticide will be quantitated, relative to inhibition of AChE and BChE.

6.3. Toxicity will be correlated with extent of phosphorylation of the new biochemical markers.

We are preparing for Task 6 by studying the in vivo response of AChE -/- and +/+ mice to the organophosphorus compound, FP-biotin.

**Abstract.** AChE -/- mice treated with a nearly lethal dose of the organophosphorus agent, FP-biotin, had acute cholinergic signs of toxicity. The cholinergic signs of toxicity could not have come from inhibition of AChE because these mice have no AChE. Their BChE was only slightly inhibited, therefore inhibition of BChE cannot explain the toxicity. The acute toxicity was reversed within 15 minutes. It was hypothesized that binding of FP-biotin to muscarinic receptors explained the cholinergic signs of toxicity. This hypothesis is supported by the findings of others that organophosphorus compounds bind to acetylcholine receptors and that this binding contributes to the biological effect of organophosphorus toxins.

FP-biotin injected i.p. crossed the blood-brain barrier and labeled a 66 kDa protein. A 66 kDa protein was also labeled in lung and muscle of AChE -/- mice. The identity of this protein will be determined by mass spectrometry. It is anticipated that this 66 kDa protein might be a new biomarker of OP exposure.

**Introduction.** The biotinylated organophosphorus compound, FP-biotin, binds to 52 proteins in mouse brain extracts when the binding studies are performed in the test tube. It was of interest to determine how many proteins bound FP-biotin when the compound was administered to living mice. The living mouse was observed for signs of toxicity after i.p. administration of FP-biotin so as to correlate toxicity with proteins covalently modified by FP-biotin. The questions of interest were the following. What is a toxic dose of FP-biotin? Is the toxic dose different for AChE -/- and +/+ mice? What are the signs of intoxication in a mouse treated with FP-biotin? Are there cholinergic signs of toxicity? What tissues bind FP-biotin? Does FP-biotin cross the blood-brain barrier? How many

proteins and what is the identity of the proteins that bind FP-biotin? Can the toxic signs be attributed to inhibition of these proteins by FP-biotin? Is toxicity the consequence of inhibition of enzymes other than AChE?

## Methods

**Materials.** FP-biotin was custom synthesized by Troy Voelker in the laboratory of Charles M. Thompson at the University of Montana, Missoula. Purity was checked by NMR and mass spectrometry and no evidence of contamination was detected. The molecular weight was 593.3. FP-biotin was stored as a dry powder at -70°C. A 1.7 mM stock solution in ethanol was stored at -70°C.

Immun-Blot PVDF membrane for protein blotting 0.2 µm, catalog # 162-0177 (Bio-Rad Laboratories, Hercules, CA); Streptavidin-Alexa 680 fluorophore (catalog # S-21378 Molecular Probes, Eugene, OR). Biotinylated molecular weight markers were from BioRad.

**Mice.** AChE -/- mice were made by gene targeting (Xie et al., 2000) at the University of Nebraska Medical Center. The animals are in strain 129Sv genetic background. The colony is maintained by breeding heterozygotes because AChE -/- mice do not breed (Duyesen et al., 2002). The AChE -/- mice require special care and feeding as described by Duyesen et al. (2002) to enable them to live to an average of 120 days. Five male AChE -/- mice, ages 34, 34, 43, 45, and 48 days and three male AChE +/+ mice ages 58, 58, and 38 days were studied. The mice weighed about 20 grams.

**Injection of FP-biotin into mice.** Mice were injected intraperitoneally with 206 µl of 4.44 mg/ml FP-biotin dissolved in 15.5% ethanol to give a dose of 55 mg/kg. After 15 min, mice received 75 µl FP-biotin to bring the total FP-biotin dose to 75 mg/kg. Control mice were injected with 15.5% ethanol. Mice were euthanized 120 min after the first injection of FP-biotin. Another set of mice was injected with 5 mg/kg FP-biotin i.p.

**Observation of FP-biotin treated animals.** Animals were observed for salivation, lacrimation, increased urination, abnormal defecation, hyperactivity or lethargy, tremor, convulsions, muscle weakness, vasodilation, response to being held, posture, gait, eyelid closing, piloerection, respiration, Straub tail, tail pinch response, and body temperature. The neurobehavioral screening battery is described by McDaniel and Moser, 1993. Surface body temperature was measured with a digital thermometer, Thermalert model TH-5, using a surface microprobe MT-D, Type T thermocouple (Physitemp Instruments, Clifton, NJ)).

**Tissue extraction.** Blood was collected from the Saphenous vein in the hind leg of mice. Then mice were euthanized and immediately perfused intracardially with phosphate buffered saline to wash the blood out of organs, before tissues were removed. Brain, lungs, liver, intestine, heart and quadriceps muscle were

collected and stored frozen. Tissues were homogenized in 10 volumes of ice-cold 50 mM potassium phosphate pH 7 containing 0.5% Tween 20 for 10 seconds in a Polytron (Brinkmann Instruments). The suspension was centrifuged in a microfuge for 10 min and the supernatant was saved for gel electrophoresis and enzyme activity assays. The extraction buffer contained Tween 20 rather than Triton X-100 because mouse BChE activity was inhibited up to 95% by 0.5% Triton X-100, but was not inhibited by 0.5% Tween 20 (Li et al., 2000).

**Enzyme activity assays in tissue extracts.** Samples were assayed in triplicate. AChE and BChE activity were measured by the method of Ellman et al. (1961) at 25°C in a Gilford spectrophotometer interfaced to MacLab 200 (ADInstruments Pty Ltd., Castle Hill, Australia) and a Macintosh computer. Samples were preincubated with 5,5-dithio-bis (2-nitrobenzoic acid) in 0.1 M potassium phosphate buffer, pH 7.0, to react free sulphydryl groups before addition of substrate. AChE activity was measured with 1 mM acetylthiocholine after inhibiting BChE activity with 0.05 mM iso-OMPA. BChE activity was measured with 1 mM butyrylthiocholine. The extinction coefficient at 412 nm was 13,600 M<sup>-1</sup> cm<sup>-1</sup>.

Carboxylesterase activity was measured with p-nitrophenyl acetate. The cuvette contained 0.865 ml of 0.1 M potassium phosphate pH 7.0, 0.025 ml of 0.5 M EDTA to inhibit paraoxonase, 0.01 ml of 1 mM eserine to inhibit AChE and BChE and 50 µl of tissue extract. Liver had such high carboxylesterase activity that the liver extract was diluted another 40-fold (400 fold dilution) before use in the assay. The mixture was preincubated for 10-20 minutes to allow complete inhibition. The carboxylesterase reaction was started by addition of 0.05 ml of 0.1 M p-nitrophenylacetate in methanol. Absorbance was recorded at 400 nm. The extinction coefficient was 9000 M<sup>-1</sup> cm<sup>-1</sup>. Tissues from two AChE -/- and 2 +/- mice were assayed with p-nitrophenylacetate. One animal of each genotype had been treated and one not treated with FP-biotin.

Acylpeptide hydrolase activity was measured in a SpectraMax 190 microtiter plate reader (Molecular Devices, Sunnyvale, CA). N-acetyl-L-alanine p-nitroanilide (Sigma) was dissolved in 0.1 M Bis-Tris, pH 7.4, to make a 4 mM solution. The rate of hydrolysis of 4 mM N-acetyl-L-alanine p-nitroanilide was measured at 405 nm at 25°C. Each 100 µl assay solution contained 5 µl of tissue extract. Absorbance was read every 5 min up to 40 min. The extinction coefficient for a 1 cm pathlength is 7530 M<sup>-1</sup> cm<sup>-1</sup> at 405 nm. The pathlength for 100 µl in a microtiter plate was determined to be 0.3 cm.

Units of activity for AChE, BChE, carboxylesterase, and acylpeptide hydrolase are defined as µmoles substrate hydrolyzed per minute. Units of activity were calculated per gram wet weight of tissue.

**Blotting onto PVDF membrane.** For determination of the number and size of proteins labeled by FP-biotin, tissue extracts were subjected to SDS gel electrophoresis, the proteins transferred to a PVDF membrane, and the protein bands visualized with a fluorescent probe. The details of the procedure follow.

A 10-20% gradient SDS-PAGE with 4% stacking gel was poured in a Hoefer

gel apparatus. The dimensions of the sandwich were 16x18x0.075 cm, with 20 wells. Thirty to 150 micrograms of protein were loaded per lane. Electrophoresis was for 4000 volt-hours in the cold room (4°C), with stirring. The bottom tank contained 4.5 L of 60 mM TrisCl buffer, pH 8.1, plus 0.1% SDS. The top tank buffer contained 0.6 L of 25 mM Tris/192 mM glycine buffer, pH 8.2, plus 0.1% SDS.

Proteins were transferred from the gel to PVDF membrane (Immun-Blot from BioRad) electrophoretically in a tank using plate electrodes (TransBlot from BioRad), at 0.5 amps, for 1 hour, in 3 L of 25 mM Tris/192 mM glycine buffer, pH 8.2, in the cold room (4°C), with stirring. The membrane was blocked with 3% gelatin (BioRad) in 20 mM TrisCl buffer, pH 7.5, containing 0.5 M NaCl for 1 hour at room temperature. The 3% gelatin solution had been prepared by heating the gelatin in buffer in a microwave oven for several seconds. The blocked membrane was washed twice with 20 mM TrisCl buffer, pH 7.5, containing 0.5 M NaCl and 0.05% Tween-20, for 20 minutes.

Biotinylated proteins were labeled with 9.5 nM Streptavidin-Alexa 680 fluorophore in 20 mM TrisCl buffer, pH 7.5, containing 0.5 M NaCl and 1% gelatin, for 2 hours, at room temperature, protected from light. Shorter reaction times resulted in less labeling. Then the membrane was washed twice with 20 mM TrisCl buffer, pH 7.5, containing 0.5 M NaCl and 0.05% Tween-20, and twice with 20 mM TrisCl buffer, pH 7.5, containing 0.5 M NaCl, for 20 minutes each. This is essentially the BioRad protocol [BioRad Lit 171 Rev D].

Membranes were scanned with the Odyssey Infrared Imaging System (LI-COR, Lincoln, NE) at 42 microns per pixel. The Odyssey employs an infrared laser to excite a fluorescent probe which is attached to the target protein, and then collects the emitted light. The emitted light intensity is directly proportional to the amount of probe. Both the laser and the detector are mounted on a moving carriage positioned directly below the membrane. The membrane can be scanned in step sizes as small as 21 microns, providing resolution comparable to x-ray film. Data are collected using a 16-bit dynamic range, and can be transferred directly to the Kodak 1D analysis program. The fluorophore is stable in the laser, making it possible to scan the membrane repeatedly, using different intensity settings to optimize data collection for both strong and weak signals.

The intensity of the signal from each labeled protein was determined using a Gaussian deconvolution routine from the Kodak 1D Image Analysis program, v 3.5.3 (Kodak).

**Protein concentration.** Protein concentration in tissue extracts was determined with the BCA Protein Assay Kit (Pierce, Rockford, IL).

**Reaction kinetics of FP-biotin with purified human AChE.** The kinetics for the inhibition of purified human AChE by FP-biotin were studied in 0.1 M potassium phosphate buffer pH 7.0 at 25°C. Bovine serum albumin (BSA), normally included to stabilize AChE, was omitted because it reduced the apparent first-order inhibition constant measured with FP-biotin. Inhibition of AChE was initiated by mixing 0.17 nM of highly purified human AChE (recombinant, from CHO-K1 cells) with variable amounts of FP-biotin. At defined times, inhibition was quenched and residual AChE

activity was determined by adding 0.5 mM DTNB and 1.0 mM acetylthiocholine (Ellman et al., 1961).

**Reaction kinetics of FP-biotin with purified human BChE.** Kinetics for the inhibition of human BChE by FP-biotin were studied in 0.1 M potassium phosphate buffer pH 7.0 at 25°C. Wild type human BChE (0.35 nM) purified from human plasma was incubated with variable amounts of FP-biotin for defined times. Inhibition was stopped and residual BChE activity was determined by addition of 0.5 mM DTNB and 1 mM butyrylthiocholine (Ellman et al., 1961).

## Results

**Toxic signs.** This is the first report of treatment of a living animal with FP-biotin. Cholinesterase inhibitors typically cause salivation, lacrimation, decreased motor activity, muscle weakness as reflected in gait changes and foot splay, tremors, decreased response to tail pinch, and hypothermia (Moser, 1995). If the cholinesterase inhibitor crosses the blood-brain barrier, the animal has convulsions.

Only some of these cholinergic signs of toxicity were observed in wild-type and AChE  $-/-$  mice after treatment with up to 75 mg/kg FP-biotin (Table 6.1). Animals had decreased motor activity, decreased tail pinch response, muscle weakness, and tremor. Hypothermia and salivation were observed only in AChE  $-/-$  mice. Animals did not lacrimate or have convulsions.

The first dose of FP-biotin at 55 mg/kg produced only mild toxic signs in AChE  $-/-$  mice. The posture became hunched, there was tremor, alertness was decreased, the gait became abnormal, motor activity decreased, and there was slight salivation. The second dose at 15 min, which increased the total to 75 mg/kg, had a dramatic effect on the AChE  $-/-$  mouse. The mouse immediately flattened its posture, had myoclonic jerks, salivated profusely, became sluggish in its movements, showed stereotypical cleaning and scratching behavior, severely abnormal gait and ataxia, increased rate of respiration, and decreased tail pinch response. The mouse was so abnormal in appearance and behavior that it was a surprise when it recovered. At 30 minutes after the first injection, the mouse had improved its posture so it was no longer flattened, the tremor had decreased, salivation decreased, the mouse became more active and alert, and its gait became more normal. Its posture continued to be hunched for the entire 120 min observation period. Its temperature started to drop at 55 minutes from 37.1°C until it reached a low of 35.8°C at 120 min when it was euthanized. The drop in body temperature was accompanied by piloerection. There was no salivation after 55 min. The tail pinch response was normal after 55 min. The 75 mg/kg FP-biotin dose was a maximally tolerated dose and was not lethal to AChE  $-/-$  mice.

Wild-type mice were less intoxicated by 75 mg/kg FP-biotin. They had a hunched posture, slightly impaired mobility, reduced tail pinch response, increased respiration rate, slight tremor, and piloerection but no salivation, no flattened posture, and no clonic jerks.

Control AChE  $-/-$  mice treated with 15.5% ethanol in saline solution briefly dropped body temperature from 37.3 to 36.2°C, but recovered normal temperature by 15 minutes after injection. No other changes were noticed. Control wild-type mice also had a drop in body temperature after being injected with 15.5% ethanol.

**Table 6.1.** Toxic signs in AChE  $-/-$  and  $+/+$  mice after injection of FP-biotin i.p. at a dose of 55 mg/kg followed by a second dose at 15 min to bring the total dose to 75 mg/kg.

Toxic sign	AChE $-/-$	AChE $+/+$
Salivation	yes	no
Lacrimation	no	no
Urination	no	no
Defecation	no	no
Vasodilation	no	no
Convulsions	no	no
Vocalization	no	no
Decreased motor activity	yes	yes
Tremor	yes	yes
Clonic jerks	yes	no
Decreased response to tail pinch	yes	yes
Straub tail	no	no
Drooping eyelids	yes	yes
Hunched posture	yes	yes
Piloerection	yes	yes
Faster respiration	yes	yes
Loss of resistance to being held	no	no
Ataxia	yes	yes
Gait changes	yes	yes
Flattened posture or splayed hind legs	yes	no
Drop in body temperature	yes	no

**Enzyme activity.** Enzyme activity was measured in tissue extracts immediately after the tissue was homogenized and clarified by centrifugation.

BChE activity was slightly inhibited in brain, serum and liver, but not at all inhibited in muscle. See Table 6.2. AChE activity was not measured because AChE  $-/-$  mice have no AChE enzyme and no AChE activity. Carboxylesterase activity was slightly inhibited in serum, liver, and brain but not at all inhibited in muscle. Acylpeptide hydrolase activity was slightly inhibited in brain but not in liver and muscle. These minor levels of inhibition do not explain the severe toxicity observed in AChE  $-/-$  mice after treatment with FP-biotin.

**Table 6.2.** Inhibition of enzyme activities after treating AChE -/- mouse with 75 mg/kg FP-biotin i.p.

Tissue	BChE activity u/g	% inhibition	Carboxyl esterase activity u/g	% inhibition	Acylpeptide hydrolase activity u/g	% inhibition
Serum	0.58		13.4			
Serum	0.49	15	9.5	29		
FP-biotin						
Liver	1.86		158		1.80	
Liver	1.29	31	138	13	1.84	0
FP-biotin						
Brain	0.066		11.0		0.50	
Brain	0.048	17	10.7	3	0.46	8
FP-biotin						
Muscle	0.10		7.8		.59	
Muscle	0.10	0	8.1	0	.68	0
FP-biotin						

**Table 6.3.** Inhibition of enzyme activities after treating AChE +/- mouse with 75 mg/kg FP-biotin i.p.

Tissue	AChE activity u/g	% inhibition	BChE activity u/g	% inhibition	Carboxyl esterase activity	% inhibition	Acylpeptide hydrolase activity u/g	% inhibition
Serum	0.16		0.67		15.1			
Serum	0.14	12.5	0.34	49	15.3	0		
FP-biotin								
Liver	0.053		1.67		155		1.88	
Liver	0.057	0	1.35	19	146	6	1.39	26
FP-biotin								
Brain	0.607		0.048		9.7		0.47	
Brain	0.538	11	0.042	12.5	9.8	0	0.44	6
FP-biotin								
Muscle	0.109		0.078		7.6		0.56	
Muscle	0.176	0	0.113	0	7.6	0	0.52	7
FP-biotin								

The pattern of inhibition was similar in wild-type (Table 6.3) and AChE -/- mice (Table 6.2). The enzymes that are normally targeted for inhibition by OP compounds, namely AChE, BChE, carboxylesterase, and acylpeptide hydrolase were only slightly inhibited. This level of inhibition does not explain the observed toxicity. These results lead to the conclusion that the toxicity of FP-biotin is due to interaction with other unidentified proteins, and is not due to inhibition of AChE, BChE, carboxylesterase or acylpeptide hydrolase.

**Proteins labeled with FP-biotin in AChE *-/-* mice.** Proteins were separated on SDS polyacrylamide gels and transferred to PVDF membrane. Biotinylated proteins were visualized by hybridization with Streptavidin-Alexafluor.

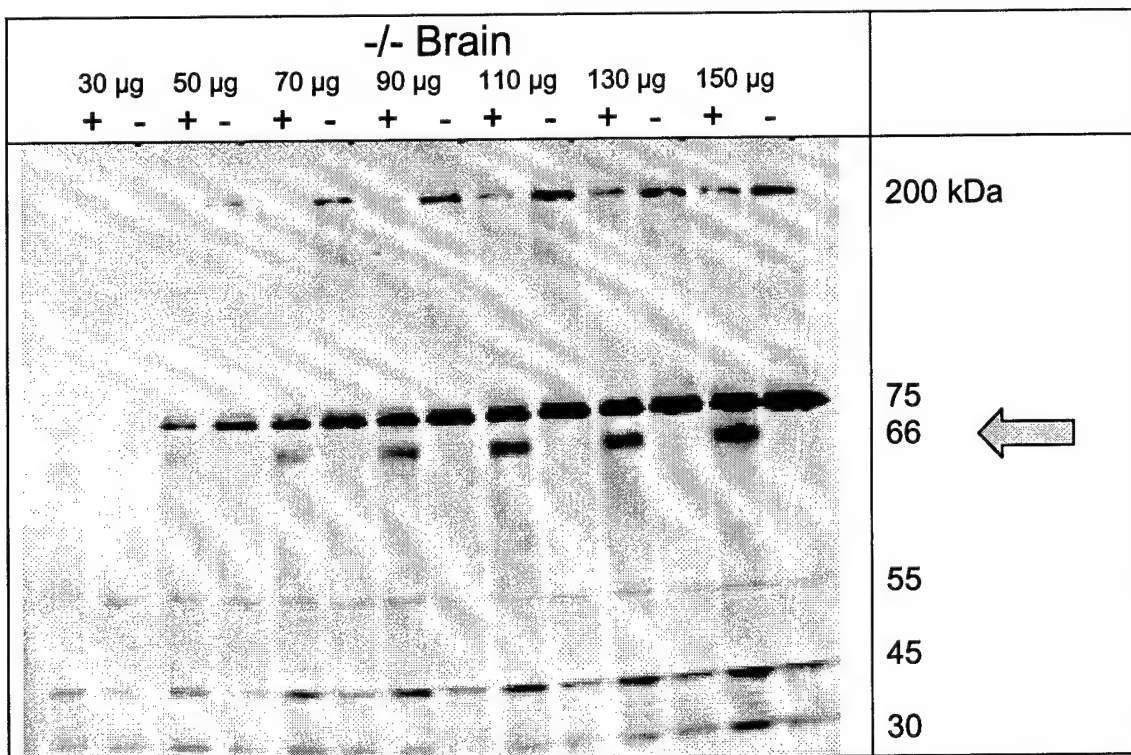


**Figure 6.1. FP-biotin 5 mg/kg injected i.p. into an AChE *-/-* mouse crossed the blood-brain barrier and labeled a 66 kDa protein in mouse brain.**  
Alternating lanes contain brain extract from mice treated with 5 mg/kg FP-biotin i.p. (+) and from untreated (-) AChE *-/-* mice. 30 to 150 µg of protein were loaded per lane.

**Brain of AChE *-/-* mouse.** Figure 6.1 shows the biotinylated proteins in brains of AChE *-/-* mice. Five bands represent endogenous biotinylated proteins found in untreated as well as FP-biotin treated mouse brain. The molecular weights of the endogenous biotinylated proteins are 200, 75, 55, 45, and 30 kDa. A novel band is present in brain of FP-biotin treated mouse, but not in untreated mouse. This novel band has a molecular weight of 66 kDa. It is noteworthy that this 66 kDa protein was labeled *in vivo* by a dose of FP-biotin that was toxic but not lethal to AChE *-/-* mice. The results in Figure 6.1 demonstrate that FP-biotin crosses the blood-brain barrier.

**Muscle of AChE *-/-* mouse.** Figure 6.2 shows the biotinylated proteins in quadriceps muscle of AChE *-/-* mice. Four endogenous biotinylated proteins have molecular weights of 200, 75, 45, and 30 kDa. An intense biotinylated protein band of 66 kDa and a weak 58 kDa band are present only in FP-biotin treated mouse, and not in untreated AChE *-/-* mouse.

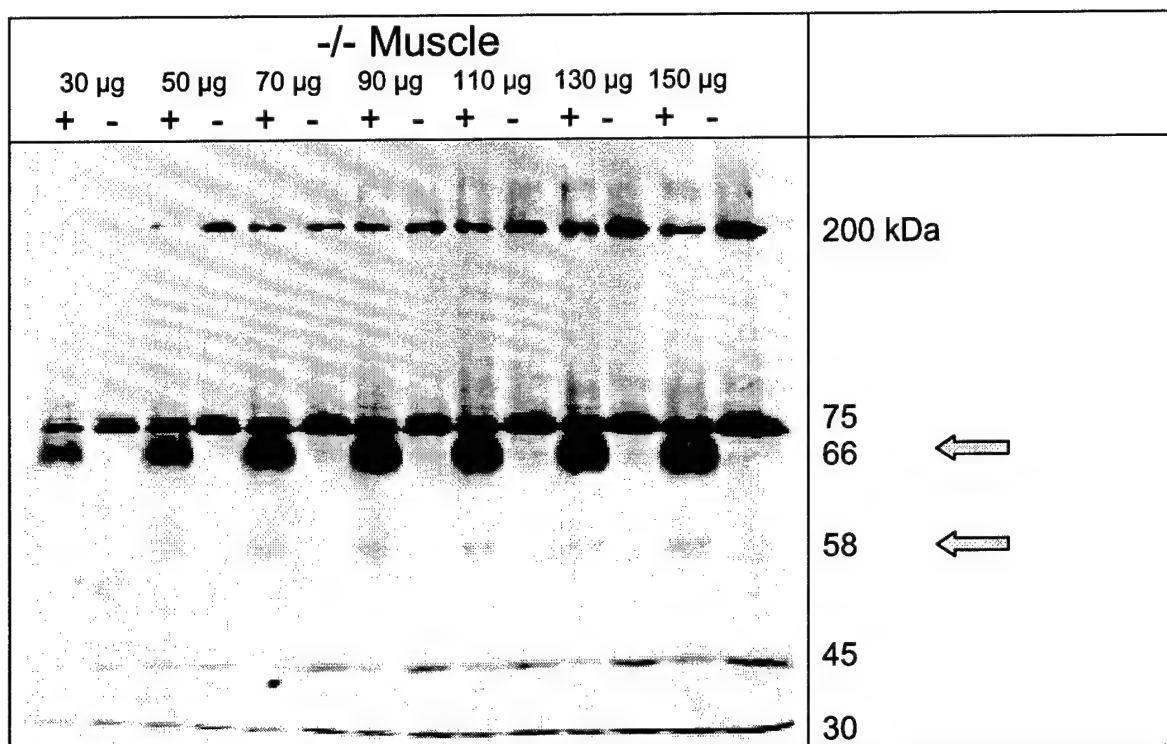


**Figure 6.2. FP-biotin 5 mg/kg injected i.p. into an AChE -/- mouse labels 66 kDa and 58 kDa proteins in quadriceps muscle.** The + and - signs at the top of each lane indicate tissue from FP-biotin treated and untreated mice respectively. Increasing amounts of protein, from 30 to 150 µg, were loaded per lane.

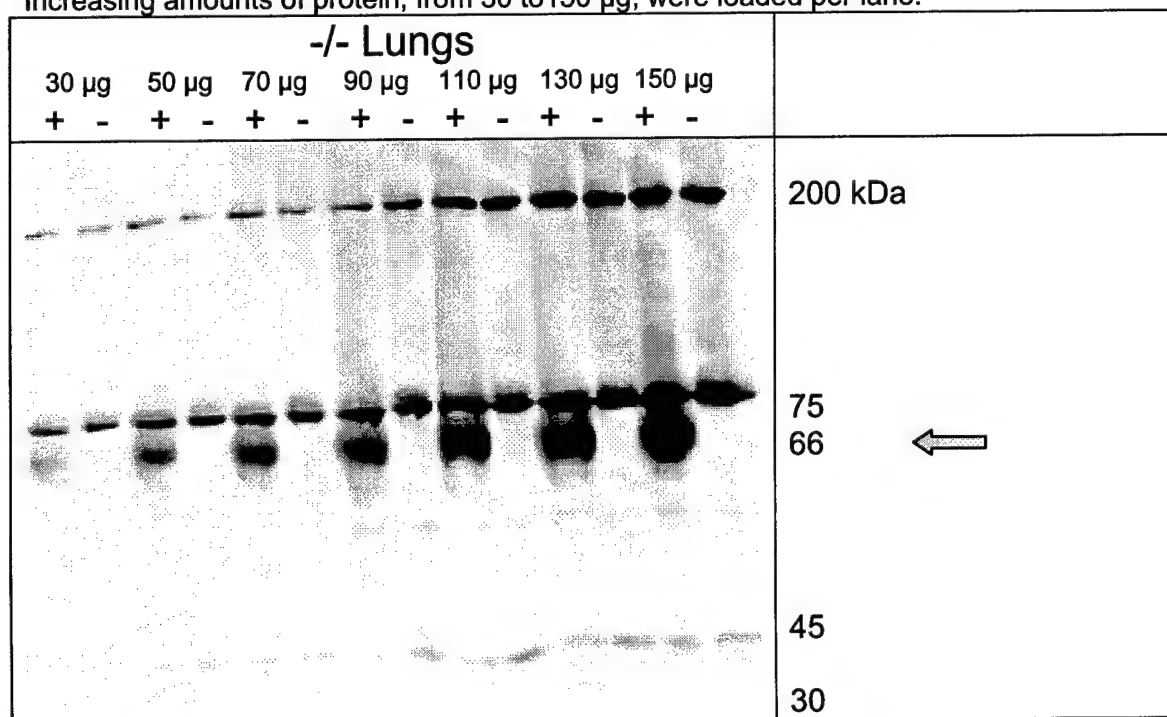


**Figure 6.3. FP-biotin 5 mg/kg injected i.p. into an AChE -/- mouse labels a 66 kDa protein in the lungs.** Lanes marked with a plus sign (+) contain protein from

FP-biotin treated mouse, while lanes marked with a minus (-) sign are from untreated mouse.

Lungs of AChE  $-/-$  mouse. Figure 6.3 shows the biotinylated proteins in the lungs of AChE  $-/-$  mice. Four endogenous biotinylated proteins have molecular weights of 200, 75, 45, and 30 kDa. An intense biotinylated protein band of 66 kDa is present only in FP-biotin treated mouse, and not in untreated AChE  $-/-$  mouse.

Liver of AChE  $-/-$  mouse. Figure 6.4 shows 20 endogenous biotinylated proteins in mouse liver in lanes from an untreated mouse. These range in size from about 10 to 200 kDa. Two weak bands are present in FP-biotin treated but not in untreated mice. A 66 kDa band is visible in lanes loaded with 40 and 60  $\mu$ g protein but is difficult to see in lanes that were loaded with larger amounts of protein. A weak band at 58 kDa is present in FP-biotin treated but not in untreated mice.

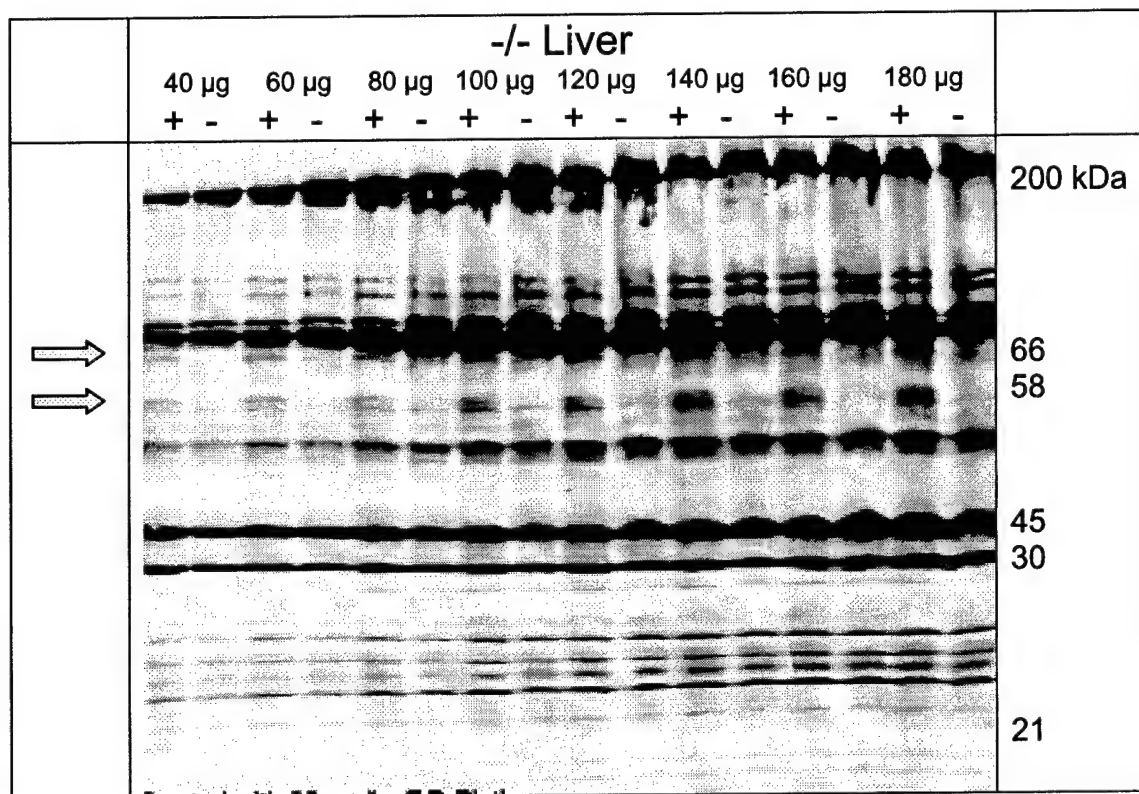


**Figure 6.4. FP-biotin injected into an AChE  $-/-$  mouse labels two proteins in the liver.** The proteins that reacted with FP-biotin are 66 and 58 kDa in size.

The above results show that a 66 kDa protein in brain, muscle, lungs, and liver was selectively labeled when a living AChE  $-/-$  mouse was treated

intraperitoneally with 5 mg/kg FP-biotin. A second protein of 58 kDa was labeled in muscle and liver.

**Proteins labeled with FP-biotin in wild-type mice.** The next question we asked was whether these same proteins reacted with FP-biotin in a wild-type mouse. Figure 6.5 shows the biotinylated proteins in the brain of a wild-type mouse treated i.p. with 5 mg/kg or 75 mg/kg FP-biotin. A weak band at 66 kDa was visible in the mouse treated with 75 mg/kg but not at the lower dose. This same 66 kDa band was seen in the AChE  $^{-/-}$  mouse brain when the mouse was treated with 5 mg/kg of FP-biotin (Figure 6.1). The band was more intense in the AChE  $^{-/-}$  mouse brain. This shows that it is easier to find OP-reactive proteins in the AChE $^{-/-}$  mouse than in the wild-type mouse.

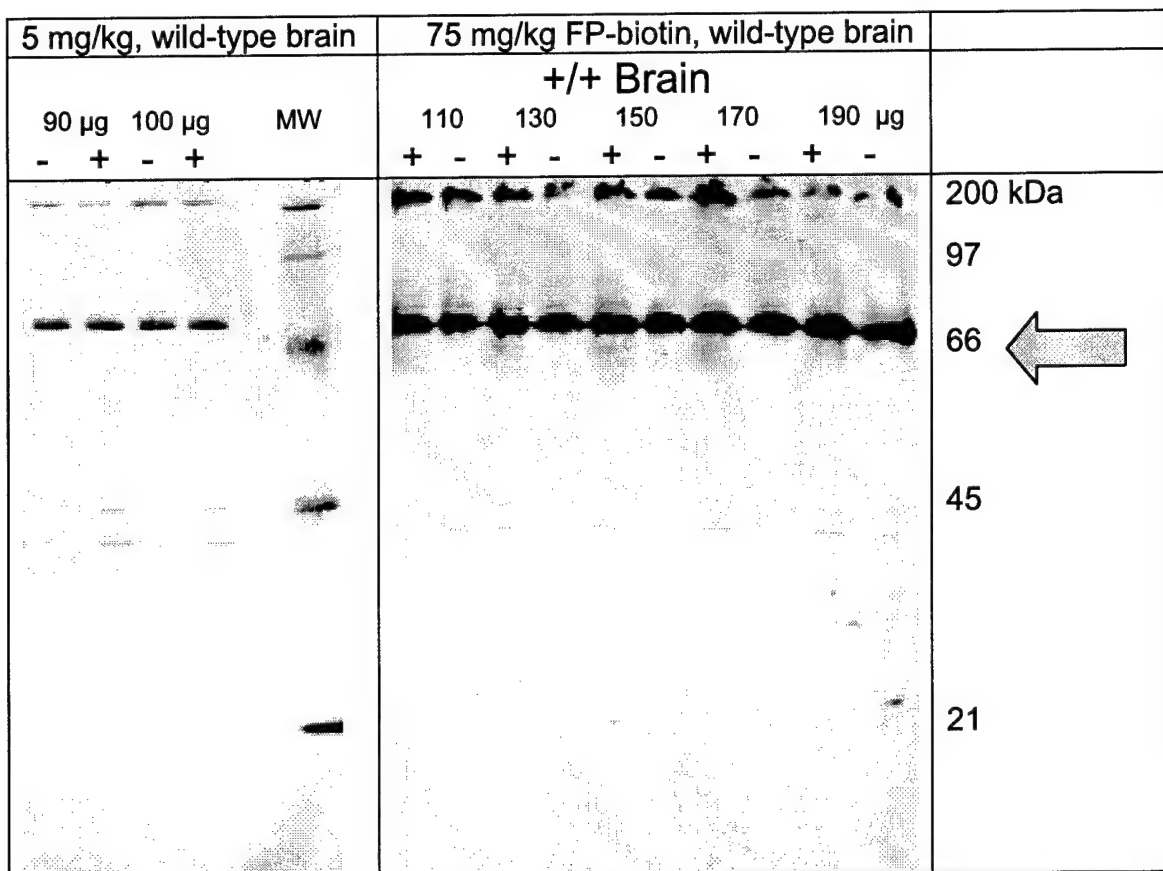


**Figure 6.5. FP-biotin injected into AChE +/+ mouse labels a 66 kDa protein in brain.** The dose of FP-biotin was 5 mg/kg i.p. in the left panel and 75 mg/kg in the right panel.

Muscle from wild-type mouse treated with 75 mg/kg FP-biotin i.p. showed two FP-biotinylated bands at 66 and 58 kDa, similar to the bands in Fig. 6.2 for AChE  $^{-/-}$  mouse. At 5 mg/kg, bands were not visible in wild-type muscle.

**Reaction kinetics of purified human AChE with FP-biotin.** The reactivity of FP-biotin with purified human AChE (wild-type AChE expressed in CHO cells) and purified human BChE (wild-type purified from human plasma) was measured for the purpose of having reference values for reaction rates.

Inhibition of human AChE by FP-biotin was first-order for at least 90% of the reaction (Figure 6.6, inset). A plot of the apparent first-order rate constant for inhibition versus the concentration of FP-biotin was linear from 0.025 to 0.25  $\mu\text{M}$  FP-biotin (Figure 6.6). The apparent second-order rate constant for the reaction of human AChE with FP-biotin was  $3.0 \times 10^6 \pm 3.9 \times 10^4 \text{ M}^{-1}\text{min}^{-1}$ .

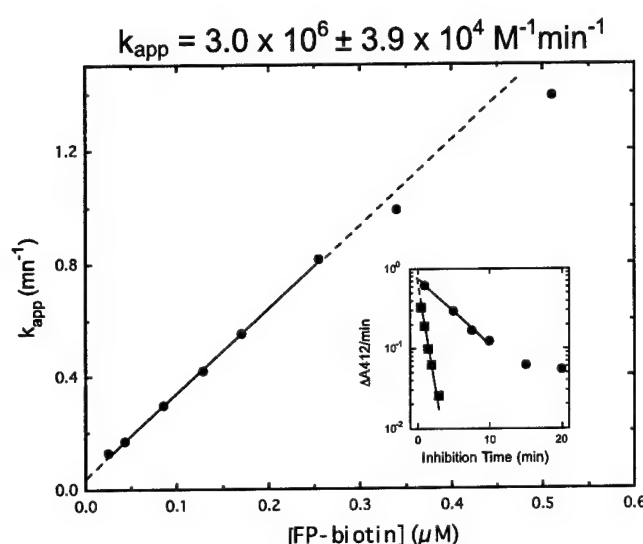


**Figure 6.6. Rate constant for inhibition of human AChE by FP-biotin.**  $k_{\text{app}}$  is the apparent first-order rate constant for the inhibition of AChE by FP-biotin. Points are the data; the solid line is from a linear fit, and the dashed line is an extrapolation of the fitted line.

Inset: Inhibition of AChE by 0.043  $\mu\text{M}$  FP-biotin (circles) and 0.34  $\mu\text{M}$  FP-biotin (squares). Solid lines are from fits to a first-order process. Data were fit using SigmaPlot.

Extrapolation of the second-order line to zero FP-biotin revealed a small non-zero Y-axis intercept, which is consistent with a minor, spontaneous loss of AChE activity due to the absence of BSA. For FP-biotin concentrations greater than 0.3  $\mu\text{M}$ , the apparent first-order rate constants fell below the extrapolated second-order line, suggesting the onset of saturation, and the existence of a non-covalent complex between FP-biotin and AChE. Data were insufficient to estimate the dissociation constant for the non-covalent complex.

**Reaction kinetics of purified human BChE with FP-biotin.** Loss of BChE activity was first-order for at least 90% of the reaction, at all concentrations of FP-biotin except for the very lowest (4.3 nM). See Figure 6.7 inset.

A plot of the apparent first-order rate constant for the loss of BChE activity versus FP-biotin concentration was linear from 8.5 to 34 nM FP-biotin (Figure 6.7). The apparent second-order rate constant for the reaction of human BChE with FP-biotin was  $2.8 \times 10^7 \pm 3.0 \times 10^5 \text{ M}^{-1}\text{min}^{-1}$ .

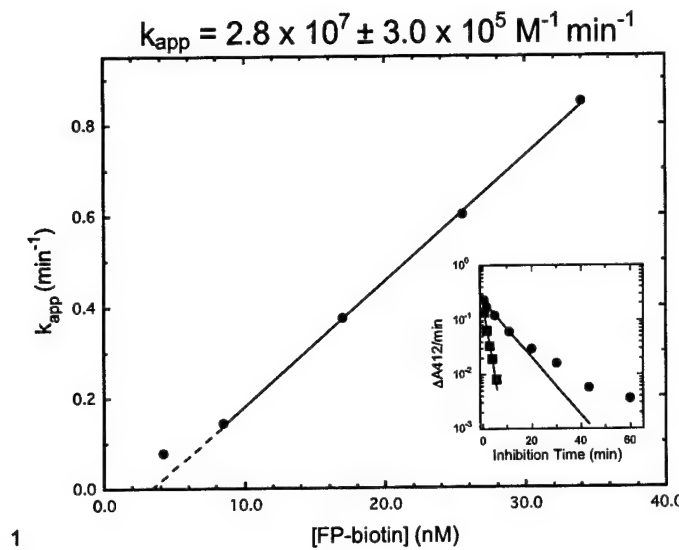


**Figure 6.7.** Inhibition of BChE by FP-biotin.  $k_{app}$  is the apparent first-order rate constant for the inhibition of human BChE by FP-biotin. Points are the data; the solid line is from a linear fit; the dashed line is an extrapolation of the fitted line.

Inset: The inhibition of BChE by 4.3 nM FP-biotin (circles) and 34 nM FP-biotin (squares). Solid lines are from fits to a first-order process. Data were fit using SigmaPlot.

Extrapolation of the second-order line to a rate constant of zero gave a non-zero X-axis intercept of 3.5 nM. This non-zero X-axis intercept suggests that the reactions are not in the pseudo-first order range, despite the fact that the concentration of BChE in the reaction was 0.35 nM and the minimum concentration of FP-biotin was 4.3 nM. This in turn suggests that BChE was reacting with a minor component of the FP-biotin preparation. The X-axis intercept should yield the concentration of the fixed member of the reaction (BChE in this case). In order to make this so, the concentration of the reactive species in the FP-biotin preparation must have been 10% of the total FP-biotin concentration. A sub-stoichiometric titration of BChE with FP-biotin confirmed this prediction.

The sub-stoichiometric titration of BChE was performed by incubating FP-biotin (0.34 to 4.93 nM) with 0.42 nM BChE, until inhibition had reached its maximum extent, that is for 4 hours. Preliminary experiments indicated that 4 hours in 0.1 M potassium phosphate buffer, pH 7.0 at 25°C was sufficient incubation time to allow the inhibition reaction to come to completion. Then 0.5 mM DTNB and 1 mM butyrylthiobacoline were added to the incubation mixture to determine the amount of active BChE remaining. A plot of {residual activity} versus {FP-biotin concentration} was linear to 93% inhibition, indicating stoichiometric inhibition of BChE (Figure 6.7). However, 2.7 nM FP-biotin was required to fully inhibit the 0.42 nM BChE, indicating that only 15% of the FP-biotin stock solution was involved in the inhibition.

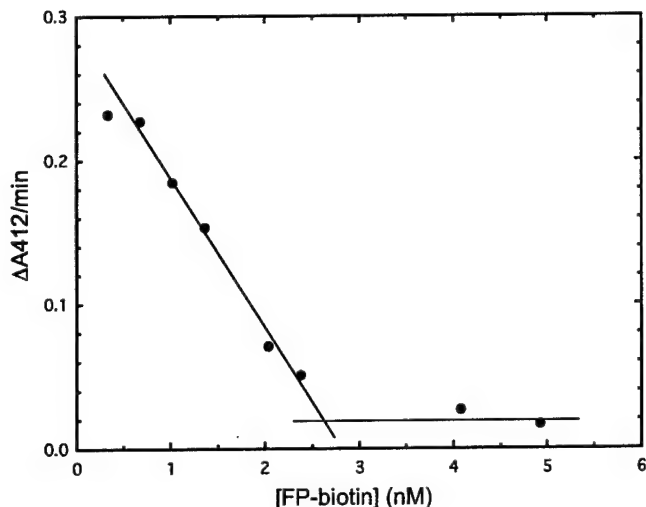


**Figure 6.8. Substoichiometric titration of BChE with FP-biotin.**  
Points are the data; lines were drawn by hand to assist in determining trends.

Though the FP-biotin appeared to be pure, a 10-15% contamination may have been undetected. To test whether intact FP-biotin was responsible for the inhibition of BChE, the inhibited BChE was checked for the presence of covalently attached biotin. It was reasoned that a contaminant in the FP-biotin preparation either would be missing the biotin moiety or would be incapable of forming a covalent adduct with BChE. 2.4 pmoles of FP-biotin-inhibited-BChE were applied to an SDS polyacrylamide gel, electrophoresed and then transferred to PVDF membrane. To measure the biotin, the membrane was treated with an avidin-horseradish peroxidase conjugate (BioRad), and then with a chemiluminescence reagent (LumiGLO from Kirkegaard & Perry). Emitted light was detected using x-ray film. The light intensity, which is directly proportional to the biotin level, was quantitated densitometrically using the Kodak EDAS 120 image analysis system and Kodak 1D software. Intensity was compared to a standard curve prepared by reacting a standardized portion of trypsin (Sigma) with FP-biotin and running various sized aliquots of this reaction mixture on the same SDS gel as the inhibited BChE. The biotin signal for BChE was equivalent to 2.0 pmoles (Figure 6.9), indicating that about 83% of the inhibited BChE carried a biotin.

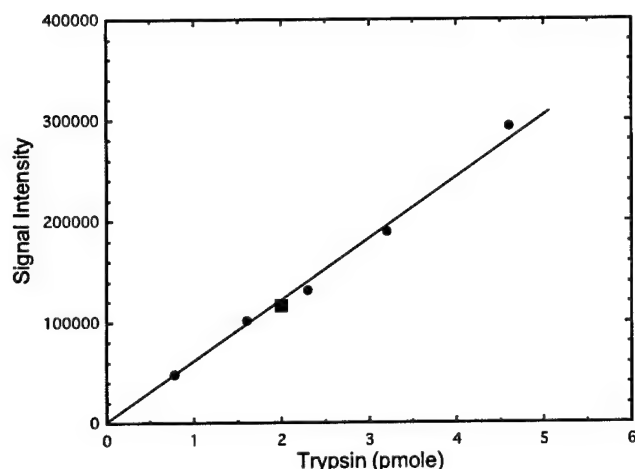


**Figure 6.9. Quantitation of biotin covalently attached to BChE.** The circles are the trypsin standards; the square is the BChE intensity reading. The line was drawn by hand.

Since the gel was run in SDS, the biotin must be covalently attached to the BChE. Therefore, inhibition of BChE does not appear to be due to a contaminant. An alternate explanation stems from the fact that FP-biotin is potentially a racemic mixture of phosphate stereoisomers (see the FP-biotin structure). Stereoselective inhibition by organophosphate stereoisomers has been reported for BChE (Millard et al., 1998; Doorn et al., 2001). If BChE reacts preferentially with a minor (10%) stereoisomeric form of FP-biotin, the observed kinetics could be rationalized. In that case, the second-order rate constant for the reaction of human BChE with FP-biotin would be  $2 \times 10^8 \text{ M}^{-1}\text{min}^{-1}$ .

## Discussion

**What is the mechanism of acute FP-biotin toxicity?** AChE  $-/-$  mice treated with 75 mg/kg FP-biotin were so severely impaired that the observer expected this dose to be lethal. However, the mice recovered significantly within 15 minutes. Recovery was not complete within 15 minutes, and some signs of toxicity were still present after 2 hours, but the posture, movement, and salivation dramatically decreased within 15 minutes. The rapid recovery is consistent with the finding that there was little inhibition of BChE. Inhibition of BChE might have explained the profuse salivation and other cholinergic signs of toxicity, but the near absence of BChE inhibition forces us to look elsewhere for an explanation.

The rapid recovery from toxicity means the FP-biotin is acting reversibly. We hypothesize that FP-biotin binds noncovalently to acetylcholine receptors to activate them, causing a response similar to excess acetylcholine. The rapid recovery indicates that the FP-biotin is rapidly removed from this binding site.

The involvement of muscarinic acetylcholine receptors in the toxicity of organophosphorus compounds has been suggested by others. Ward et al. (1993) measured the ability of anticholinesterase OP compounds to compete for binding of a high affinity agonist (cis-methyldioxolane,  $K_D = 3.5$  nM) to M2 muscarinic receptor. They found that echothiophate, DFP, and the oxon forms of parathion, malathion, and disulfoton were potent inhibitors of binding. Echothiophate concentrations as low as  $4 \times 10^{-9}$  M inhibited binding of the agonist. OP binding to this high-affinity binding site was reversible. They concluded that the biological effects of OP are due not just to their ability to inhibit AChE but also to OP binding to muscarinic receptors.

Binding of OP to muscarinic receptors has also been demonstrated by Silveira et al. (1990), Jett et al. (1991), Huff et al. (1994), and Bomser and Casida (2001). These studies used membrane preparations rather than living animals. Toxicity studies in wild-type mice have not been able to clearly demonstrate binding of OP to muscarinic receptors because of competition by binding to AChE. The absence of AChE in the AChE  $^{-/-}$  mouse makes the AChE  $^{-/-}$  mouse a better model to test the role of muscarinic receptors in OP toxicity.

In our study of the toxicity of VX (Duysen et al., 2001) we reported that VX treated AChE  $^{-/-}$  mice had the same cholinergic signs of toxicity as VX treated wild-type mice. In the VX experiments it was possible that the cholinergic signs of toxicity in AChE  $^{-/-}$  mice were due to inhibition of BChE because BChE in the brain and other tissues was inhibited 50%. In contrast, the present results with FP-biotin cannot invoke inhibition of BChE as a cause of cholinergic signs of toxicity in AChE  $^{-/-}$  mice. Instead, the present study supports the conclusion that organophosphorus agents bind to muscarinic receptors and that this binding accounts for some of the acute toxic effects of OP.

**What is the mechanism of nonacute FP-biotin toxicity?** AChE  $^{-/-}$  animals had signs of toxicity, including hunched posture and drop in body temperature, long after the acute signs had disappeared. A search of proteins irreversibly alkylated by FP-biotin revealed a protein with a molecular weight of 66 kDa. This protein was biotinylated in brain, muscle, and lung of FP-biotin treated AChE  $^{-/-}$  mice, but not in FP-biotin treated wild-type mice. It is possible that derivatization of this protein by FP-biotin accounts for long-term toxicity.

We plan to identify this protein by mass spectroscopy. Identification of this protein could be important because this protein could be a biomarker of OP toxicity.

**Test tube experiments did not predict live animal results.** Studies of the reaction of purified BChE with FP-biotin showed a very fast reaction rate even with low concentrations of FP-biotin. These test tube results led to the expectation that animals treated with FP-biotin would show high levels of BChE inhibition. However, significant BChE inhibition was not found in animals. Furthermore, no FP-biotin labeled BChE band was seen on blots. The OP-reactive proteins labeled with FP-biotin are expected to have a higher binding affinity than AChE and BChE for FP-biotin, and to account for low dose toxicity.

## Response to Reviewer's comments on the 2002 annual review

**Comment 2.** "In Task 5, the proposal required testing rate constants for reaction of the probe with the target proteins essentially following the method of Richard et. al. (1999). The research group decided that this approach would be too tedious and thus decided to evaluate alternative approaches, i.e., competitive reaction and IC<sub>50</sub> approaches. While the original approach may indeed be laborious and time-consuming, it should have been conducted as it was evaluated in the original proposal. At the least, a comparison between the original and the second choice, the IC<sub>50</sub> approach, should take place to determine if it might be worthwhile to pursue the original approach."

At the time this proposal was written, the determination of rate constants for the reaction of OP with proteins from mouse tissue fractions was an appealing objective. However, experience with the Western blotting technique has shown that reliable quantitation is not easily obtained, especially from weak bands. This combined with the fact that most of the proteins of interest appear in overlapping clusters, which further complicates the quantitation, makes it unlikely that determination of rate constants would be productive. It is our opinion that time would be better spent on other objectives.

**Comment 5.** "The second and related weakness is the focus on the nervous system. It is not clear whether other tissues also contain targets to OP. It may be worth considering non-neural tissues in the broad search for proteins that are phosphorylated by OPs."

The possibility that OP targets may exist in non-neural tissues is an interesting prospect. We initiated our screening with brain because that seemed the most probable place to find interesting alternate targets. However, as shown in our 2003 report for Task 6, we have begun looking at other tissues as well.

**Comment 6.** "Finally, it is not clear how the results of the binding studies will inform us about the toxicity of 10-(fluroethoxyphosphinyl)-N-(biotinamidopentyl) decanamide (FP-biotin), much less of other OPs. First, FP-biotin is a specific OP, and its binding (and toxicity) may not reflect the activity of other OPs. Second, binding does not necessarily indicate toxic action (e.g., inhibition of an enzyme). A protein that binds to FP-biotin may or may not be important in the toxic response. It will not be easy to sort this out, and it would be helpful for the PI to discuss how these elegant studies will yield causal relationships between the binding of an OP to a protein and its toxic action."

We agree that the connection between an OP binding to an enzyme and a role for that enzyme in the toxic response to that OP is not an easy issue to sort out. However, the main purpose of the current study is to identify candidate

targets which react with OP as well as or better than AChE does. Binding of OP to these candidates might cause toxic response, but that possibility must be addressed by studying each candidate individually. We plan to do in vivo studies in live mice to determine whether inhibition of a particular set of enzymes is related to toxicity. The AChE -/- mouse is particularly useful for identifying proteins involved in OP toxicity, as demonstrated in our 2003 report for Task 6.

Regarding the binding and toxicity of FP-biotin itself, the reviewer is correct; it is a highly specialized OP, which may not reflect the reactivity of other OPs. We do not intend to argue that proteins which react with FP-biotin are important in the toxic response to OP insecticides. The primary purpose of FP-biotin in this study is to provide a means by which the reaction of other OP can be studied. We use the loss of FP-biotin reaction in the presence of another OP as an indication of reaction by that other OP. An inherent limitation with this approach is that FP-biotin is expected to react with a select subset of OP-reactive proteins. Proteins which react readily with FP-biotin may react poorly with other OP, and vice versa. On the chance that important, alternate-target proteins may react poorly with FP-biotin, the reaction time with FP-biotin has been extended so that all observable proteins are completely reacted. In addition, we have tried to monitor even very weak FP-biotin signals, on the chance that interesting targets are present at low levels. The overall goal is to use FP-biotin to visualize as many OP-reactive proteins as possible. This effort to monitor as many OP-reactive proteins as possible has greatly complicated the quantitation of the reactions, but the increased breath of the screen justifies the decreased accuracy of the quantitation.

Finally, the reviewer argues that binding of an OP to a protein does not necessarily indicate toxic action, an example of which is given as inhibition of an enzyme. We agree with this in general. For example, by extending the breath of our study to as many FP-biotin reactive proteins as possible, we have identified a variety of FP-biotin reactive proteins which are not hydrolases (i.e. heat shock proteins, dehydrogenases, tubulin, and peroxiredoxin). For some of these proteins, it is likely that reaction with FP-biotin does not cause inhibition of the enzyme activity. However, none of these proteins are particularly reactive toward the insecticidal OP in our test set, and are therefore of little interest. The proteins which do react well with the insecticidal OP are all hydrolases. Hydrolases would be expected to react with OP at the active site, thereby fully inhibiting enzyme activity. In that sense, OP binding to hydrolases would fit the reviewers example of a reaction which leads to a toxic action. However it is unclear whether inhibition of these hydrolase enzymes would lead to physiological signs of toxicity. There is no direct, causal relationship between OP inhibition of an enzyme and the toxic action of that OP at the physiological level. But, in order for a protein to be important in a toxicological sense, it must be capable of reacting with low levels of the toxin. The overall goal of the current studies is to identify proteins which react with OP toxicants at a low level, i.e. at a level lower than that at which the OP reacts with AChE, the traditional toxicologically important target for OP. Thus, the screening is merely the first step in identifying new, toxicologically significant OP targets.

**Key Research Accomplishments**

- A method to label, visualize, and isolate OP-reactive proteins was established.
- Mass spectral analysis identified 26 OP-reactive proteins in mouse brain soluble fraction.
- Chlorpyrifos oxon, dichlorvos, diazoxon, and malaoxon were found to react with incompletely overlapping sets of proteins. Each OP reacted with a unique set of 1-7 proteins, in test tube experiments.
- Platelet activating factor acetylhydrolase reacted with dichlorvos faster than AChE reacted with dichlorvos. This means platelet activating factor acetylhydrolase is a good candidate for a new biomarker of OP exposure
- Two additional candidates for biomarkers of low dose OP exposure are fatty acid amide hydrolase and acylpeptide hydrolase.
- Toxicity testing with FP-biotin in mice revealed 1 or 2 labeled proteins depending on the tissue.
- Evidence was obtained that FP-biotin acts directly on muscarinic receptors to give cholinergic signs of toxicity in living mice. The literature has examples of OP binding to muscarinic receptors in membrane preparations. This is the first study in living mice to support the idea that OP bind directly to acetylcholine receptors where they act as agonists.

**Reportable Outcomes**Published manuscripts

Lockridge O, Duysen EG, Li B (2003) Butyrylcholinesterase function in the acetylcholinesterase knockout mouse. Chapter 2 in "Butyrylcholinesterase Its Function and Inhibitors". (Editor, Ezio Giacobini). Martin Dunitz, London, pp 21-28

Haux JE, Lockridge O, Casida JE (2002) Specificity of ethephon as a butyrylcholinesterase inhibitor and phosphorylating agent. *Chem Res Toxicol* 15: 1527-1533

Duysen EG, Fry DL, Lockridge O (2002) Early weaning and culling eradicated *Helicobacter hepaticus* from an acetylcholinesterase knockout 129S6/SvEvTac mouse colony. *Comparative Medicine* 52: 461-466

Submitted manuscript

Lockridge O, Duysen EG, Voelker T, Thompson CM, Schopfer LM (2003) Life without acetylcholinesterase: the implications of cholinesterase inhibitor toxicity in AChE-knockout mice. Submitted to *Environmental Toxicology and Pharmacology* June 22, 2003.

**Conclusions**

- Each OP is unique in terms of the set of proteins with which it reacts. This supports the findings of toxicologists that each OP causes a unique set of toxic symptoms when the dose of OP is low.
- Acetylcholinesterase and butyrylcholinesterase are not significantly inhibited by low doses of OP. Other proteins are the targets of OP

- reactivity. These other proteins may include platelet activating factor acetylhydrolase, fatty acid amide hydrolase, and acylpeptide hydrolase.
- The acetylcholinesterase knockout mouse is useful for identifying new biomarkers of OP exposure because lack of competition from acetylcholinesterase allows greater reactivity of OP with alternative OP-reactive proteins.

### Literature Cited

Amitai G, Moorad D, Adani R, Doctor BP (1998) Inhibition of acetylcholinesterase and butyrylcholinesterase by chlorpyrifos-oxon, *Biochem Pharmacol* 56: 293-299

Black RM, Harrison JM, Read RW (1999) The interaction of sarin and soman with plasma proteins: the identification of a novel phosphorylation site. *Arch Toxicol* 73: 123-126

Bomser JA, Casida JE (2001) Diethylphosphorylation of rat cardiac M2 muscarinic receptor by chlorpyrifos oxon in vitro. *Toxicol Lett* 119: 21-26

Carrington CD, Abou-Donia MB (1985) Characterization of [<sup>3</sup>H]di-isopropyl phosphorofluoridate-binding proteins in hen brain. *Biochem J* 228: 537-544

Chaiken IM, Smith EL (1969) Reaction of a specific tyrosine residue of papain with diisopropylfluorophosphate. *J Biol Chem* 244: 4247-4250

Derewenda ZS, Derewenda U (1991) Relationships among serine hydrolases: evidence for a common structural motif in triacylglyceride lipases and esterases. *Biochemistry Cell Biol* 69: 842-851

Doorn JA, Schall M, Gage DA, Talley TT, Thompson CM, Richardson RJ (2001) Identification of butyrylcholinesterase adducts after inhibition with isomalathion using mass spectrometry: difference in mechanism between (1R)- and (1S)- stereoisomers. *Toxicol Appl Pharmacol* 176: 73-80

Duysen EG, Li B, Xie W, Schopfer LM, Anderson RS, Broomfield CA, Lockridge O (2001) Evidence for nonacetylcholinesterase targets of organophosphorus nerve agent: supersensitivity of acetylcholinesterase knockout mouse to VX lethality. *J Pharmacol Exp Ther* 299: 528-535

Duysen EG, Stribley JA, Fry DL, Hinrichs SH, Lockridge O (2002) Rescue of the acetylcholinesterase knockout mouse by feeding a liquid diet;phenotype of the adult acetylcholinesterase deficient mouse. *Dev Brain Res* 137: 43-54

Ellman GL, Courtney KD, Andres V, Featherstone RM (1961) A new and rapid colorimetric determination of acetylcholinesterase activity. *Biochem Pharmacol* 7: 88-95

Gray EG, Whittaker VP (1962) The isolation of nerve endings from brain: An electron-microscopic study of cell fragments derived by homogenization and centrifugation, *J Anat* 96: 79-88

Ho YS, Swenson L, Derewenda U, Serre L, Wei Y, Dauter Z, Hattori M, Adachi T, Aoki J, Arai H, Inoue K, Derewenda ZS (1997) Brain acetylhydrolase that inactivates platelet-activating factor is a G-protein-like trimer. *Nature* 385: 89-93

Huff RA, Corcoran JJ, Anderson JK, Abou-Donia MB (1994) Chlorpyrifos oxon binds directly to muscarinic receptors and inhibits cAMP accumulation in rat striatum. *J Pharmacol Exp Ther* 269: 329-335

Jett DA, Abdallah EAM, El-Fakahany EE, Eldefrawi, ME, Eldefrawi AT (1991) High-affinity activation by paraoxon of a muscarinic receptor subtype in rat brain striatum. *Pest Biochem Physiol* 39: 149-157

Johnson JA, Wallace KB (1987) Species-related differences in the inhibition of brain acetylcholinesterase by paraoxon and malaoxon, *Tox Appl Pharmacol* 88: 234-241

Keshavarz-Shokri A, Suntornwat O, Kitos PA (1999) Identification of serine esterases in tissue homogenates. *Anal Biochem* 267: 406-411.

Kidd D, Liu Y, Cravatt BF (2001) Profiling serine hydrolase Activities in complex proteomes, *Biochemistry* 40: 4005-4015

Korza G, Ozols J (1988) Complete covalent structure of 60-kDa esterase isolated from 2,3,7,8-tetrachlorodibenzo-p-dioxin-induced rabbit liver microsomes. *J Biol Chem* 263: 3486-3495

Li B, Stribley JA, Tici A, Xie W, Schopfer LM, Hammond P, Brimijoin S, Hinrichs SH, Lockridge O (2000) Abundant tissue butyrylcholinesterase and its possible function in the acetylcholinesterase knockout mouse, *J. Neurochem.* 75: 1320-1331

McDaniel KL, Moser VC (1993) Utility of neurobehavioral screening battery for differentiating the effects of two pyrethroids, permethrin and cypermethrin. *Neurotoxicol Teratol* 15: 71-83

Main AR (1979) Mode of action of anticholinesterases. *Pharmac Ther* 6:579-628

Millard CB, Lockridge O, Broomfield CA (1998) Organophosphorus acid anhydride hydrolase activity in human butyrylcholinesterase: synergy results in a somanase. *Biochemistry* 37: 237-247

Moser VC (1995) Comparisons of the acute effects of cholinesterase inhibitors using a neurobehavioral screening battery in rats. *Neurotoxicol Teratol* 17: 617-625

Quistad GB, Sparks SE, Casida JE(2001)Fatty acid amide hydrolase inhibition by neurotoxic organophosphorous pesticides, *Tox Appl Pharmacol* 173: 48-55

Quistad GB, Sparks SE, Segall Y, Nomura DK, Casida JE (2002) Selective inhibitors of fatty acid amide hydrolase relative to neuropathy target esterase and acetylcholinesterase: toxicological implications, *Tox Appl Pharmacol* 179: 57-63

Richards PG, Johnson MK, Ray DE (2000) Identification of acylpeptide hydrolase as a sensitive site for reaction with organophosphorous compounds and a potential target for cognitive enhancing drugs, *Mol Pharmacol* 58: 577-583

Richards P, Lees J (2002) Functional proteomics using microchannel plate detectors. *Proteomics* 2: 256-261

Rodriguez OP, Muth GW, Berkman CE, Kim K, Thompson CM (1997) Inhibition of various cholinesterases with the enantiomers of malaoxon, *Bull Environ Contam Toxicol* 58: 171-176

Skrinjaric-Spoljar M, Simeon V, Reiner E (1973) Spontaneous reactivation and aging of dimethylphosphorylated acetylcholinesterase and cholinesterase. *Biochim Biophys Acta* 315: 363-369

Ward TR, Ferris DJ, Tilson HA, Mundy WR (1993) Correlation of the anticholinesterase activity of a series of organophosphates with their ability to compete with agonist binding to muscarinic receptors. *Toxicol Appl Pharmacol* 122: 300-307

Xie W, Sibley JA, Chatonnet A, Wilder PJ, Rizzino A, McComb RD, Taylor P, Hinrichs SH, Lockridge O (2000) Postnatal developmental delay and supersensitivity to organophosphate in gene-targeted mice lacking acetylcholinesterase. *J Pharmacol Exp Ther* 293: 896-293

### Appendices

Lockridge O, Duysen EG, Li B (2003) Butyrylcholinesterase function in the acetylcholinesterase knockout mouse. Chapter 2 in "Butyrylcholinesterase: Its Function and Inhibitors". (Ed, Ezio Giacobini). Martin Dunitz, London, pp21-28

Haux JE, Lockridge O, Casida JE (2002) Specificity of ethephon as a butyrylcholinesterase inhibitor and phosphorylating agent. *Chem Res Toxicol* 15: 1527-1533

Duysen EG, Fry DL, Lockridge O (2002) Early weaning and culling eradicated *Helicobacter hepaticus* from an acetylcholinesterase knockout 129S6/SvEvTac mouse colony. *Comparative Medicine* 52: 461-466

Lockridge O, Duysen EG, Voelker T, Thompson CM, Schopfer LM (2003) Life without acetylcholinesterase: the implications of cholinesterase inhibitor toxicity in AChE-knockout mice. Submitted to *Environmental Toxicology and Pharmacology* June 22, 2003

# BUTYRYLCHOLINESTERASE ITS FUNCTION AND INHIBITORS

*Ezio Giacobini MD PhD*

*Department of Geriatrics  
University of Geneva  
School of Medicine  
Geneva  
Switzerland*

*Editor*

© 2003 Martin Dunitz, an imprint of the Taylor & Francis Group plc

First published in the United Kingdom in 2003  
by Martin Dunitz, an imprint of the Taylor and Francis Group plc,  
11 New Fetter Lane,  
London EC4P 4EE

Tel.: +44 (0) 20 7583 9855  
Fax.: +44 (0) 20 7842 2298  
E-mail: [info@dunitz.co.uk](mailto:info@dunitz.co.uk)  
Website: <http://www.dunitz.co.uk>

All rights reserved. No part of this publication may be reproduced, stored in a retrieval system, or transmitted, in any form or by any means, electronic, mechanical, photocopying, recording, or otherwise, without the prior permission of the publisher or in accordance with the provisions of the Copyright, Designs and Patents Act 1988 or under the terms of any licence permitting limited copying issued by the Copyright Licensing Agency, 90 Tottenham Court Road, London W1P 0LP.

A CIP record for this book is available from the British Library.

ISBN 1 84184 209 5

Distributed in the USA by  
Fulfilment Center  
Taylor & Francis  
10650 Toebben Drive  
Independence, KY 41051, USA  
Toll Free Tel.: +1 800 634 7064  
E-mail: [taylorandfrancis@thomsonlearning.com](mailto:taylorandfrancis@thomsonlearning.com)

Distributed in Canada by  
Taylor & Francis  
74 Rolark Drive  
Scarborough, Ontario M1R 4G2, Canada  
Toll Free Tel.: +1 877 226 2237  
E-mail: [tal\\_fran@istar.ca](mailto:tal_fran@istar.ca)

Distributed in the rest of the world by  
Thomson Publishing Services  
Cheriton House  
North Way  
Andover, Hampshire SP10 5BE, UK  
Tel.: +44 (0)1264 332424  
E-mail: [salesorder.tandf@thomsonpublishingservices.co.uk](mailto:salesorder.tandf@thomsonpublishingservices.co.uk)

Composition by EXPO Holdings, Malaysia  
Printed and bound in Spain by Gratos SA, Arte Sobre Papel

## 2

### Butyrylcholinesterase function in the acetylcholinesterase knockout mouse

Oksana Lockridge, Ellen G Duysen and Bin Li

#### Introduction

All vertebrates have two distinct cholinesterases, acetylcholinesterase (AChE, EC 3.1.1.7) and butyrylcholinesterase (BuChE, EC 3.1.1.8). However, *Drosophila* flies and zebrafish have only AChE. The fact that mice can live to adulthood without AChE,<sup>1,2</sup> whereas insects and zebrafish cannot,<sup>3,4</sup> suggests that BuChE partly compensates for the loss of AChE. It is hypothesized that BuChE functions in nerve impulse transmission. This chapter summarizes the new view of BuChE function based on observations of the AChE knockout mouse.

#### Historical

When Mendel and Rudney first identified BuChE as an enzyme distinct from AChE, they named it pseudocholinesterase.<sup>5</sup> They were convinced that BuChE has no vital function. Dogs treated with cholinesterase inhibitor could lose 95% of their serum BuChE activity, yet show no toxic signs.<sup>6</sup> This view was reinforced by the finding that people with zero BuChE activity were healthy. About 2% of the Inuit population in Alaska, and 1 in 100,000 Caucasians have zero BuChE activity due to a genetic variant called 'silent' BuChE.<sup>7</sup> People with silent BuChE have no obvious health problems, though a detailed study has never been done.

#### AChE knockout mouse

The AChE knockout mouse was made by deleting 5 kb of the ACHE gene, making it impossible to produce any AChE protein.<sup>1</sup> All tissues in AChE<sup>-/-</sup> mice are completely deficient in AChE activity. Their BuChE activity is normal, and is not higher than in wild-type mice.<sup>8,9</sup> The genetic background of the knockout mice is strain 129Sv.

It was a surprise that AChE<sup>-/-</sup> mice were born alive, and that they could breathe and move. In our first report their average life span was 14 days.<sup>1</sup> Later we learned to keep them alive to adulthood by feeding them a liquid diet of Ensure (Abbott Laboratories, Abbott Park, IL).<sup>2</sup>

AChE<sup>-/-</sup> mice are not normal. They have a number of problems described below. Their phenotype suggests that, if BuChE is indeed responsible for the fact they are alive, BuChE is an inadequate substitute for AChE. The poor performance of BuChE can be attributed to location, low abundance in the brain, and slower rate of catalysis. BuChE is not in the right location for optimal function in nerve impulse transmission. BuChE is in glial cells, adjacent to rather than inside nerve synapses.<sup>9</sup> BuChE is highly abundant in most tissues, so that the total amount of BuChE in the mouse body is 10 times higher than the total AChE content.<sup>10</sup> However, the brain has low amounts of BuChE compared to AChE. The

affinity of BuChE for acetylcholine is the same as the affinity of AChE for acetylcholine,<sup>11</sup> though the catalytic activity of BuChE is about 4-fold lower.

### *Weak muscles*

AChE-/- mice have very weak muscles. Pups are incapable of sucking enough milk to sustain life. When the diet of the dams was enriched by feeding them 11% fat food pellets and liquid Ensure, the dam's milk acquired more nutritional value with the result that AChE-/- pups survived. AChE-/- pups are weaned on day 14 and fed liquid Ensure in a dish.<sup>2</sup> They do not eat solid food. They never bite the handler or each other.

Their weak muscles cause them to have an unusual posture of splayed feet, an abnormal gait with the abdomen and tail dragging on the ground, and absence of grip strength. They are less active than their littermates. Young AChE-/- mice run, climb, and take a bipedal stance to look over the edge of a barrier. After 1 year of age AChE-/- mice are inactive; they walk to their food dish, but they do not climb or run. Adult AChE-/- mice have a hunched back. Weak muscles can be explained by the absence of AChE in the neuromuscular junction. People with end-plate AChE deficiency, due to mutations in the collagen tail protein (COLQ) gene, have the same weak muscles and scoliosis as AChE-/- mice.<sup>12,13</sup>

BuChE activity is found in the neuromuscular junction as shown by colocalization of BuChE activity and nicotinic receptors in AChE-/- muscle.<sup>8</sup> Electrophysiological experiments show that AChE-/- muscle is capable of contracting and of functioning. However, twitch tension, rise, and decay times in response to a single supramaximal stimuli are abnormal.<sup>14</sup> Diaphragm muscles from AChE-/- mice maintain tension when repetitively stimulated at

70 and 100 Hz, but show tetanic fade at 20, 50, 200, and 400 Hz. Two mechanisms explain the ability of AChE-/- muscle to maintain tension: downregulation of nicotinic acetylcholine receptors and reliance on BuChE activity. A role for BuChE in acetylcholine hydrolysis was shown by exposing AChE-/- diaphragm muscle to the selective BuChE inhibitor (BuChEI) tetra-(monoisopropyl)-pyrophosphortetramide (iso-OMPA). Inhibition of BuChE induced tetanic fade at 70 and 100 Hz. It was concluded that BuChE hydrolysed acetylcholine in the muscle of AChE-/- mice.

Minic et al<sup>15</sup> measured release of quanta of acetylcholine from AChE-/- muscle and came to a different conclusion regarding BuChE function. They found that inhibition of BuChE decreased evoked-quantal transmitter release. They concluded that BuChE has a role in the release of acetylcholine quanta from presynaptic membranes and that BuChE is not involved in regulating the duration of acetylcholine action at the post-synaptic membrane.

### *Sexual dysfunction*

Male and female AChE-/- mice are housed together, from postnatal day 14 to the end of their lives. No AChE-/- mouse has become pregnant in 4 years (n = 700). No mating behavior has been noticed; there is no sniffing and no mounting. An explanation for this sexual dysfunction is not yet available. Males have normal levels of testosterone and females have normal levels of estradiol. The seminiferous tubules contain sperm, and evidence of estrous has been found in females.<sup>2</sup>

Another behavioral abnormality is the absence of competition between males. Unrelated sexually mature wild-type males cannot be housed together because they fight to death. In contrast, AChE-/- males display no aggression to other males.

### Eyes

AChE<sup>-/-</sup> mice have pinpoint pupils all their life, an observation consistent with the presence of excess acetylcholine. Other than the pinpoint pupils, the eyes of young mice look normal to visual inspection. However, by 1 year of age many AChE<sup>-/-</sup> mice have gross deformations in their eyes. In some mice the eyes bulge out, suggesting excessive pressure within the eye as in glaucoma. A vascular carpet covers the bulging eyes of some animals. Other mice have a different deformity; their eyes are resorbed. Mucus covers the sunken eyes, and a hairless ring of skin surrounds the eye.

The laboratory of Paul Layer has found degeneration of inner retina neural layers as early as postnatal day 60. By day 86, the photoreceptor layer is gone.<sup>16</sup> It is unknown whether young AChE<sup>-/-</sup> mice can see, but they are certainly blind when the photoreceptor layer is gone at day 86.

### Postnatal developmental delay

AChE<sup>-/-</sup> pups can be distinguished from littermates from the day of birth. They tremble more, and hold their head and tail in unnatural, characteristic positions. With each day the differences become more pronounced. AChE<sup>-/-</sup> pups are smaller. The average weight of a 4-month-old AChE<sup>-/-</sup> female is 18 g, whereas a wild-type female weighs 27–32 g. Male AChE<sup>-/-</sup> mice also average 18 g though a few have grown to be 20–30 g, almost as large as wild-type males (30–35 g). Despite their small size, AChE<sup>-/-</sup> mice are not gaunt or emaciated. They have body fat and do not appear to be starving. Their body length to weight ratio is equivalent to that of wild-type animals.

AChE<sup>-/-</sup> mice are late in displaying the following developmental milestones. They open their eyes one day late (day 13 vs 12); they

acquire the righting reflex 6 days late (day 18 vs 12); they acquire the ability to maintain their body temperature 7 days late (day 22 vs 15); their testes descend 4 weeks late (week 7–8 vs 4); estrous is up to 10 weeks late (week 15–16 vs 6–7).<sup>2</sup>

### Gastrointestinal tract bloating

Wild-type and AChE<sup>+/+</sup> mice infected with *Helicobacter hepaticus* showed no symptoms. In contrast, infected AChE<sup>-/-</sup> mice had severe gastrointestinal (GI) bloating. Gas distended the walls of the stomach and the intestines. Gas filled the GI tract from the esophagus to the anus in some living animals. After our colony was freed of infection,<sup>17</sup> bloating was never seen again.

The bloating had caused distress to the animals as indicated by loss of body weight, loss of body temperature, and premature death. Currently no premature death is caused by GI ileus.

An explanation for the unusual response to infection is not yet available. The hypothesis was tested that intestinal motility might be reduced in AChE<sup>-/-</sup> mice.<sup>18</sup> To test motility, Evans blue dye was gavaged into 12 wild-type and six AChE<sup>-/-</sup> mice. Twenty minutes later the animals were euthanized and the distance traveled by the dye was measured relative to the length of the GI tract. Motility in AChE<sup>-/-</sup> mice was 16% higher than in wild-type mice. This experiment ruled out the possibility that reduced motility in AChE<sup>-/-</sup> mice fostered growth of inappropriate intestinal flora. Other possibilities being tested are that the immune function might be compromised, or that the environment in the GI tract might be abnormal due to improper functioning of pancreatic and gall bladder sphincters.

### *Seizures*

Many AChE-/- mice have seizures when they are startled or undergo prolonged restraint. Pups less than 15 days of age do not have seizures. A critical period for seizure activity is postnatal days 20–50. AChE-/- mice older than 100 days have seizures less frequently. Many mice recover, but some die from the seizures. The major cause of early death in AChE-/- mice is seizures.

### *Normal brain structure*

Mesulam et al<sup>9</sup> stained brain sections for choline acetyltransferase immunoreactivity. They reported that AChE-/- brains displayed an overall pattern of choline acetyltransferase immunoreactivity that did not qualitatively differ from wild-type. This indicated that cholinergic perikarya, axons, and terminals are viable even in the absence of AChE. It was concluded that AChE is not absolutely essential for the development or maintenance of cholinergic pathways. Staining for BuChE activity showed that the brain contains widespread BuChE activity which can be used to hydrolyse acetylcholine. In the wild-type mouse brain, BuChE activity is 10% of AChE activity. BuChE is found in capillaries, glial cells, and a few neurons, while AChE activity is found in axons and neurons. Mesulam et al<sup>9</sup> reported that BuChE activity extended to all regions known to have cholinergic neurotransmission. These studies were at the light microscopic level. More subtle quantitative studies are needed before it is known whether absence of AChE causes changes in connectivity, dendritic branching, cell number, and cell size.

Darvesh et al<sup>19</sup> stained human brain for BuChE activity. They concluded that BuChE may have specific functions including coregulation of cholinergic and noncholinergic neu-

rotransmission in amygdala and in the hippocampal formation.

### *Downregulation of muscarinic and nicotinic receptors*

BuChE is an inefficient substitute for AChE. The AChE-/- mouse has had to make drastic adaptations to survive in the absence of AChE. Muscarinic receptor levels are downregulated to 50% of normal.<sup>20</sup> The low level of muscarinic receptors suggests overstimulation by excess acetylcholine. This in turn suggests that BuChE does not adequately protect receptors from overstimulation. Nicotinic receptors are also downregulated as shown by the work of Adler et al<sup>14</sup> and Minic et al<sup>15</sup> in isolated muscle preparations.

### *Memory and learning*

Memory and learning are difficult to measure in an animal that is blind, cannot swim well or for an extended period, and has poor locomotor activity. Thus, no measures of this type are available for AChE-/- mice. A clue to higher brain function is housekeeping behavior. Adult wild-type mice select one corner of their cage for urination. In contrast, AChE-/- mice urinate and defecate in their nest. This lack of housekeeping behavior suggests that higher brain function is undeveloped in AChE-/- mice.<sup>2</sup>

### *AChE is not present in excess concentrations in the mammalian brain*

It is generally thought that AChE is present in excess concentrations in the mammalian brain and that AChE activity is not a limiting factor in brain acetylcholine metabolism.<sup>21</sup> Our results question this. Heterozygote AChE+/- mice with 50% of normal AChE activity have intermedi-

ate levels of muscarinic receptors in the brain.<sup>20</sup> This means that 50% AChE activity is too little to handle normal levels of acetylcholine. There is too much acetylcholine, and the receptors are overstimulated. In response to overstimulation, receptors are downregulated.

### *Inhibition of BuChE is lethal to AChE-/- mice*

AChE-/- mice are supersensitive to the lethality of organophosphorus agents and carbamate inhibitors. Doses of the specific BuChEIs iso-OMPA and bambuterol, which are not toxic to wild-type mice, are lethal to AChE-/- mice. VX, the most potent nerve agent known, is lethal to AChE-/- mice at a lower dose ( $LD_{50} = 12 \mu\text{g/kg}$ ) than the dose for lethality in wild-type mice ( $LD_{50} = 24 \mu\text{g/kg}$ ).<sup>10</sup> The organophosphorus agents, DFP and chlorpyrifos oxon, which are relatively selective for BuChE over AChE, are lethal to AChE-/- mice at a lower dose compared to the lethal dose for wild-type mice. AChE-/- mice die when 50% of their brain BuChE is inhibited.<sup>10</sup>

### *Possible function of BuChE and implications for treatment of Alzheimer's disease*

BuChE appears to have a function based on the following observations. (1) Mice live to adulthood despite the complete absence of AChE. It is thought that the presence of BuChE in mice partly compensates for AChE deficiency. (2) Inhibition of BuChE in the AChE-/- mouse is lethal. Low doses of DFP, iso-OMPA, and chlorpyrifos oxon are lethal to AChE-/- mice but not to AChE+/+ mice. (3) There is 10 times more BuChE than AChE in a wild-type mouse.

Would the body have so much BuChE if BuChE had no function? (4) BuChE is widely distributed in the brain of mice<sup>9</sup> and humans,<sup>19</sup> though its cellular localization is different from that of AChE. BuChE is present mainly in glial cells and capillaries, whereas AChE is in neurons and axons. (5) BuChE hydrolyses acetylcholine and therefore could have a role in terminating nerve impulse transmission.

The normal brain structure and intact cholinergic system found by Mesulam et al<sup>9</sup> suggested that BuChE compensated for the absence of AChE in AChE knockout brains. It was hypothesized that BuChE hydrolysed acetylcholine after the acetylcholine diffused out of synapses. Thus, BuChE could have a function in terminating nerve impulse transmission. This conclusion is supported by the work of Giacobini.<sup>21</sup> Giacobini specifically inhibited BuChE activity in the rat brain by perfusing a selective carbamate, MF-8622, into the cortex. Extracellular fluid was removed by microdialysis for quantitation of acetylcholine. A 15-fold increase in the concentration of acetylcholine was found in cortical cholinergic synapses (from 5 nM to 75 nM). There were no cholinergic adverse effects, thus supporting the finding that AChE was not significantly inhibited. Another specific BuChEI, phenethylcymserine, improved learning in elderly rats.<sup>22</sup> Mesulam et al's and Giacobini's results lead to the conclusion that inhibition of BuChE will increase the amount of acetylcholine in the brain, and thus BuChEIs are expected to be beneficial to Alzheimer's disease patients.

### *Acknowledgments*

Supported by the US Army Medical Research and Materiel Command grant DAMD17-01-2-0036. The opinions and assertions contained

herein belong to the authors and should not be construed as the official views of the US Army or the Department of Defense.

## References

1. Xie W, Sibley JA, Chatonnet A et al. Postnatal developmental delay and supersensitivity to organophosphate in gene-targeted mice lacking acetylcholinesterase. *J Pharmacol Exp Ther* 2000; 293:896-902.
2. Duysen EG, Sibley JA, Fry DL et al. Rescue of the acetylcholinesterase knockout mouse by feeding a liquid diet; phenotype of the adult acetylcholinesterase deficient mouse. *Brain Res Dev Brain Res* 2002; 137:43-54.
3. Greenspan RJ, Finn JA, Hall JC. Acetylcholinesterase mutants in *Drosophila* and their effects on the structure and function of the central nervous system. *J Comp Neurol* 1980; 189: 741-774.
4. Behra M, Cousin X, Bertrand C et al. Acetylcholinesterase is required for neuronal and muscular development in the zebrafish embryo. *Nat Neurosci* 2002; 5:111-118.
5. Mendel B, Rudney H. Studies on cholinesterase. I. Cholinesterase and pseudocholinesterase. *Biochem J* 1943; 37:59-63.
6. Hawkins RD, Gunter JM. Studies on cholinesterase. 5. The selective inhibition of pseudocholinesterase in vivo. *Biochem J* 1946; 40: 192-197.
7. Primo-Parmo SL, Bartels CF, Wiersema B et al. Characterization of 12 silent alleles of the human butyrylcholinesterase (BCHE) gene. *Am J Hum Genet* 1996; 58:52-64.
8. Li B, Sibley JA, Ticu A et al. Abundant tissue butyrylcholinesterase and its possible function in the acetylcholinesterase knockout mouse. *J Neurochem* 2000; 75:1320-1331.
9. Mesulam MM, Guillozet A, Shaw P et al. Acetylcholinesterase knockouts establish central cholinergic pathways and can use butyrylcholinesterase to hydrolyze acetylcholine. *Neuroscience* 2002; 110:627-639.
10. Duysen EG, Li B, Xie W et al. Evidence for nonacetylcholinesterase targets of organophosphorus nerve agent: supersensitivity of acetylcholinesterase knockout mouse to VX lethality. *J Pharmacol Exp Ther* 2001; 299:528-535.
11. Radic Z, Pickering NA, Vellom DC et al. Three distinct domains in the cholinesterase molecule confer selectivity for acetyl- and butyrylcholinesterase inhibitors. *Biochemistry* 1993; 32:12074-12084.
12. Hutchinson DO, Walls TJ, Nakano S et al. Congenital endplate acetylcholinesterase deficiency. *Brain* 1993; 116:633-653.
13. Ohno K, Brengman J, Tsujino A, Engel AG. Human endplate acetylcholinesterase deficiency caused by mutations in the collagen-like tail subunit (COLQ) of the asymmetric enzyme. *Proc Natl Acad Sci USA* 1998; 95:9654-9659.
14. Adler M, Deshpande SS, Oyler G et al. Contractile and morphological properties of diaphragm muscle in acetylcholinesterase knockout mice. US Army Medical Defense Bioscience Review. Hunt Valley, MD June 2-5, 2002.
15. Minic J, Barbier J, Chatonnet A et al. Synaptic transmission at AChE-/- and COLQ-/- knockout mouse neuromuscular junctions. Seventh International Meeting On Cholinesterases; Pucon, Chile; November 8-12, 2002.
16. Bytyqi AH, Duysen EG, Lockridge O, Layer PG. Complete postnatal degeneration of the photoreceptor layer in an AChE knockout mouse. Seventh International Meeting On Cholinesterases; Pucon, Chile; November 8-12, 2002.
17. Duysen EG, Fry DL, Lockridge O. Early weaning and culling eradicated *Helicobacter hepaticus* from an acetylcholinesterase knockout 129S6/SvEvTac mouse colony. *J Comp Med* 2002; 52:461-466.
18. Duysen EG, Kolar CH, Lockridge O. *H. hepaticus* infection in acetylcholinesterase knockout mice results in severe intestinal distension. Seventh International Meeting On Cholinesterases; Pucon, Chile; November 8-12, 2002.
19. Darvesh S, Grantham DL, Hopkins DA. Distribution of butyrylcholinesterase in the human amygdala and hippocampal formation. *J Comp Neurol* 1998; 393:374-390.
20. Li B, Duysen EG, Lockridge O. Acetylcholinesterase knockout mice are resistant to oxotremorine-induced hypothermia and pilocarpine-induced seizures. Seventh International Meeting On Cholinesterases; Pucon, Chile; November 8-12, 2002.

21. Giacobini E. Selective inhibitors of butyrylcholinesterase. A valid alternative for therapy of Alzheimer's Disease? *Drug Aging* 2001; 18: 891-898.
22. Greig NH, Utsuki T, Yu Q et al. A new therapeutic target in Alzheimer's disease treatment: attention to butyrylcholinesterase. *Curr Med Res Opin* 2001; 17:159-165.

# Early Weaning and Culling Eradicated *Helicobacter hepaticus* from an Acetylcholinesterase Knockout 129S6/SvEvTac Mouse Colony

Ellen Gail Duysen,<sup>1</sup> Debra Lucie Fry, and Oksana Lockridge, PhD

The finding of *Helicobacter hepaticus* infection in our acetylcholinesterase (AChE) knockout mouse colony led to a search for a treatment. One-hundred percent of AChE  $+/+$ , 100% of AChE  $+/$ , and 35% of AChE  $-/-$  mice tested positive. The lower infection rate in AChE  $-/-$  mice, who are routinely weaned on day 15, suggested that early weaning might be an effective eradication strategy. The AChE  $+/+$  and  $+/$  mice were weaned on days 13, 14, 15, or 16. Litters were placed in sterile, heated, isolator cages. Animals were fed liquid Ensure Fiber and 11% fat pelleted diet. Feces were tested for the presence of *H. hepaticus* by use of DNA amplification. Litters weaned on days 14, 15, or 16 had a high rate (68, 63, and 100%, respectively), whereas litters weaned on day 13 had a lower (8%) rate of infection. Uninfected animals have remained free of *H. hepaticus* through day 120. Pups weaned on day 13 lost body weight, beginning on day 14, but recovered by day 16. It is concluded that the non-coprophagic behavior of AChE  $-/-$  mice accounts for a low infection rate and that the combination of early weaning, routine testing, and culling provide an effective method for eradication of *H. hepaticus*.

*Helicobacter hepaticus* contamination of commercial and private mouse colonies has presented a treatment dilemma for researchers. Characterized as a novel bacterium in 1994 (1, 2), the gram-negative *H. hepaticus* bacterium has since been associated with chronic active hepatitis and liver tumors in various strains of mice (A/JCr, DBA/2NCr, C3H/HeNCr, B6C3F<sub>1</sub>) (2-5). Colitis, typhlitis, and inflammatory bowel disease in immunodeficient mice have been linked to infection with *H. hepaticus* (6-10). Transmission of *H. hepaticus* has been reported to be by the oral-fecal route (11), an effective means of infection in coprophagic animals such as mice. Exposure of sentinel mice to *H. hepaticus*-contaminated bedding results in high rates of infection. (12, 13). A study by Truett and co-workers (14) indicated that pups raised by *Helicobacter*-positive dams all tested positive for the bacteria by day 19.

Initial identification of the *H. hepaticus* bacterium in this laboratory's acetylcholinesterase (AChE) knockout mouse colony was made during serologic and fecal screening of sentinel animals. Samples were analyzed at The Missouri University Research Animal Diagnostic Laboratory (RADIL, Columbia, Mo.). In-house testing of bacterial DNA from fecal pellets led to the discovery of widespread *H. hepaticus* infection. A surprise finding was that, although 100% of AChE wild type (AChE  $+/+$ ) and heterozygote (AChE  $+/$ ) mice tested positive for *H. hepaticus*, only 35% of the group-housed AChE nullizygote (AChE  $-/-$ ) mice were infected. An investigation into a feasible method for reestablishment of a *H. hepaticus*-negative breeding colony was undertaken. Reports of successful drug therapy involved oral gavage of affected animals three times daily, using a triple drug regimen

(15). The labor and cost involved in treating our large colony, as well as reports of inconsistent results, eliminated drug therapy as a practical treatment method. Neonatal transfer of pups from *H. hepaticus*-positive dams to negative dams was documented to be an effective method of eradication (14). Fostering the AChE knockout litters on an *H. hepaticus*-negative dam was worrisome because the AChE  $-/-$  pups are substantially smaller and weaker than their littermates and would have been targets for cannibalism or abandonment. This would have resulted in loss of valuable AChE  $-/-$  pups. Cross-fostering the pups would have required additional time to establish uninfected dams in the colony and would have necessitated implementing a protocol for synchronization of the dams' reproductive cycle prior to breeding. Re-deriving the colony by embryo transfer would have been cost and time prohibitive.

The AChE knockout mouse was developed in our laboratory by use of gene targeting and homologous recombination (16). All tissues of the AChE  $-/-$  animals are devoid of acetylcholinesterase enzyme activity and protein (16, 17). The AChE  $-/-$  animals, produced by heterozygote breeding, are characterized by weak muscles, manifested in lack of bite and suckling strength, no fore or hind limb grip strength, splayed limbs, and reduced locomotor activity. In addition, the AChE  $-/-$  animals do not manifest aggressive behaviors, do not breed, have continuous mild tremors, and have reduced body weight and body temperature, compared with their AChE  $+/+$  and  $+/$  littermates (18). Consequences of the bite strength deficit are that AChE  $-/-$  animals are unable to efficiently eat pelleted diet and are not coprophagic. Raised by *H. hepaticus*-positive dams, AChE  $-/-$  mice are weaned on day 15, placed on a heating pad through day 21, and fed a diet of liquid Ensure Fiber. The AChE  $-/-$  mice remain on the Ensure Fiber diet for the duration of their life, which averages 100 days. In a previous study conducted in this labora-

Received: 3/06/02. Revision requested: 5/03/02, 6/11/02. Accepted: 6/14/02.  
Eppley Institute, University of Nebraska Medical Center, Omaha, Nebraska  
68198-6805.

\*Corresponding author.

tory, feeding of a liquid diet of Ensure Fiber ad libitum to AChE  $+/+$  and  $+/$ - mice did not reduce survival time or cause any detrimental health effects (18). Early weaning and lack of coprophagia are believed to be the factors responsible for the reduced incidence of infection in AChE  $-/-$  animals. Thus, the objective of the study reported here was to devise and describe use of an early-weaning regimen to prevent infection of the AChE  $+/+$  and  $+/$ - mice with *H. hepaticus*.

## Materials and Methods

**Animals and husbandry.** All animal procedures were performed in accordance with the Public Health Service Policy on Humane Care and Use of Laboratory Animals (PHS 1996). Protocols were approved by the University of Nebraska Medical Center Institutional Animal Care and Use Committee. Facilities were maintained at a temperature of 20–22°C, humidity of 35 to 40%, with lighting on a 12/12-h light/dark cycle. The AChE  $-/-$  mice were housed in a 17  $\times$  8.5  $\times$  8-in. hamster cage lined with paper towels in place of bedding. Cages were lined with paper towels to eliminate contamination of the liquid diet by loose bedding. Early-weaned pups and animals determined to be *H. hepaticus* free were housed in sterile static isolator top standard mouse cages. All procedures were conducted under a laminar flow hood, using Clidox spray as a decontaminant.

The animals studied were derived from an original breeding of Taconic 129S6/SvEvTac mice with a chimera from R1 embryonic stem cells, in which five kilobases of the ACHE gene from intron one through exon five had been deleted (16). Nullizygote mice, generated from AChE  $+/+$  breeding, have no AChE activity in any of their tissues (16, 17). By visual observation, AChE  $+/+$  and AChE  $+/$ - mice are indistinguishable.

Males and nonpregnant females were fed a pelleted 5% (wt./wt.) fat maintenance diet (catalog No. 7912, Harlan Teklad LM-485 Harlan Teklad, Madison, Wis.). Gestating females were fed a pelleted 11% (wt./wt.) fat diet (catalog No. 7904, Harlan Teklad S-2335, Harlan Teklad). Early weaned pups (from day 13 to 21) and AChE  $-/-$  mice (from day 15 throughout their lifetime) were fed a liquid diet of Ensure Fiber, vanilla flavor (catalog No. 50650, Abbott Laboratories, Ross Products division, Columbus, Ohio). In addition, early-weaned pups were offered 11% (wt./wt.) fat diet pellets, placed on the floor of the cage for easy access.

**Colony health status.** Serologic testing of the colony was conducted quarterly at the RADIL. The Cri:CD-1(ICR)BR sentinels from Charles River Laboratories, Inc. (Wilmington, Mass.) were exposed to dirty bedding three times a week for three months. One sentinel was analyzed for every 21 cages of test animals. Serum samples from sentinel animals were tested for the presence of antibodies to: mouse hepatitis virus, Sendai virus, pneumonia virus of mice, reovirus 3, Theiler's murine encephalomyelitis virus, ectromelia virus, mouse adenovirus type I and mouse adenovirus type II, polyoma virus, *Mycoplasma pulmonis*, parvovirus, mouse rotavirus, lymphocytic choriomeningitis virus, *E. cuniculi*, cilia-associated respiratory bacillus, *Clostridium piliforme*, and Hantaan virus. Fecal samples were analyzed by use of a polymerase chain reaction (PCR) assay for the presence of *Helicobacter* species (*H. bilis*, *H. hepaticus*, *H. rodentium*, and *H. typhlonicus*) at the RADIL as well as at Charles River Diagnostic Laboratories (Wilmington, Mass.).

**Detection methods for *H. hepaticus*.** A DNA purification and amplification method was used to determine the presence

of *H. hepaticus* bacteria in fecal pellets. Using sterile forceps, feces were collected from the cage floor and placed in a sterile 2.0-ml microcentrifuge tube. The samples were tested within two hours of collection and were stored at 4°C in the interim. The bacterial DNA from the feces was purified, using the QIAamp DNA Stool Mini Kit (catalog No. 51504, QIAGEN Inc., Valencia, Calif.). This kit contains a matrix and a buffer that are designed to remove enzyme inhibitory substances and DNA degradation products from the fecal sample. The purified DNA was amplified by use of a PCR assay with primer sequences that recognized an *H. hepaticus*-specific region of the 16S rRNA gene (15). The oligonucleotides, 5' GCA TTT GAA ACT GTT ACT CTG 3', and 5' CTG TTT TCA AGC TCC CC 3' produced a 416-bp product. The PCR materials and conditions used were those outlined by Foltz and co-workers (15), with the exception that *Taq* polymerase in storage buffer B (catalog No. M116B-1, Promega, Madison, Wis.) was used. Samples were visualized by electrophoresis on a 1% agarose gel containing ethidium bromide and viewing by UV illumination.

***Helicobacter hepaticus* testing of group-housed AChE  $-/-$  mice.** The AChE  $-/-$  mice were group-housed, four to eight animals per cage, in hamster cages lined with paper towels. Mice were housed together beginning on postpartum day (PPD) 15, and remained together throughout their lifetime. The AChE  $-/-$  mice (n = 23) housed in four cages were individually tested for *H. hepaticus* infection. Mice ranged in age from 29 to 392 days. For fecal collection, mice were placed in separate cages lined with paper towels. Fecal samples were collected, and the DNA was purified and detected as described previously.

**Weaning from contaminated breeding colony.** During gestation and after parturition, *H. hepaticus*-positive heterozygote dams were housed in a cage containing nesting material, with 11% (wt./wt.) fat diet and water available ad libitum. Cage bedding was changed three times weekly. On PPD 13, 14, 15, or 16, AChE  $+/+$  and AChE  $+/$ - pups from 56 litters (264 animals) were removed from the birth cage and placed in a sterile standard mouse cage lined with paper towels and fitted with an isolator top. The 37 AChE  $-/-$  mice of the 56 litters were not included in this part of the study. These developmentally delayed pups do not have their eyes open and are not fully mobile until PPD 15; therefore, weaning prior to this time would result in death of the pup. Day 13 was chosen as the earliest day of weaning of AChE  $+/+$  and  $+/$ - pups because, by PPD 12, the pup's eyes are open, the animals are mobile, and they are able to regulate their body temperature.

A 12  $\times$  8.3  $\times$  3.2-cm sterile plastic box with a hole in the side was lined with paper towels and inverted in the cage to provide shelter and additional warmth. Shallow plastic petri dishes were placed on the floor of the cage to hold the Ensure Fiber liquid diet. Several 11% (wt./wt.) diet pellets were placed on the floor. Additional pellets and a water bottle were placed in the hopper on the cage lid. Approximately a third of the cage, the portion containing the lined box, was placed on a 11  $\times$  13-in. heating pad, providing a surface temperature of 42°C. Cage bedding was changed, food dishes were washed, and the Ensure diet was replenished daily.

**Determination of body weight and surface body temperature.** Body weight and surface body temperature of pups in nine litters (45 pups) were measured daily from day 10 through day 21. Half the animals in each litter were weaned on

**Table 1.** Detection of *Helicobacter hepaticus* in group-housed acetylcholinesterase (AChE) *-/-* mice (n = 29)

Cage no.	Age at testing (days)	No. of <i>H. hepaticus</i> -positive mice	No. of <i>H. hepaticus</i> -negative mice
1	222-392	1	5
2	92-249	1	4
3	31-70	4	3
4	29-33	2	3

Mice were group housed from postpartum day (PPD) 16 onward.

day 13, while the remainder were left with the dam through day 21. Body weight was measured daily, using a top-loading balance. The axial body temperature was measured daily by use of a digital thermometer (Thermalert model TH-5 and a surface Microprobe MT-D, Type T thermocouple, Physitemp Instruments Inc., Clifton, N.J.). Data from male and female pups were analyzed separately to avoid having sex as a confounding variable in the results.

**Statistical analysis.** Body weight, surface temperature data, and litter size were analyzed, using the Microsoft Excel data analysis program. Statistical differences were determined by use of a two-tailed independent *t* test, with significance set at *P* = 0.05.

## Results

**Initial *H. hepaticus* detection.** In one routine quarterly screening of our AChE knockout colony by RADIL, all sentinel mice (n = 6) were determined to be free of antibodies to MHV and all other pathogens. These same mice were all found to be infected with *H. hepaticus* on the basis of results of fecal analysis. Subsequent random testing of feces from the colony indicated that the infection was widespread, with 100% of the AChE *++* (11/11) and AChE *+-* (13/13) mice testing positive. Infection status was determined in house by PCR analysis of purified DNA from fecal samples.

**Group-housed AChE *-/-* infection rate.** Twenty three AChE *-/-* mice group-housed in four cages were individually tested for *H. hepaticus* infection (Table 1). The four cages had a total of 15 mice testing negative for *H. hepaticus* and eight testing positive, for a 35% infection rate.

**Lack of coprophagia in AChE *-/-* mice.** Observations that the AChE *-/-* mice are not coprophagetic were made over a two-year period. The AChE *-/-* mice were never observed consuming feces, a behavior common to the AChE *++* and *+-* mice. The solid fecal pellets were not held or consumed by the AChE *-/-* mice, as they lack grip and bite strength (18). Although the AChE *-/-* mice do not have a deficit in their olfactory sense (18), they did not manifest interest in the feces of other animals when introduced to a new cage.

**Early weaning.** A total of 56 litters of mice, 264 AChE *++* and *+-* pups, were weaned on PPD 13 (n = 25 litters), 14 (n = 19 litters), 15 (n = 8 litters) or 16 (n = 4 litters) (Table 2). Average litter size for each group was: PPD 13, 6.1 pups/litter; PPD 14, 5.5 pups/litter; PPD 15, 5.8 pups/litter; and PPD 16, 6.1 pups/litter. There was no significant difference among litter sizes. Because of delayed eye opening and reduced locomotor activity, AChE *-/-* mice cannot be weaned until day 15; therefore, these mice were not included in this experiment. Each litter was tested for *H. hepaticus* infection on PPD 21 to 30. Because of time and cost considerations, pups were not housed or tested individually. Litters were group-housed, and it was assumed

**Table 2.** Effect of early weaning on infection rate

PPD of weaning	No. of litters <i>H. hepaticus</i> pos.	No. of litters <i>H. hepaticus</i> neg.	% of mice <i>H. hepaticus</i> pos.	% of mice converting to pos. status
13	2	23	8.0	0
14	19	6	68.4	0
15	5	3	62.5	0
16	4	0	100.0	NA

Mice in 56 litters (n = 264; AChE *++* and *+-* pups) were weaned on postpartum day (PPD) 13, 14, 15 or 16, and were tested for *H. hepaticus* on days 21 to 30 and again every 3 weeks through 120 days. Mice that were test negative in the first test period, remained negative in subsequent test periods. Pos. = test positive; NA = all animals weaned on day 16 tested positive for *H. hepaticus*; therefore, the % conversion parameter is not applicable.

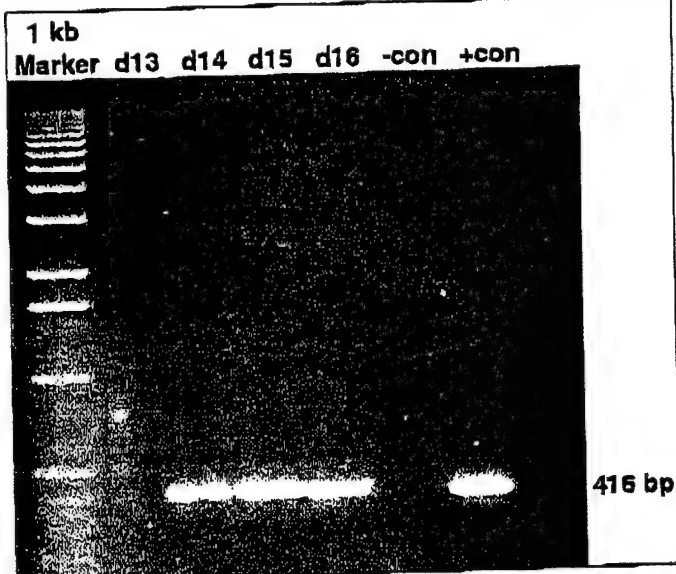


**Figure 1.** Detection of *Helicobacter hepaticus* by use of polymerase chain reaction (PCR) analysis. The DNA from the feces of acetylcholinesterase (AChE) *++* and *+-* mice pups was amplified by PCR analysis and was visualized on a 1% agarose gel containing ethidium bromide with a 1-kb marker. The 416-bp band indicates presence of *H. hepaticus* in mice weaned on postpartum day (PPD) 14, 15, and 16. The absence of the band on day 13 indicates that the animal was not infected. The PCR product from a known infected animal was included as a positive control (+ con). The negative control (- con) is a PCR reaction containing no fecal DNA.

that if one animal became infected, the remainder would become infected (12, 13). Only two of 25 litters (8%) weaned on day 13 tested positive for *H. hepaticus*; however, 13 of 19 (68%) and three of five (60%) litters whose members were weaned on days 14 and 15, respectively, tested positive. All four (100%) of the litters whose members were weaned on PPD 16 tested *H. hepaticus* positive. An example of the PCR results from AChE *++* and *+-* mice weaned on PPD 13, 14, 15 or 16 is shown in Fig. 1. The 416-bp band is indicative of infection with *H. hepaticus*. Absence of the band on day 13 indicates that the pups in this litter were not infected. The litters whose members were deemed to be *H. hepaticus* negative were retested every three weeks after the initial testing. None of the previously test-negative litters converted to a positive status through 120 days of testing. The RADIL and Charles River Diagnostic Laboratories substantiated the findings by analyzing random samples previously tested in house.

**Body weight and surface temperature of early-weaned pups.** Body temperature (Fig. 2) and body weight (Fig. 3) were

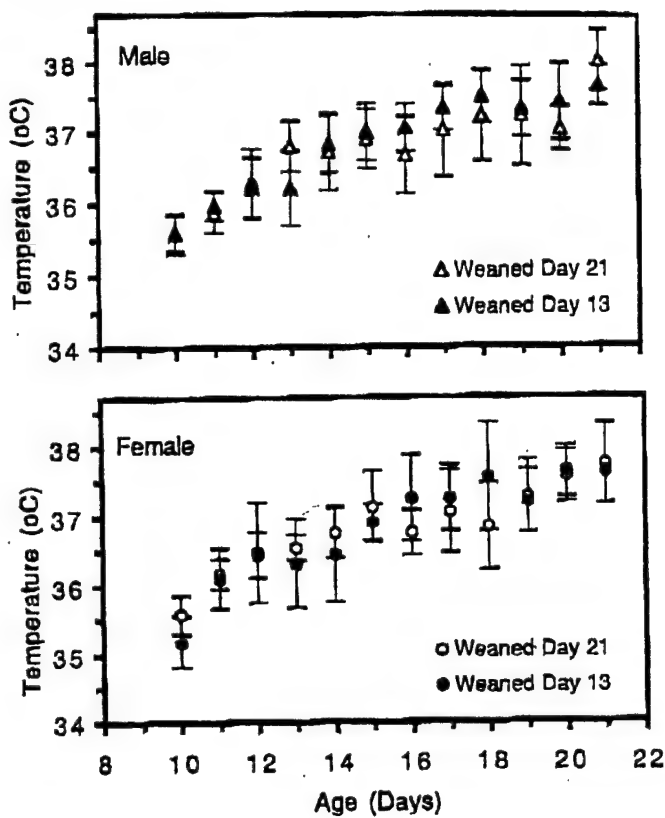


Figure 2. Surface body temperature of AChE  $^{+/+}$  and  $^{+/-}$  pups weaned on day 13 (male,  $n = 13$ ; female,  $n = 12$ ) or day 21 (male,  $n = 11$ ; female,  $n = 9$ ). There was no significant difference at any time point (two-tailed independent  $t$ -test with significance level of  $P < 0.05$ ). Error bars represent  $\pm$  SD.

measured daily for nine litters. One half of each litter was weaned on day 13, and the other half was left with the dam through day 21, the routine day of weaning. There was no significant difference between surface body temperature of the early-weaned male ( $n = 13$ ) and female ( $n = 12$ ) pups and the day-21 weaned male ( $n = 11$ ) and female ( $n = 9$ ) pups (two-tailed independent samples  $t$ -test significance level,  $P = 0.05$ ). Body weight of the male pups weaned on day 13 was significantly lower on days 14 ( $P = 0.001$ ) and 15 ( $P = 0.007$ ), compared with the weight of male pups that were left with the dam through day 21. From days 16 to 21, body weight did not differ significantly between the two male groups. There was no significant difference in body weight in pups of the female group at any time. Although it was not significant, there was a trend toward lower weight in pups of the early-weaned group from days 14 to 20, compared with that in the female pups weaned on day 21.

**Mortality/morbidity of early-weaned pups.** There were 264 individual pups in the 56 early-weaned litters. One animal died on day 18 during the weaning process (0.4% mortality). This animal did not manifest any untoward signs of disease prior to death. Other indicators of morbidity were not observed in any of the early-weaned pups.

**Sexual development.** On PPD 50 to 58, eight heterozygote, early-weaned, *H. hepaticus*-negative females were bred to sexually mature, heterozygote, early-weaned, *H. hepaticus*-negative males. All of the females (8/8) gave birth from 21 to 26 days after exposure to the males. Average litter size was 5.3 pups.

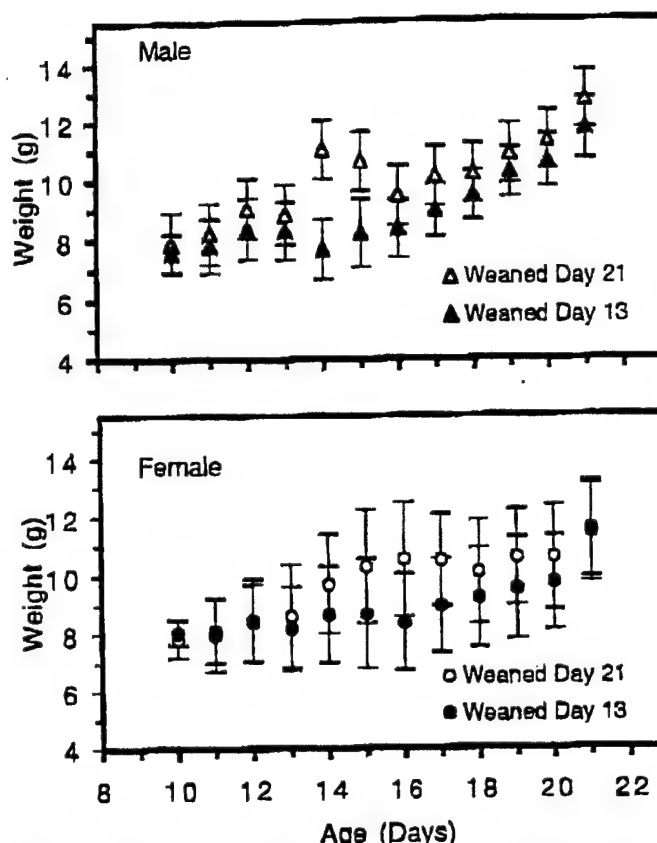


Figure 3. Body weight of AChE  $^{+/+}$  and  $^{+/-}$  pups weaned on day 13 (male,  $n = 13$ ; female,  $n = 12$ ) or day 21 (male,  $n = 11$ ; female,  $n = 9$ ). Pups weaned on day 13 had significantly lower body weight on day 14 ( $P = 0.001$ ) and on day 15 ( $P = 0.007$ ) than did the male littermates weaned on day 21 (two-tailed independent  $t$ -test with significance level of  $P < 0.05$ ). See Fig. 2 for key.

## Discussion

Concerns regarding the long-term health of our *H. hepaticus*-infected AChE knockout colony prompted this laboratory to investigate a method of eradication of the organism. The possibility that infection could prove to be a confounding factor in the data generated from these animals was considered. Although clinical signs of disease ascribed to this infection were not apparent, and signs of disease were not observed by gross and microscopic examinations, long-term effects could not be ruled out. Infected animals could not be shipped to other facilities because of their *H. hepaticus*-positive status, resulting in delay in collaborative research efforts.

**Early-weaning rationale.** To facilitate feeding and to provide a constant warm environment, AChE  $^{-/-}$  mice are weaned on day 15. This early-weaning protocol has made it possible to raise a high percentage of these fragile pups to adulthood (18). Remarkably, only 35% of the early-weaned, group-housed, non-coprophagous AChE  $^{-/-}$  mice tested positive for *H. hepaticus*. The oldest AChE  $^{-/-}$  animal in the colony (392 days) as well as four other animals in the same cage were negative for *H. hepaticus* even though they had been housed with an *H. hepaticus*-positive animal for seven months. This finding is in contrast to results of studies indicating rapid infection with *H. hepaticus*, either after exposure to contaminated bedding (12, 13) or by exposure to the bacteria in the birth cage (14). The AChE  $^{-/-}$  mice testing positive may have originally contracted the bacteria from the dam's coat

Eradication of *Helicobacter hepaticus* by early weaning and culling

while suckling. Our results substantiate the reported link between coprophagia and infection with *H. hepaticus*. It follows that, by using the same early-weaning protocol, the AChE +/- and +/- mice could be weaned prior to becoming coprophagetic, thereby eliminating spread of the bacteria. The stronger and more developmentally mature AChE +/- and +/- mice were able to be weaned prior to day 15. Truett and co-workers (14) reported that, when 13-day-old *Helicobacter*-free mice were housed with *Helicobacter*-contaminated dams, they became *Helicobacter* positive by day 16. Ebino and co-workers (19) reported that suckling ICR mice manifested coprophagetic behavior at 17 to 18 days of age. Considering these data we focused on a range of weaning times from days 13 to 16. Our data indicated marked difference in the infection rate between pups weaned on PPD 13 versus those weaned one day later. This may represent a transition period between non-coprophagetic and coprophagetic behavior in 129S6/SvEvTac mice. This 13- to 14-day postpartum period may also represent a time when the pups become more susceptible to intestinal invasion by the *Helicobacter* organism. There may be strain differences when it comes to the appropriate day to wean. Physically larger mouse strains may develop faster and become coprophagetic by day 13, requiring that they be weaned before day 13. Smaller, fragile or slower developing strains may not yet have their eyes open, or be mobile enough to feed from a petri dish. The appropriate day to wean would have to be established for each colony.

**Stress associated with early weaning.** Concern about the stress that early weaning might cause prompted additional parameters, such as weight loss, decrease in body temperature, increase in morbidity or mortality, and delayed time to sexual development, to be examined. Although we saw significant weight loss in the early weaned male pups beginning on day 14, there was rapid and sustained recovery by day 16. Body temperature between the two groups was not significantly different. Morbidity was not observed in any of the early-weaned pups. There have been 225 pups weaned on day 13 and only one pup has died. Early-weaned females were successfully bred at eight weeks of age, producing 5.3 pups/litter. Females weaned on day 21 have routinely been bred in this time frame. The average litter size of 5.3 pups from the early-weaned dams (n = 8) is similar to the average litter (5.7 pups/litter) for a non-early-weaned first-litter dam (n = 27).

The lower body weight from days 14 through 16 after weaning suggested a minimal degree of stress involved in the early-weaning process. Reduction in the level of stress was accomplished by addition of a covered secure area in the cage for the pups to hide, by providing additional warmth, and by feeding a liquid diet. Different strains of mice may be more or less prone to stress than is the 129S6/SvEvTac strain used in this study.

**Labor and cost factors.** The early-weaning protocol is labor intensive. Cage bedding and liquid diet must be changed daily. If the early-weaned pups are housed in a room with infected animals, they must be handled prior to handling infected animals. Using sterile technique and isolator housing is important because fecal contamination can be easily transmitted from gloves, infected cages, or bedding that may be scattered from infected cages (12). The animals must be screened after weaning on day 13 and routinely screened to ensure that the test-negative animals have not converted to test-positive status. Animals testing positive for *H. hepaticus* must be culled from

the colony. Screening of feces from an entire cage verses individual animals saved time and expense. Using the commercially available QIAGEN fecal DNA purification kit proved to be convenient and rapid. The expense of screening numerous samples by use of this method could become prohibitive. An inexpensive alternative was proposed by Truett and co-workers (14), using a reagent termed HotSHOT for the purification procedure.

In conclusion, our experience with the successful early weaning of non-coprophagetic AChE +/- mice led us to develop a safe, rapid, inexpensive procedure for eradication of *H. hepaticus*. By weaning pups on day 13, using sterile technique, reducing stress by feeding a liquid diet, providing a supplementary heat source and a sheltered area in the cage, and conducting routine fecal screening, we were able to re-establish a breeding colony free of infection with *H. hepaticus*.

---

### Acknowledgments

This work was supported by U.S. Army Medical Research and Materiel Command Grants DAMD17-01-2-0036 and DAMD17-01-1-0776. The opinions or assertions contained herein belong to the authors and should not be construed as the official views of the U.S. Army or the Department of Defense.

---

### References

1. Fox, J. G., F. E. Dewirst, J. G. Tully, B. J. Paster, L. Yan, N. S. Taylor, M. J. Collins, Jr., P. L. Gorelick, and J. M. Ward. 1994. *Helicobacter hepaticus* sp. nov., a microaerophilic bacterium isolated from livers and intestinal mucosal scrapings from mice. *J. Clin. Microbiol.* 32:1238-1245.
2. Ward, J. M., J. G. Fox, M. R. Anver, D. C. Haines, C. V. George, M. J. Collins, Jr., P. L. Gorelick, K. Nagashima, M. A. Gonda, R. V. Gilden, J. G. Tully, R. J. Russell, R. E. Benveniste, B. J. Paster, F. E. Dewirst, J. C. Donovan, L. M. Anderson, and J. M. Rice. 1994. Chronic active hepatitis and associated liver tumors in mice caused by a persistent bacterial infection with a novel *Helicobacter* species. *J. Natl Cancer Inst.* 86:1222-1227.
3. Ward, J. M., M. R. Anver, D. C. Haines, and R. E. Benveniste. 1994. Chronic active hepatitis in mice caused by *Helicobacter hepaticus*. *Am. J. Pathol.* 145:959-968.
4. Fox, J. G., X. Li, L. Yan, R. J. Cahill, R. Hurley, R. Lewis, and J. C. Murphy. 1996. Chronic proliferative hepatitis in A/JCr mice associated with persistent *Helicobacter hepaticus* infection: a model of *Helicobacter*-induced carcinogenesis. *Infect. Immun.* 64:1548-1558.
5. Fox, J. G., J. A MacGregor, Z. Shen, X. Li, R. Lewis, and C. A. Dangler. 1998. Comparison of methods of identifying *Helicobacter hepaticus* in B6C3F<sub>1</sub> mice used in a carcinogenesis bioassay. *J. Clin. Microbiol.* 36:1382-1387.
6. Fox, J. G., L. Yan, B. Shames, J. Campbell, J. C. Murphy, and X. Li. 1998. Persistent hepatitis and enterocolitis in germ-free mice infected with *Helicobacter hepaticus*. *Infect. Immun.* 66:3673-3681.
7. Cahill, R. J., C. J. Foltz, J. G. Fox, C. A. Dangler, F. Powrie, and D. B. Schauer. 1997. Inflammatory bowel disease: an immunity-mediated condition triggered by bacterial infection with *Helicobacter hepaticus*. *Infect. Immun.* 65:3126-3131.
8. Whary, M. T., T. J. Morgan, C. A. Dangler, K. J. Gaudes, N. S. Taylor, and J. G. Fox. 1998. Chronic active hepatitis induced by *Helicobacter hepaticus* in the A/JCr mouse is associated with a Th1 cell-mediated immune response. *Infect. Immun.* 66:3142-3148.
9. Foltz, C. J., J. G. Fox, R. Cahill, J. C. Murphy, L. Yan, B. Shames, and D. B. Schauer. 1998. Spontaneous inflammatory bowel disease in multiple mutant mouse lines: association with colonization by *Helicobacter hepaticus*. *Helicobacter* 3:69-78.

Vol 52, No 5  
Comparative Medicine  
October 2002

10. Kullberg, M. C., J. M. Ward, P. L. Gorelick, P. Caspar, S. Hieny, A. Cheever, D. Jankovic, and A. Sher. 1998. *Helicobacter hepaticus* triggers colitis in specific-pathogen-free interleukin-10 (IL-10)-deficient mice through an IL-12- and gamma interferon-dependent mechanism. *Infect. Immun.* 66:5157-5166.
11. Rice, J. M. 1995. *Helicobacter hepaticus*, a recently recognized bacterial pathogen, associated with chronic hepatitis and hepatocellular neoplasia in laboratory mice. *Emerg. Infect. Dis.* 1:1-2.
12. Whary, M. T., J. H. Cline, A. E. King, C. A. Corcoran, S. Xu, and J. G. Fox. 2000. Containment of *Helicobacter hepaticus* by use of husbandry practices. *Comp. Med.* 50:78-81.
13. Livingston, R. S., L. K. Riley, C. L. Besch-Williford, R. R. Hook, Jr., and C. L. Franklin. 1998. Transmission of *Helicobacter hepaticus* infection to sentinel mice by contaminated bedding. *Lab. Anim. Sci.* 48:291-293.
14. Truett, G. E., J. A. Walker, and D. G. Baker. 2000. Eradication of infection with *Helicobacter* spp. by use of neonatal transfer. *Comp. Med.* 50:444-451.
15. Foltz, C. J., J. G. Fox, L. Yan, and B. Shamer. 1995. Evaluation of antibiotic therapies for eradication of *Helicobacter hepaticus*. *Antimicrob. Agents Chemother.* 39:1292-1294.
16. Xie, W., J. A. Stribley, A. Chatonnet, P. J. Wilder, A. Rizzino, R. D. McComb, P. Taylor, S. H. Hinrichs, and O. Lockridge. 2000. Postnatal developmental delay and supersensitivity to organophosphate in gene-targeted mice lacking acetylcholinesterase. *J. Pharmacol. Exp. Ther.* 293:898-902.
17. Li, B., J. A. Stribley, A. Tieu, W. Xie, L. M. Schopfer, P. Hammond, S. Brimijoin, S. H. Hinrichs, and O. Lockridge. 2000. Abundant tissue butyrylcholinesterase and its possible function in the acetylcholinesterase knockout mouse. *J. Neurochem.* 75:1320-1331.
18. Duysen, E., J. A. Stribley, D. L. Fry, S. H. Hinrichs, and O. Lockridge. 2002. Rescue of the acetylcholinesterase knockout mouse by feeding a liquid diet; phenotype of the adult acetylcholinesterase deficient mouse. *Dev. Brain Res.* 137:43-54.
19. Ebino K. Y., T. Suwa, Y. Kuwabara, T. R. Saito, and K. W. Takahashi. 1987. Lifelong coprophagy in male mice. *Jikken Dobutsu.* 36:273-276.

---

---

## **Specificity of Ethephon as a Butyrylcholinesterase Inhibitor and Phosphorylating Agent**

---

**J. Eric Haux, Oksana Lockridge, and John E. Casida**

Environmental Chemistry and Toxicology Laboratory, Department of  
Environmental Science, Policy and Management, University of  
California, Berkeley, California 94720-3112, and Eppley Cancer  
Institute, University of Nebraska Medical Center,  
Omaha, Nebraska 68198-6805

# **Chemical Research in Toxicology<sup>®</sup>**

Reprinted from  
Volume 15, Number 12, Pages 1527-1533

# Specificity of Ethepron as a Butyrylcholinesterase Inhibitor and Phosphorylating Agent

J. Eric Haux,<sup>†</sup> Oksana Lockridge,<sup>‡</sup> and John E. Casida\*,<sup>†</sup>

*Environmental Chemistry and Toxicology Laboratory, Department of Environmental Science, Policy and Management, University of California, Berkeley, California 94720-3112, and Eppley Cancer Institute, University of Nebraska Medical Center, Omaha, Nebraska 68198-6805*

Received May 28, 2002

Butyrylcholinesterase (BChE) is inhibited by the plant growth regulator (2-chloroethyl)-phosphonic acid (ethepron) as observed 25 years ago both in vitro and in vivo in rats and mice and more recently in subchronic studies at low doses with human subjects. The proposed mechanism is phosphorylation of the BChE active site at S198 by ethepron dianion. The present study tests this hypothesis directly using [<sup>33</sup>P]ethepron and recombinant BChE (rBChE) with single amino acid substitutions and further evaluates if BChE is the most sensitive esterase target in vitro and with mice in vivo. [<sup>33</sup>P]Ethepron labels purified rBChE but not enzymatically inactive diethylphosphoryl-rBChE (derivatized at S198 by preincubation with chlorpyrifos oxon) or several other esterases and proteins. Amino acid substitutions that greatly reduce rBChE sensitivity to ethepron are G117H and G117K in the oxyanion hole (which may interfere with hydrogen bonding between glycine-N–H and ethepron dianion) and A328F, A328W, and A328Y (perhaps by impeding access to the active site gorge). Other substitutions that do not affect sensitivity are D70N, D70K, D70G, and E197Q which are not directly involved in the catalytic triad. The effect of pH and buffer composition on inhibition supports the hypothesis that ethepron dianion is the actual phosphorylating agent without activation by divalent cations. Human plasma BChE in vitro and mouse plasma BChE in vitro and in vivo are more sensitive to ethepron than any other esterases detected by butyrylthiobaline or 1-naphthyl acetate hydrolysis in native-PAGE. All mouse liver esterases observed are less sensitive than plasma BChE to ethepron in vitro and in vivo. More than a dozen other esterases examined are 10–100-fold less sensitive than BChE to ethepron. Thus, BChE inhibition continues to be the most sensitive marker of ethepron exposure.

## Introduction

Ethepron [(2-chloroethyl)phosphonic acid] (Figure 1) is one of the most important plant growth regulators to promote pre- and postharvest ripening in food and fiber crops (1). The annual use is about 5.4 million pounds in the United States (2) and 0.9 million pounds in California (3), mostly on cotton. In rats, the acute oral LD<sub>50</sub> is 3030 mg/kg and the chronic (2 year) dietary no observable effect level is 3000 ppm (1). Most organophosphorus (OP)<sup>1</sup> pesticides are insecticides acting as acetylcholinesterase (AChE) inhibitors, often with even greater inhibition of butyrylcholinesterase (BChE). Ethepron as an OP, even though it gives no cholinergic signs of poisoning, was tested the same way as an OP insecticide. The result was very surprising. It markedly inhibited plasma BChE with much less effect on brain or erythrocyte AChE in rats and mice both in vitro and in vivo (4, 5). BChE inhibition is expected for an OP triester insecticide but certainly not for a phosphonic acid plant growth regulator. Impor-



**Figure 1.** Structures of ethepron (molecular weight 144.5) and ethepron dianion ( $pK_{a1}$  2.5,  $pK_{a2}$  7.2) (1).

tantly, BChE sensitivity extends to subchronic human studies where a dose of 0.5 or 1.8 mg/kg/day for 16 and 28 days, respectively, gives significant BChE inhibition from which the reference dose of 0.018 mg/kg/day was established as the chronic dietary end point (6).

The mechanism for ethepron inhibition of BChE has many similarities to that for triester OPs with AChE or BChE. In both cases the inhibition is progressive and irreversible, suggesting a covalent derivatization reaction. Further, ethepron blocks human plasma BChE postlabeling with [<sup>3</sup>H]diisopropyl fluorophosphonate (DFP) at S198 (7) (Figure 2) leading to the proposal that it forms S198-phospho-BChE (7). Although the sensitivity of BChE to ethepron is clearly defined and the mechanism partially understood, it is not known if other enzymes might be even more sensitive as markers of exposure. This study uses three new approaches in examining the mechanism and specificity of ethepron as an esterase inhibitor. First, the proposed inhibition of human BChE by a phosphorylation reaction at S198 is evaluated using [<sup>33</sup>P]ethepron (Figure 2). Second, recombinant BChE (rBChE) mutants are used to determine the importance of specific amino acids near the active site in the inhibition reaction. Third, esterase specificity studies are made for the first time to determine if BChE is the most

\* To whom correspondence should be addressed. Phone: (510) 642-5424. Fax: (510) 642-6497. E-mail: ectl@nature.berkeley.edu.

<sup>†</sup> University of California.

<sup>‡</sup> University of Nebraska Medical Center.

<sup>1</sup> Abbreviations: AChE, acetylcholinesterase; ATCh, acetylthiobaline; BChE, butyrylcholinesterase; BME, 2-mercaptoethanol; BTCh, butyrylthiobaline; CPO, chlorpyrifos oxon; DFP, diisopropyl fluorophosphonate; DTT, dithiothreitol; IC<sub>50</sub>, median inhibitory concentration; NA, 1-naphthyl acetate; NB, 1-naphthyl butyrate; NPA, 4-nitrophenyl acetate; NPB, 4-nitrophenyl butyrate; OP, organophosphorus; PAGE, polyacrylamide gel electrophoresis; rBChE, recombinant BChE; SDS, sodium dodecyl sulfate.

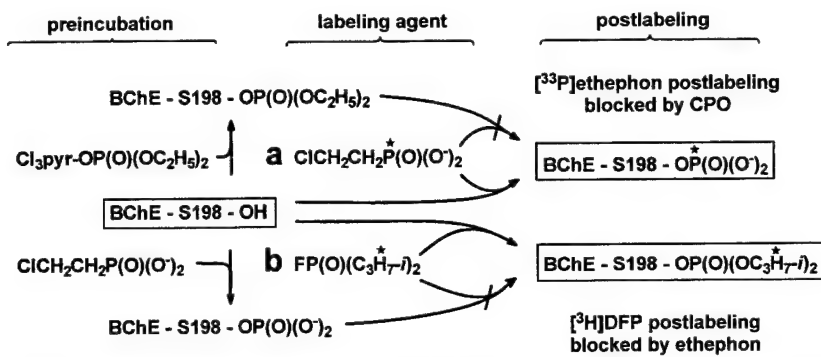


**Figure 2.** BChE is labeled at S198 by  $[^{33}\text{P}]$ ethephon or  $[^3\text{H}]$ DFP. (a) Preincubation with unlabeled chlorpyrifos oxon ( $\text{Cl}_3\text{pyr} = 3,5,6$ -trichloro-2-pyridinyl) blocks postlabeling with  $[^{33}\text{P}]$ ethephon (this study). (b) Preincubation with unlabeled ethephon blocks postlabeling with  $[^3\text{H}]$ DFP (7). The site of BChE dialkylphosphorylation is S198 for DFP (8) and by analogy for CPO.

sensitive esterase in vitro and in vivo or if it is only one of many undergoing inhibition.

## Materials and Methods

**Chemicals.** Ethepron was obtained from Chem Service (West Chester, PA) and  $[^{33}\text{P}]$ ethephon (0.42 mCi/mmol) was prepared in the Berkeley laboratory (9). Reagents for native- and sodium dodecyl sulfate (SDS)-polyacrylamide gel electrophoresis (PAGE) included SDS from Boehringer Mannheim (Indianapolis, IN); Coomassie Brilliant Blue R-250 and 2-mercaptoethanol (BME) from Bio-Rad (Hercules, CA); bromophenol blue and dithiothreitol (DTT) from Fisher (Fair Lawn, NJ); molecular weight marker proteins from Bio-Rad and GibcoBRL (Gaithersburg, MD). Other chemicals were obtained as follows: acetylthiocholine (ATCh) iodide, butyrylthiocholine (BTCh) iodide, 1-naphthyl acetate (NA), 1-naphthyl butyrate (NB), 4-nitrophenyl acetate (NPA), 4-nitrophenyl butyrate (NPB), Fast Garnet GBC, and dithiooxamide from Sigma (St. Louis, MO); chlorpyrifos oxon (CPO) from Dow Agrosciences (Indianapolis, IN).

**Electrophoresis.** For SDS- or native-PAGE, an 8% resolving gel and 5% stacking gel were used in a Bio-Rad Mini-PROTEAN II vertical electrophoresis cell unless specified otherwise. For SDS-PAGE, samples were solubilized in 30–50  $\mu\text{L}$  sample loading dye [62.5 mM Tris-HCl pH 7.4, 37.5% glycerol, 2% SDS, 6.25% BME and 0.04% bromophenol blue; modified from Laemmli (10)] and/or 30–50  $\mu\text{L}$  of modified sample loading buffer (50 mM Tris-HCl pH 8.0, 1% SDS, 5 mM EDTA, and 10 mM DTT), then denatured at 65 °C in a water bath for 5 min, cooled, and quickly centrifuged. For native-PAGE, the sample loading dye contained no SDS or BME and samples were not denatured. The running buffer was Tris-glycine (5 mM Tris, 50 mM glycine) with 0.02% SDS for denaturing gels or no SDS for native gels. Gels were run at 50–100 V according to the manufacturer's instructions until the dye front reached the bottom. Proteins were stained with Coomassie Brilliant Blue R-250 (0.1% in 40% aqueous methanol with 10% acetic acid) for 4 h followed by destaining overnight and then rehydrated in distilled water. Gels were dried on Whatman 3 MM chromatography paper for 2 h in a Bio-Rad Model 543 Gel Dryer. Protein markers were used for determination of kD (SDS-PAGE) or apparent kD (native-PAGE).

**Enzymes and Tissue Preparations.** Human and mouse plasma were obtained from CalBiochem (La Jolla, CA). rBChE secreted by Chinese Hamster Ovary cells was used as the wild-type at 90–95% purity (11) or for comparison of wild-type with various mutants (D70G, D70N, D70K, G117H, G117K, E197Q, A328F, A328W, and A328Y) (12–19). Human erythrocyte AChE, serum albumins (human, mouse, and bovine), bovine pancreas trypsin and  $\alpha$ -chymotrypsin, porcine liver carboxylesterase, porcine pancreas cholesterol esterase, rabbit muscle phosphorylase a and b, and jack bean urease were obtained from Sigma (St. Louis, MO). Protein content was provided by the supplier or determined by the method of Bradford (20).

Sprouts of mung bean (*Phaseolus aureus*) were processed to extract cholinesterase according to Kasturi and VasanthaRajan (21) and Fluck and Jaffe (22). Roots at 50% (w/v) in 50 mM Tris-HCl pH 8.0 were ground in a Waring blender. The pellet from centrifugation (5,000  $\times$  g, 4 °C, 5 min) of the homogenate was reground in half the original volume of 5%  $(\text{NH}_4)_2\text{SO}_4$  to extract the esterase, shaken on ice for 1 h, and centrifuged (25000g, 4 °C, 15 min). Proteins in the supernatant were concentrated in an Amicon Centrifuge YM-30 (Millipore, Bedford, MA). Enzymatic activity was determined with 1 mM ATCh by the method of Ellman et al. (23).

Plasma, liver, and brain from male albino Swiss-Webster mice were used as sources of esterases. The mice received either ethephon (200 mg/kg i.p., neutralized in 600 mM  $\text{Na}_2\text{CO}_3$ ) in 250 mM Tris-HCl pH 8.0 or Tris-HCl only as a control. They were sacrificed 1 h after these asymptomatic treatments and tissues were fractionated and frozen immediately. Blood was collected in 105 mM sodium citrate and centrifuged to obtain plasma. Liver and brain were homogenized at 20% (w/v) in buffer (250 mM sucrose for liver or 350 mM sucrose for brain, 1 mM EDTA, and 10 mM Tris-HCl, pH 7.4). For in vitro experiments, the liver homogenate was compared with the cytosol fraction (supernatant, 50000g, 60 min, 4 °C). For in vivo experiments, the membrane fraction (500g supernatant, 100000g pellet) from liver and brain was resuspended to the original volume with buffer for comparison with the supernatant or cytosol fraction.

**Phosphorylation of Human rBChE by  $[^{33}\text{P}]$ Ethepron.** rBChE (90–95% pure) was incubated with  $[^{33}\text{P}]$ ethephon and the labeled phosphoprotein analyzed by SDS-PAGE. More specifically,  $[^{33}\text{P}]$ ethephon (1.2 mg, 3.5  $\mu\text{Ci}$ ) in methanol (15  $\mu\text{L}$ ) was placed in an Eppendorf tube (0.5 mL), the solvent was allowed to evaporate at 25 °C, and the diacid was converted to the dianion by adding  $\text{Na}_2\text{CO}_3$  (15  $\mu\text{L}$  of 1.2 M). rBChE (200  $\mu\text{g}$  of protein) was then added in phosphate buffer (200 mM, pH 8.0) to make a final volume of 170  $\mu\text{L}$ . rBChE pretreated with CPO (120  $\mu\text{M}$ , 15 min, 25 °C) to inhibit esteratic activity was used as a control. After incubation for 18 h at 25 °C, aliquots of the samples (30 or 100  $\mu\text{g}$  of protein) were subjected to SDS-PAGE in comparison with untreated rBChE (3  $\mu\text{g}$ ) visualized by Coomassie staining. Labeled proteins on the dried gels were detected with a Storm 860 PhosphorImager (Molecular Dynamics, Sunnyvale, CA) or by autoradiography with a Biomass or Biomax screen and film (Kodak, Rochester, NY).

**Sensitivity of rBChE Mutants and Esterases to Ethepron with Colorimetric Analysis.** The Ellman method (23) was used to determine cholinesterase activity of rBChE mutants, serum albumin, plasma, and tissue homogenates and their inhibition by ethephon. The described procedure (7) was modified in BTCh or ATCh substrate concentration (1 mM). The buffer was phosphate (100 mM, pH 7.4, unless specified otherwise). The absorbance change was measured at 405 nm in 10 s intervals for 5–7 min on a UVmax plate reader (Molecular Devices, Sunnyvale, CA), and three to four replicates were used. NPA and NPB were also used as substrates at

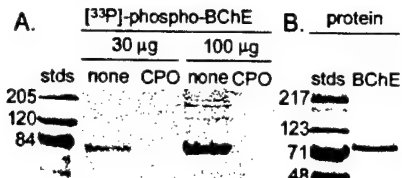


**Figure 3.**  $[^{33}\text{P}]$ Phospho-BChE from reaction of human rBChE with  $[^{33}\text{P}]$ ethephon. Analyses by SDS-PAGE. (A) Labeling of BChE (30 or 100  $\mu\text{g}$  of protein) by  $[^{33}\text{P}]$ ethephon but not of BChE pretreated with CPO as detected by phosphorimaging. (B) BChE protein (3  $\mu\text{g}$ ) detected by Coomassie blue.

1 mM monitoring the absorbance change at 405 nm. Concentrations for 50% inhibition ( $IC_{50}$ s) were calculated from linear activity rate data with ethephon at 1, 3, 10, 30  $\mu\text{M}$ , etc.

**Sensitivity of Esterases to Ethepron with Native-PAGE Analysis.** Esterases in human and mouse plasma, mouse liver homogenate, and mouse liver and brain membranes and cytosol (200  $\mu\text{g}$  of protein) analyzed by native-PAGE were detected specifically for BChE with BTCh (24) and generally with NA or NB (25–27). For BChE detection, the gel was first shaken at room temperature in buffer (67 mM phosphate pH 6.1, 10 mM glycine, 2 mM  $\text{Cu}_2\text{SO}_4$ , and 30 mM  $\text{Na}_2\text{SO}_4$ ) for 30 min, then with fresh buffer containing 0.1% BTCh for 2–4 h. The reaction was stopped by holding the gel in 3 M  $(\text{NH}_4)_2\text{SO}_4$  at 4 °C overnight. BChE isozymes were revealed as dark green bands after 2–4 h incubation at room temperature in 3 M  $(\text{NH}_4)_2\text{SO}_4$  saturated with dithiooxamide. Several rinses in 7% acetic acid rehydrated the gel and restored a clear background. For general esterase detection, gels were gently shaken at room temperature in 50 mM Tris-HCl pH 8.0 (50 mL) containing 200 mM 1-naphthyl ester substrate (added to the buffer in 400  $\mu\text{L}$  of ethanol containing 2% Triton X-100) for up to 1 h. The gel was rinsed with several changes of distilled water and stained with Fast Garnet GBC (0.05% in 50 mM Tris-HCl pH 8.0) until bands developed. To stop the reaction the gel was rinsed thoroughly, first with distilled water and finally with 1% acetic acid, before drying. Incubation times with substrate and dye were optimized for high sensitivity with reduced background. The substrates NA and NB were both used successfully without significant difference. For in vitro inhibition studies, the esterase preparation was incubated with ethephon for 90 min at 25 °C prior to loading and running native-PAGE. For in vivo studies, mice and tissues were treated as above.

**Data Presentation.** SigmaPlot, HP PrecisionScan LT, and Adobe PhotoDeluxe software were used to generate graphs and acquire images.

## Results

**$[^{33}\text{P}]$ Phospho-BChE from Reaction of Human rBChE with  $[^{33}\text{P}]$ Ethepron.** According to the proposed inhibition mechanism, BChE-S198 should be labeled on incubation with  $[^{33}\text{P}]$ ethephon in a mole for mole reaction (Figure 2). To test this hypothesis purified rBChE was required in microgram amounts because of the low specific activity of  $[^{33}\text{P}]$ ethephon at the time of the experiment. The analysis is straightforward since the enzyme appears as a single band at about 80 kDa by SDS-PAGE with Coomassie blue (Figure 3B). Treatment with  $[^{33}\text{P}]$ ethephon labels this same band as detected by phosphorimaging (Figure 3A) and, in a separate experiment, also by autoradiography (data not shown). Importantly, in both experiments, pretreatment with CPO blocks all labeling with  $[^{33}\text{P}]$ ethephon. The site at which CPO reacts to inhibit esteratic activity is therefore the same as that phosphorylated by ethephon.

**Attempted Phosphorylation of Other Proteins by  $[^{33}\text{P}]$ Ethepron.** The labeling reaction with  $[^{33}\text{P}]$ ethephon

**Table 1. Effect of Amino Acid Substitutions on Sensitivity of rBChE to Ethepron**

rBChE	$IC_{50}$ ( $\mu\text{M}$ $\pm$ SD, $n = 3$ –8) <sup>a</sup>	
	90 min	24 h
wild-type	more sensitive to ethephon	
D70N	38 $\pm$ 2	0.3 $\pm$ 0.1 <sup>b</sup>
D70K	13 $\pm$ 15	
D70G	13 $\pm$ 4	
E197Q	121 $\pm$ 5	
	45 $\pm$ 30	<2
A328F	less sensitive to ethephon	
A328W	173 $\pm$ 13	
A328Y	>256	
G117H	>256	33 $\pm$ 2
G117K	>256	34 $\pm$ 3

<sup>a</sup> Preincubation of rBChE with ethephon for 90 min or 24 h before BTCh added. <sup>b</sup> Human plasma instead of rBChE.

at low specific activity was successful for BChE but not for several other proteins (30  $\mu\text{g}$  each) in the same experiment as analyzed by SDS-PAGE and phosphorimaging. Thus, purified BChE gave a labeled band of appropriate kilodaltons and blocked by CPO but none of the following proteins showed labeling: human serum albumin, bovine serum albumin, trypsin,  $\alpha$ -chymotrypsin, phosphorylase a, phosphorylase b, and urease. In addition, labeling was not observed with human plasma since its BChE content was only about  $1 \times 10^{-5}$  of the total protein.

**Effect of Amino Acid Substitutions on Sensitivity of rBChE to Ethepron (Table 1).** The rBChE variants examined fall into two groups in their sensitivity to ethephon. The more sensitive set is the wild type and mutants at D70 (D70N, D70K, and D70G) and E197 (E197Q) with  $IC_{50}$ s of 13–121  $\mu\text{M}$ . The less sensitive set has mutations at A328 (A328F, A328W, and A328Y) and G117 (G117H and G117K) with  $IC_{50}$ s of 173  $\rightarrow$  256  $\mu\text{M}$ . Thus, substitutions at D70 and E197 do not greatly alter sensitivity to ethephon while those at A328 and G117 have a much greater effect in lowering the sensitivity.

**Effect of pH, Divalent Cations and Albumin on Human Plasma BChE Sensitivity to Ethepron.** The inhibitory potency of ethephon should vary with pH if the reactive species is the dianion (7) (Figure 1). To test this hypothesis, the inhibition reaction was carried out in 50 or 100 mM phosphate at pH 5, 6, 7.4, 8, or 9 for 90 min then the pH was adjusted to 7.4 with the addition of BTCh and DTNB for assay of residual enzymatic activity. The same high inhibitory potency ( $IC_{50}$  20–30  $\mu\text{M}$ ) was observed at pH 7.4, 8, and 9 with much lower potency (essentially no inhibition at 300  $\mu\text{M}$ ) at pH 5 and 6 (Figure 4).

Divalent cations ( $\text{Mg}^{2+}$ ,  $\text{Ca}^{2+}$ , and  $\text{Mn}^{2+}$ ) were examined for possible effects on the inhibition reaction. There was no significant change in BChE activity with 10–3000  $\mu\text{M}$  of any divalent cation examined and no change in the  $IC_{50}$  when  $\text{Mg}^{2+}$  was 0.1, 1, and 10 times the ethephon concentration (data not shown). With high divalent cation concentration the  $IC_{50}$  decreased 2-fold with  $\text{Mg}^{2+}$ , 1.4-fold with  $\text{Ca}^{2+}$ , and remained unchanged with  $\text{Mn}^{2+}$  compared to the control (Table 2).

Human serum albumin was examined as a major plasma component potentially altering BChE sensitivity to ethephon. There was no difference in the sensitivity of human plasma and human albumin ( $IC_{50}$  31–34  $\mu\text{M}$ ). The  $IC_{50}$  also changed less than 2-fold for ethephon and

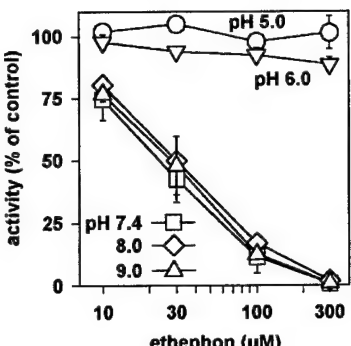


**Figure 4.** Effect of pH on human plasma BChE sensitivity to ethephon. The buffer was 50 mM phosphate at pH 5 and 6 and 100 mM phosphate at pH 7.4, 8, and 9.

**Table 2. Effect of Divalent Cations on Human Plasma BChE Sensitivity to Ethepron**

cation (mM) <sup>a</sup>	treatment	control
Mg <sup>2+</sup> (11)	9.2 ± 0.9	21.1 ± 1.4
Ca <sup>2+</sup> (23) <sup>b</sup>	15.7 ± 0.5	21.5 ± 0.8
Mn <sup>2+</sup> (0.007)	15.5 ± 2.1	17.1 ± 2.6

<sup>a</sup> Concentration 10 times greater than that of normal plasma (28). <sup>b</sup> Poor reproducibility in other experiments, possibly due to some precipitation.

eserine (a selective BChE inhibitor) comparing human plasma (1:30 dilution) and human plasma (1:30 dilution) in 5% albumin (data not shown).

**Specificity of Ethepron as a BChE Inhibitor. (1) Esterases in Human and Mouse Plasma Assayed by Native-PAGE with BTCh and NA Substrates (Figure 5).** Esterases in human and mouse plasma were examined for sensitivity to ethephon in vitro (0, 1, 10, and 100 μM) and in mouse plasma for inhibition in vivo (0 and 200 mg/kg, 1 h). BTCh with human and mouse plasma revealed two principal bands, i.e., 1 at >170 apparent kDa and 2 at 150–170 apparent kDa, plus a doublet for mouse plasma at 90–120 apparent kDa in position 3. The BChE isozymes in both human and mouse plasma are inhibited by ethephon detectably with 1 μM, strongly with 10 μM and completely with 100 μM, with bands 2 and 3 probably more sensitive than 1. A faint band (not evident in the figure) appeared with both human and mouse plasma at position 5 at or near albumin but was not sensitive to ethephon at 100 μM. In the in vivo study, as in vitro, BChE activity from plasma of treated mice was either strongly inhibited (band 1) or abolished (band 2) and band 5 was detected weakly and not inhibited.

NA detects BChE in human plasma (band 1 strongly plus 2 and 3 weakly and not evident in the figure) and mouse plasma (bands 1 and 2). Albumin or another esterase of similar position appears in both cases as band 5 and mouse plasma also gives a doublet band 4 and (only with NB) a weak band 6 (not evident in the figure). With both human and mouse plasma, the BChE bands are sensitive to ethephon (10 and 100 μM) in vitro as are also mouse bands 4 and 6 whereas band 5 is not sensitive. In the in vivo experiment only BChE band 1 was clearly inhibited.

**(2) Esterases in Mouse Liver (Figure 6) and Brain Assayed by Native-PAGE with BTCh and NA Substrates.** A BTCh-hydrolyzing esterase, probably BChE, from liver homogenate appears as band 1 at >200 kDa

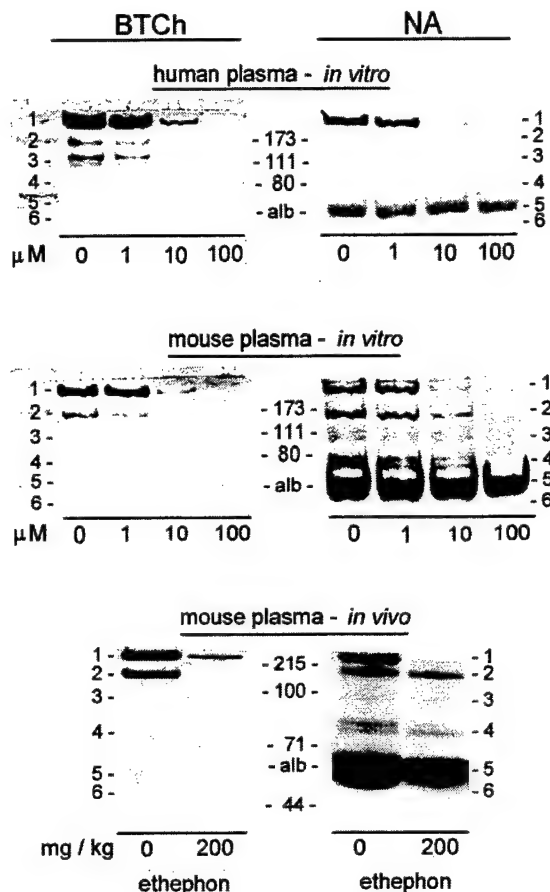


**Figure 5.** Sensitivity of human plasma esterases in vitro and mouse plasma esterases in vitro and in vivo to ethephon. Assays by native-PAGE with BTCh and NA substrates. Incubations in vitro for 90 min at 25 °C. Mice in vivo sacrificed 1 h after ip dose. kDa values are shown based on marker proteins. The esterase components are referred to by number and apparent kDa relative to the marker proteins.

and is clearly inhibited by ethephon in vitro at 10–100 μM. Liver cytosolic BChE in band 1 is also strongly inhibited in vivo (200 mg/kg) whereas membrane esterases in bands 1 and 5 are not inhibited.

With NA as the substrate, at least 11 esterase bands (not all designated by number) appear in mouse liver homogenate of which bands 1 and 3 are most sensitive to 10 μM ethephon, bands 2 and 5 (each with two or more esterases present) and 6 are inhibited at 100 μM, and 4 is insensitive in vitro. Although not illustrated, in cytosol only bands 1 and 3 are sensitive to 10 μM ethephon and band 6 is sensitive with 100 μM. In vivo inhibition is evident with liver esterase band 1 in cytosol but not with any of the other esterases in cytosol or membranes.

Brain esterases from in vivo treatment (200 mg/kg) were also examined and BChE in the cytosol assayed with BTCh was sensitive (data not shown). Activity in membranes was not sufficient for assay with BTCh. No ethephon-sensitive esterase was detected with NA either in the cytosol or membranes.

**(3) Esterases from Several Sources Assayed Colorimetrically with Thiocholine and 4-Nitrophenyl Esters as Substrates (Table 3).** The comparisons included plasma, liver homogenate, serum albumin, purified enzymes, and a plant cholinesterase. The three most sensitive preparations with IC<sub>50</sub> values of 27–34 μM were human and mouse plasma and human serum

**Table 3. Sensitivity to Ethepron of Esterases from Several Sources Assayed Colorimetrically with Thiocholine and 4-Nitrophenyl Esters as Substrates**

enzyme or preparation	BTCh or ATCh <sup>a</sup>	IC <sub>50</sub> ( $\mu$ M $\pm$ SD, n = 3-4)	NPA	NPB
human plasma	31 $\pm$ 11 <sup>b</sup>			700 $\pm$ 180
mouse plasma	27 $\pm$ 16			770 $\pm$ 78
mouse liver homogenate	250 $\pm$ 52		670 $\pm$ 32	580 $\pm$ 35
human albumin	34 $\pm$ 3 <sup>b</sup>		>1000 (0) <sup>c,d</sup>	>1000 (30) <sup>c</sup>
mouse albumin			>1000 (35) <sup>c,d</sup>	720 $\pm$ 220
bovine albumin			>1000 (35) <sup>c,d</sup>	380 $\pm$ 520
AChE	1300 $\pm$ 600			
trypsin			>1000 (25) <sup>c</sup>	>1000 (0) <sup>c</sup>
$\alpha$ -chymotrypsin			>1000 (35) <sup>c</sup>	>1000 (45) <sup>c</sup>
cholesterol esterase				>300 (10) <sup>c</sup>
carboxylesterase				>1000 (45) <sup>c</sup>
mung bean cholinesterase	2200 $\pm$ 220 <sup>c</sup>			

<sup>a</sup> BTCh for plasma, liver homogenate, and albumin; ATCh for human erythrocyte AChE and mung bean preparation. <sup>b</sup> The same IC<sub>50</sub> is observed with BTCh and human plasma or human albumin because BChE is a component in plasma and an impurity in the albumin preparation used. <sup>c</sup> Inhibition (%) at 1000  $\mu$ M. <sup>d</sup> Low activity required 500  $\mu$ g protein per assay. <sup>e</sup> Inhibition of 65% with 6 mM eserine (30 min).

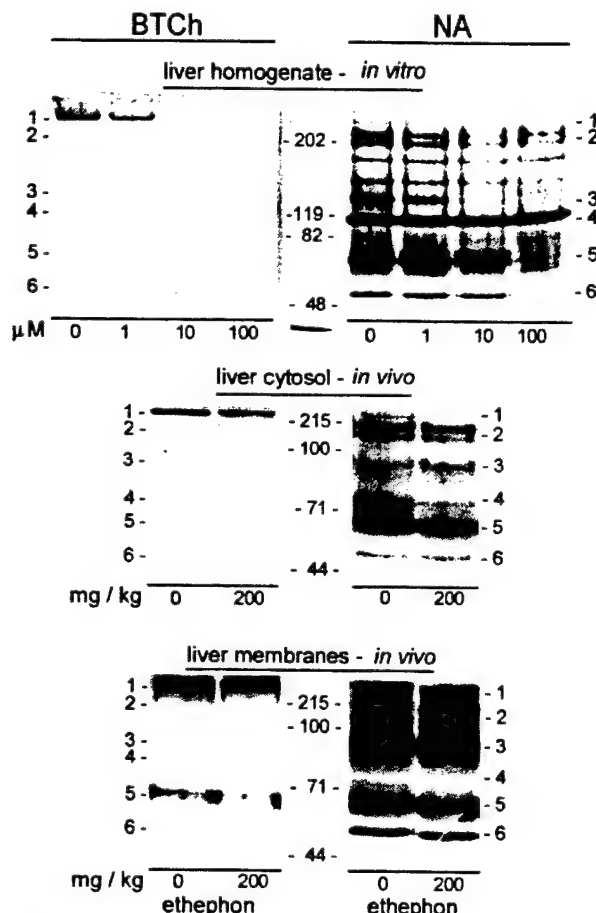


**Figure 6.** Sensitivity to ethephon of mouse liver homogenate esterases in vitro and mouse liver cytosolic and membrane esterases in vivo. Inhibition and assay conditions were the same as those in Figure 5 except for analysis of the homogenate (top panels) which utilized a 6% resolving gel in a Bio-Rad PROTEAN II system.

albumin assayed with BTCh. Intermediate sensitivities (IC<sub>50</sub>s 250–770  $\mu$ M) were observed for mouse liver homogenate with BTCh and NPA and plasma (human and mouse), liver homogenate, and serum albumin (bovine and mouse) with NPB. Other serum albumin assays (human, mouse, and bovine with NPA and human with NPB) are less sensitive (IC<sub>50</sub> > 1000  $\mu$ M). All other enzymes or preparations assayed gave IC<sub>50</sub> values of > 1000  $\mu$ M including AChE, trypsin,  $\alpha$ -chymotrypsin,

cholesterol esterase, and carboxylesterase from mammals and a cholinesterase preparation from mung bean.

## Discussion

**Phosphorylation of Alcohols, BChE and Other Proteins by Ethepron.** Ethepron as the dianion phosphorylates primary alcohols in the presence of water (29, 30). This observation serves as the model for the proposed phosphorylation by ethephon of the BChE active site (7, 29–32). BChE in human plasma is inhibited slowly but progressively by ethephon, leading to the proposal that it undergoes covalent derivatization at its active site (7, 30, 31). More specifically, ethephon inhibition of enzymatic activity is correlated with inhibition of postlabeling by [<sup>3</sup>H]DFP, thereby indicating that ethephon competes for the same position as [<sup>3</sup>H]DFP, i.e., S198 (7) (Figure 2). Ethephon could inhibit by phosphorylation, by derivatization with the chloroethyl moiety, or by reaction of the liberated ethylene. Ethephon is a very poor alkylating agent relative to phosphorylating agent (29–32). Further, it might not derivatize only S198 but also other sites in BChE. These questions can be answered with [<sup>33</sup>P]ethephon, prompting its radiosynthesis (9) at low but adequate specific activity for use with purified BChE, but not with plasma due to its low BChE content. The experiment used unlabeled CPO for diethylphosphorylation of purified rBChE, specifically at S198, resulting in complete block of postlabeling by [<sup>33</sup>P]ethephon, i.e., ethephon phosphorylates S198 and no other site under the reaction conditions examined (Figure 2). As a further test of specificity, [<sup>33</sup>P]ethephon was incubated with other enzymes or proteins having esteratic activity, but no phosphorylation was detected with human or bovine serum albumin, trypsin,  $\alpha$ -chymotrypsin, phosphorylase a and b, or urease.

**Proposed Mechanisms of Activation of BChE and Ethepron Dianion Leading to Phosphorylation at S198.** The observed effects of amino acid substitutions on the sensitivity of rBChE to ethephon dianion, combined with earlier studies cited above, lead to the proposed mechanisms shown in Figure 7. It is suggested that E325 and H438 activate S198 in the catalytic triad and the main chain NH groups of G116, G117, and A199 in the oxyanion hole stabilize ethephon dianion as a tetrahedral intermediate. Mutations at D70 and E197 have much less effect on the potency of ethephon than those at A328 and G117. Retention of most of the

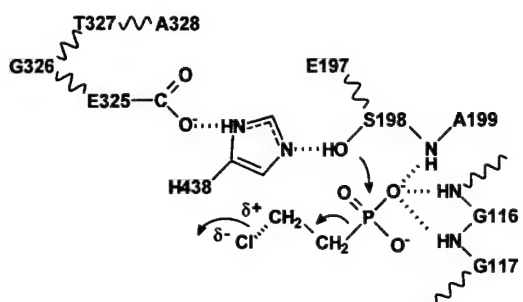


**Figure 7.** Proposed mechanism of BChE inhibition by ethephon dianion as a tetrahedral intermediate analogue leading to phosphorylation at S198. In the catalytic triad (upper portion), E325 and H438 activate S198 in the usual manner. In the oxyanion hole (right portion), the main chain NH groups of G116, G117, and A199 stabilize one of the negatively charged oxygens and the other one may be stabilized by residues at the bottom of the gorge. Slow dissociation of chloride is the first and rate-limiting step in the phosphorylation with liberation of ethylene. Proposal based on Haux et al. (7), Lockridge et al. (14), and Zhang and Casida (32).

sensitivity in the D70N, D70K, and D70G mutants, lacking the carboxylate moiety of aspartic acid, indicates that the phosphorylation reaction is not affected by either charge-state alterations in the peripheral anionic site or the resulting conformational changes relative to W82 in the active-site gorge (13). The E197Q mutation, perturbing the strength of H-bonds and the arrangement of water molecules in the vicinity of S198 (19), does not affect the inhibition reaction. Replacement of A328 with an aromatic amino acid (A328F, A328W, and A328Y) reduces the sensitivity, perhaps due to impeded access to the active site gorge (17). The equivalent residues F and Y in Torpedo and human AChE, respectively (11), may account for their low sensitivity to ethephon. The G117H and G117K mutations in the oxyanion hole reduce the rate of phosphorylation at S198, probably by interfering with hydrogen bonding between the glycine-N-H substituents (12, 14) and ethephon dianion. As an alternative, the G117H mutant is known to hydrolyze paraoxon, sarin, echothiophate, and VX (12, 14) and perhaps might also hydrolyze ethephon to account for the difference from wild type in  $IC_{50}$  values of  $>200 \mu M$  at 90 min or  $>100$ -fold at 24 h.

**Factors Affecting Human Plasma BChE Sensitivity to Ethepron.** The apparent high sensitivity of human plasma BChE to ethephon in vivo, i.e., significant inhibition at 0.5 mg/kg/day for 16 days (6), is somewhat surprising in light of its relatively low potency in vitro, i.e.,  $IC_{50}$  10–30  $\mu M$  with 90 min incubation at 25 °C (7 and this study). Perhaps the reaction of ethephon with plasma or purified rBChE in vitro does not truly reflect the inhibitory conditions in vivo. Factors that could affect either BChE or ethephon in their reaction together include pH, divalent cations, and albumin. The pH effect was examined during the phosphorylation reaction with readjustment to standard pH for the activity assay. Much higher inhibition occurs at pH values where ethephon is the dianion than when it is a monoanion. Phosphorylation of BChE by ethephon dianion bound at the active site is proposed to involve dissociation of chloride as the first and rate-limiting step (32). This proposal is based on ethephon dianion being the reactive species. Alternatively, the poor inhibition at lower pH could also be due to an unfavorable protonation state of the active site, e.g., H438.

The divalent cations  $Ca^{2+}$ ,  $Mg^{2+}$ , and  $Mn^{2+}$  increase cholinesterase activity (33) and might therefore alter the potency of ethephon for BChE inhibition. At concentrations 10-fold greater than those in normal human plasma (28), there was little, if any, difference in ethephon inhibition. It is therefore unlikely that plasma divalent cations influence the effects of ethephon.

Albumin has esterase activity (34) and catalyzes some reactions of OP esterase inhibitors (35). It is present in plasma at a much higher level than BChE and might therefore alter the effectiveness of ethephon as a BChE inhibitor. However, this was not the case since the sensitivity of BChE activity to ethephon in vitro was not altered by albumin at plasma levels.

**Specificity of Ethepron as a BChE Inhibitor.** The discovery that ethephon is a BChE and to a lesser extent AChE inhibitor (4, 5) was not initially followed up by considering other esterases that might be even more sensitive. This is done here with native-PAGE separation of plasma, liver, and brain proteins and determination of esterase activity with BTCh and NA. Human and mouse plasma contain many esterases (36, 37), including BChE isozymes sensitive to ethephon in vitro and in vivo. In various plasma, the BChE sensitivity to ethephon decreases in the order of dog (most sensitive) > human = mouse > rat (7), suggesting mouse BChE as a model for human BChE. Other esterases in plasma are also observed with NA and NB, but they are less sensitive than BChE to ethephon. Although several plasma and liver esterases are sensitive in vitro, BChE is most sensitive in vivo. An esterase behaving like BChE was the only enzyme in mouse brain observed to be sensitive to ethephon in vitro and in vivo. Colorimetric assays were also used to survey purified enzymes, but none of those tested showed high sensitivity. The apparent sensitivity of human serum albumin is probably due to BChE as a contaminant. The colorimetric determination survey included tissue preparations, each containing several esterases evident by electrophoresis. Human and mouse plasma BChE remained the most sensitive with  $IC_{50}$  values of approximately 30  $\mu M$ . Plasma esterases detected with NPB were also sensitive, but at concentrations typically 20-fold greater. Of all the esterases considered, BChE remained the most sensitive in vitro and in vivo to ethephon.

Many plants have cholinesterases (38) and acetylcholine (39), suggesting a cholinergic system somewhat like that in animals (40). Mung bean cholinesterase is similar to AChE in being inhibited by methylcarbamate and organophosphorus compounds (41). Since ethephon is both a BChE inhibitor and phosphorylating agent in mammals, perhaps plant cholinesterase or other plant enzymes are also sensitive and phosphorylated as a possible contributor or alternative to ethylene in regulating plant growth; this possibility is neither supported nor ruled out by the present findings.

**Toxicological Relevance of Esterase Inhibition.** BChE in human and mouse plasma is the most sensitive esterase target for ethephon under the test conditions. Although BChE inhibition may sensitize animals experimentally to compounds detoxified by this enzyme, e.g., succinylcholine (42), aspirin (43), and cocaine (44), these are unlikely combinations under normal use conditions. The physiological significance of other ethephon-sensitive esterases is poorly defined. No other proteins examined in vitro were radiolabeled by ethephon. In conclusion,

BChE inhibition continues to be the most sensitive marker of ethepron exposure.

**Acknowledgment.** We thank our Berkeley colleagues Nanjing Zhang, Yoffi Segall, Gary Quistad, and Susan Sparks for their suggestions and assistance. The project described was supported by Grant R01 ES008762 (to J.E.C.) from the National Institute of Environmental Health Sciences (NIEHS), National Institutes of Health (NIH), and its contents are solely the responsibility of the authors and do not necessarily represent the official views of the NIEHS (NIH). It was also supported by Grant DAMD17-01-1-0776 (to O.L.) from the U.S. Medical Research and Material Command.

## References

- Tomlin, C. D. S., Ed. (2000) *The Pesticide Manual*, 12th ed., pp 359–360, British Crop Protection Council, Farnham, Surrey, U.K.
- Gianessi, L. P., and Marcelli, M. B. (2000) *Pesticide Use in U.S. Crop Production: 1997. National Summary Report*, National Center for Food and Agricultural Policy, Washington, DC.
- California Department of Pesticide Regulation (2001) *Summary of Pesticide Use Report Data 2000 Indexed by Chemical*, Sacramento, CA.
- Hennighausen, G., Tiefenbach, B., and Lohs, Kh. (1977) Der Einfluss von 2-Chloräthylphosphonsäure (Ethepron) auf die Aktivität von Cholinesterasen in vivo und in vitro in Beziehung zur akuten Toxizität. *Pharmazie* 32, 181–182.
- Hennighausen, G., and Tiefenbach, B. (1978) Über die Mechanismen der akuten toxischen Wirkung von Chlortholinchlorid und 2-Chloräthylphosphonsäure (Ethepron). *Arch. Exp. Veterinaermed* 32, 609–621.
- Environmental Protection Agency (1997) Rhône-Poulenc Ag Company; Pesticide Tolerance Petition Filing. *Fed. Regist.* 62 (10), 2149–2154.
- Haux, J. E., Quistad, G. B., and Casida, J. E. (2000) Phosphobutyrylcholinesterase: phosphorylation of the esteratic site of butyrylcholinesterase by ethepron [(2-chloroethyl)phosphonic acid] dianion. *Chem. Res. Toxicol.* 13, 646–651.
- Jansz, H. S., Brons, D., and Warringa, M. G. P. J. (1959) Chemical nature of the DFP-binding site of pseudocholinesterase. *Biochim. Biophys. Acta* 34, 573–575.
- Zhang, N., and Casida, J. E. (2001) Novel synthesis of [<sup>33</sup>P]-{(2-chloroethyl)phosphonic acid}. *J. Org. Chem.* 66, 327–329.
- Laemmli, U. K. (1970) Cleavage of structural proteins during the assembly of the head of bacteriophage T4. *Nature* 227, 680–685.
- Nachon, F., Nicolet, Y., Viguié, N., Masson, P., Fontecilla-Camps, J. C., and Lockridge, O. (2002) Engineering of a monomeric and low-glycosylated form of human butyrylcholinesterase. Expression, purification, characterization, and crystallization. *Eur. J. Biochem.* 269, 630–637.
- Millard, C. B., Lockridge, O., and Broomfield, C. A. (1995) Design and expression of organophosphorus acid anhydride hydrolase activity in human butyrylcholinesterase. *Biochemistry* 34, 15925–15933.
- Masson, P., Froment, M.-T., Bartels, C. F., and Lockridge, O. (1996) Asp70 in the peripheral anionic site of human butyrylcholinesterase. *Eur. J. Biochem.* 235, 36–48.
- Lockridge, O., Blong, R. M., Masson, P., Froment, M.-T., Millard, C. B., and Broomfield, C. A. (1997) A single amino acid substitution, Gly117His, confers phosphotriesterase (organophosphorus acid anhydride hydrolase) activity on human butyrylcholinesterase. *Biochemistry* 36, 786–795.
- Masson, P., Froment, M.-T., Bartels, C. F., and Lockridge, O. (1997) Importance of aspartate-70 in organophosphate inhibition, oxime re-activation and aging of human butyrylcholinesterase. *Biochem. J.* 325, 53–61.
- Masson, P., Legrand, P., Bartels, C. F., Froment, M.-T., Schopfer, L. M., and Lockridge, O. (1997) Role of aspartate 70 and tryptophan 82 in binding of succinylthiobutyrylcholinesterase to human butyrylcholinesterase. *Biochemistry* 36, 2266–2277.
- Saxena, A., Redman, A. M. G., Jiang, X., Lockridge, O., and Doctor, B. P. (1997) Differences in active site gorge dimensions of cholinesterases revealed by binding of inhibitors to human butyrylcholinesterase. *Biochemistry* 36, 14642–14651.
- Millard, C. B., Lockridge, O., and Broomfield, C. A. (1998) Organophosphorus acid anhydride hydrolase activity in human butyrylcholinesterase: synergy results in a somanase. *Biochemistry* 37, 237–247.
- Masson, P., Xie, W., Froment, M.-T., and Lockridge, O. (2001) Effects of mutations of active site residues and amino acids interacting with the  $\Omega$  loop on substrate activation of butyrylcholinesterase. *Biochim. Biophys. Acta* 1544, 166–176.
- Bradford, M. M. (1976) A rapid and sensitive method for the quantitation of microgram quantities of protein utilizing the principle of protein-dye binding. *Anal. Biochem.* 72, 248–254.
- Kasturi, R., and Vasantharajan, V. N. (1976) Properties of acetylcholinesterase from *Pisum sativum*. *Phytochemistry* 15, 1345–1347.
- Fluck, R. A., and Jaffe, M. J. (1974) Cholinesterases from plant tissues. III. Distribution and subcellular localization in *Phaseolus aureus* Roxb. *Plant Physiol.* 53, 752–758.
- Ellman, G. L., Courtney, K. D., Andres, V., Jr., and Featherstone, R. M. (1961) A new and rapid colorimetric determination of acetylcholinesterase activity. *Biochem. Pharmacol.* 7, 88–95.
- Dewald, B., Dulaney, J. T., and Touster, O. (1974) Solubilization and polyacrylamide gel electrophoresis of membrane enzymes with detergents. *Methods Enzymol.* 32, 82–91.
- Harris, H., and Hopkinson, D. A. (1976) *Handbook of Enzyme Electrophoresis in Human Genetics*, North-Holland Publishing: Amsterdam.
- Richardson, B. J., Baverstock, P. R., and Adams, M. (1986) *Allozyme Electrophoresis*, pp 175–176, Academic Press, NY.
- Pond, A. L., Coyne, C. P., Chambers, H. W., and Chambers, J. E. (1996) Identification and isolation of two rat serum proteins with A-esterase activity toward paraoxon and chlorpyrifos-oxon. *Biochem. Pharmacol.* 52, 363–369.
- Hill, R., and Mills, C. F. (1961) In *Biochemists' Handbook* (Long, C., Ed.) pp 839–885, Van Nostrand, Princeton, NJ.
- Maynard, J. A., and Swan, J. M. (1963) Organophosphorus compounds. I. 2-Chloroalkylphosphonic acids as phosphorylating agents. *Aust. J. Chem.* 16, 596–608.
- Segall, Y., Toia, R. F., and Casida, J. E. (1993) Mechanism of the phosphorylation reaction of 2-haloalkylphosphonic acids. *Phosphorus, Sulfur, Silicon* 75, 191–194.
- Segall, Y., Grendell, R. L., Toia, R. F., and Casida, J. E. (1991) Composition of technical ethepron [(2-chloroethyl)phosphonic acid] and some analogues relative to their reactivity and biological activity. *J. Agric. Food Chem.* 39, 380–385.
- Zhang, N., and Casida, J. E. (2002) Novel irreversible butyrylcholinesterase inhibitors: 2-chloro-1-(substituted-phenyl)ethylphosphonic acids. *Bioorg. Med. Chem.* 10, 1281–1290.
- Augustinsson, K.-B. (1948) Cholinesterases. A Study in Comparative Enzymology. *Acta Physiol. Scand.* 15 (Suppl. 52), 1–182.
- Casida, J. E., and Augustinsson, K.-B. (1959) Reaction of plasma albumin with 1-naphthyl *N*-methylcarbamate and certain other esters. *Biochim. Biophys. Acta* 36, 411–426.
- Eto, M., Oshima, Y., and Casida, J. E. (1967) Plasma albumin as a catalyst in cyclization of diaryl o-( $\alpha$ -hydroxyl)tolyl phosphates. *Biochem. Pharmacol.* 16, 295–308.
- Hunter, R. L., and Strachan, D. S. (1961) The esterases of mouse blood. *Ann. N. Y. Acad. Sci.* 94, 861–867.
- Augustinsson, K.-B. (1958) Electrophoretic separation and classification of blood plasma esterases. *Nature* 181, 1786–1789.
- Fluck, R. A., and Jaffe, M. J. (1974) The distribution of cholinesterases in plant species. *Phytochemistry* 13, 2475–2480.
- Tretyn, A., and Kendrick, R. E. (1991) Acetylcholine in plants: presence, metabolism and mechanism of action. *Botanical Rev.* 57, 33–73.
- Hartmann, E., and Gupta, R. (1989) Acetylcholine as a signaling system in plants. In *Second Messengers in Plant Growth and Development* (Boss, W. F., and Morré, J., Eds.) pp 257–287, A. R. Liss, NY.
- Riov, J., and Jaffe, M. J. (1973) Cholinesterases from plant tissues. I. Purification and characterization of a cholinesterase from mung bean roots. *Plant Physiol.* 51, 520–528.
- Sparks, S. E., Quistad, G. B., and Casida, J. E. (1999) Organophosphorus pesticide-induced butyrylcholinesterase inhibition and potentiation of succinylcholine toxicity in mice. *J. Biochem. Mol. Toxicol.* 13, 113–118.
- Masson, P., Froment, M.-T., Fortier, P.-L., Visicchio, J.-E., Bartels, C. F., and Lockridge, O. (1998) Butyrylcholinesterase-catalysed hydrolysis of aspirin, a negatively charged ester, and aspirin-related neutral esters. *Biochim. Biophys. Acta* 1387, 41–52.
- Sun, H., Yazal, J. E., Lockridge, O., Schopfer, L. M., Brimijoin, S., and Pang, Y.-P. (2001) Predicted Michaelis–Menten complexes of cocaine–butyrylcholinesterase. Engineering effective butyrylcholinesterase mutants for cocaine detoxification. *J. Biol. Chem.* 276, 9330–9336.

Submitted to Environmental Toxicology and Pharmacology June 2003

## **Life Without Acetylcholinesterase: The Implications of Cholinesterase Inhibitor Toxicity in AChE-Knockout Mice**

Oksana Lockridge<sup>a</sup>, Ellen G. Duysen<sup>a</sup>, Troy Voelker<sup>b</sup>, Charles M. Thompson<sup>b</sup>, Lawrence M. Schopfer<sup>a</sup>

<sup>a</sup>University of Nebraska Medical Center, Eppley Institute, Omaha NE 68198-6805 USA  
olockrid@unmc.edu

<sup>b</sup>University of Montana, Dept Pharmaceutical Sciences, Missoula, MT 59812-1552

**Abstract.** The acetylcholinesterase (AChE) knockout mouse is a new tool for identifying physiologically relevant targets of organophosphorus toxicants (OP). If AChE were the only important target for OP toxicity, then mice with zero AChE would have been expected to be resistant to OP. The opposite was found. AChE  $^{-/-}$  mice were supersensitive to the lethality of DFP, chlorpyrifos oxon, iso-OMPA, and the nerve agent VX. A lethal dose of OP caused the same cholinergic signs of toxicity in mice with zero AChE as in mice with normal amounts of AChE. This implied that the mechanism of toxicity of a lethal dose of OP in AChE  $^{-/-}$  mice was the same as in mice that had AChE, namely accumulation of excess acetylcholine followed by overstimulation of receptors. OP lethality in AChE- $^{-/-}$  mice could be due to inhibition of BChE, or to inhibition of a set of proteins. A search for additional targets used biotinylated-OP as a marker. Test tube experiments found that biotinylated-OP appeared to label as many as 55 proteins in the 100,000xg supernatant of mouse brain. Chlorpyrifos oxon bound a set of proteins (bands 12, 41, 45) that did not completely overlap with the set of proteins bound by diazoxon (bands 9, 12, 41, 47) or dichlorvos (bands 12, 23, 24, 32, 44, 45, 51) or malaoxon (band 9). These results support the idea that a variety of proteins could be interacting with a given OP to give the neurotoxic symptoms characteristic of a particular OP.

**1. Introduction.** The biochemical event that triggers convulsions and death after exposure to organophosphorus agents is inhibition of acetylcholinesterase. When AChE is inhibited, excess acetylcholine overstimulates acetylcholine receptors. This starts a cascade of neuronal excitation involving the glutamate receptors and excessive influx of calcium ions, that is responsible for the onset and maintenance of seizure activity (McDonough & Shih, 1997). Inhibition of AChE has been documented in thousands of papers, and is the gold standard for measuring exposure to OP. This understanding of the mechanism of OP toxicity has led to effective therapies against OP poisoning. Administration of atropine to block muscarinic receptors, of 2-PAM to reactivate AChE, and of anticonvulsant drugs, is standard clinical practice for treatment of OP toxicity. In view of the overwhelming evidence for a critical role for AChE in OP toxicity, it was of interest to determine the response of a mouse that had no AChE. If AChE were the only important target of OP, then mice with no AChE were expected to be resistant to OP toxicity.

## **2. Methods**

**2.1. Mice.** AChE knockout mice were made by gene-targeting (Xie et al., 2000). 5 kb of the ACHE gene including the signal peptide, the catalytic triad, and 93% of the coding sequence were deleted. No AChE protein is made, and no AChE activity is present in any tissue.

**2.2. Organophosphorus agents and dose.** The nerve agent O-ethyl S-(2-(diisopropylamino)ethyl) methylphosphonothioate (VX) was from the Edgewood Chemical Biological Center (Aberdeen Proving Ground, MD). Animals were shipped to the U.S. Army Institute of Chemical Defense, Aberdeen Proving Ground, for experiments with VX. Tetraisopropyl pyrophosphoramide (iso-OMPA) and diisopropylfluorophosphate (DFP) were from Sigma (St. Louis, MO). Chlorpyrifos oxon (CPO), diazoxon, dichlorvos,

and malaoxon were from Chem Service, Inc (West Chester, PA). FP-biotin (10-(fluoroethoxyphos phinyl)-N-(biotinamidopentyl) decanamide) was synthesized by Troy Voelker in the laboratory of Charles Thompson (Univ Montana, Missoula). FP-biotin has a reactive phosphonofluoridate group tethered to biotin via a spacer arm (Liu et al., 1999).

VX was dissolved in sterile saline and injected subcutaneously in the back of the neck at a dose of 8.0 – 25.0 µg/kg. Male and female animals were 34-55 days old. The number of animals for LD<sub>50</sub> experiments was n = 21 AChE +/+, n = 18 AChE +/-, n = 16 AChE -/-.

DFP was dissolved in sterile phosphate buffered saline and injected intraperitoneally at a dose of 2.5 mg/kg. Male and female animals were 12 days old. The number of animals was n = 8 AChE +/+, n = 15 AChE +/-, n = 3 AChE -/-.

Chlorpyrifos oxon was dissolved in dimethylsulfoxide and injected intraperitoneally at a dose of 0.1 to 4.0 mg/kg. Male animals were 49-200 days old. The number of animals was n = 13 AChE +/+, n = 3 AChE +/-, n = 9 AChE -/-.

Iso-OMPA was dissolved in sterile water and injected intraperitoneally at a dose of 1 – 550 mg/kg. Female mice were 90-210 days old. The number of animals was n = 21 AChE +/+, n = 42 AChE +/-, n = 11 AChE -/-.

### **2.3. Enzyme activity assays in tissue extracts.**

Tissues were collected at time of death or 6 h after treatment, and frozen. Age and sex matched untreated control tissues were collected and stored in the same manner as the treated samples. Tissues were homogenized in 10 volumes of 50 mM potassium phosphate, pH 7.4, containing 0.5% Tween 20, in a Tissumizer (Tekmar, Cincinnati, OH) for 10 seconds. The suspension was centrifuged in a microfuge for 10 min, and the supernatant was saved for enzyme activity assays. The extraction buffer contained Tween 20 rather than Triton X-100 because mouse BChE activity was inhibited up to 95% by 0.5% Triton X-100, but was not inhibited by 0.5% Tween 20 (Li et al., 2000).

AChE and BChE activity was measured by the method of Ellman et al. (1961) at 25°C, in a Gilford spectrophotometer interfaced to MacLab 200 (ADIInstruments Pty Ltd., Castle Hill, Australia) and a Macintosh computer. Samples were preincubated with 5,5-dithio-bis (2-nitrobenzoic acid) in 0.1 M potassium phosphate buffer, pH 7.0, to react free sulfhydryl groups before addition of substrate. AChE activity in tissues from VX treated animals was measured with 1 mM acetylthiocholine after inhibiting BChE activity with 0.1 mM iso-OMPA (liver required 1 mM for complete BChE inhibition). AChE activity in tissues from iso-OMPA treated mice was measured with 1 mM acetylthiocholine after inhibiting BChE with 0.01 mM ethopropazine. BChE activity was measured with 1 mM butyrylthiocholine. Units of activity are defined as µmoles substrate hydrolyzed per minute. Units of activity were calculated per gram wet weight of tissue.

### **2.4. Observations of OP treated animals.** Mice treated with organophosphorus toxicant (OP) were monitored up to 24 hours. Observations included salivation, lacrimation, increased urination, abnormal defecation, hyperactivity or lethargy, tremor, convulsions, muscle weakness, vasodilation. Body temperature was measured with a digital thermometer using a surface microprobe.

**2.5. Preparation of sub-cellular fractions from mouse brain, and protein quantitation.** Mouse brain was separated into its sub-cellular fractions by centrifugation, essentially as described by Gray and Whittaker (1962). Brain tissue was homogenized by two 1-minute disruptions with a Potter-Elvehjem homogenizer (Teflon pestle with glass vessel) rotating at 840 rpm (in 10-volumes of ice cold 50 mM Tris/Cl buffer, pH 8.0, containing 0.32 M sucrose, to prevent disruption of organelles). The suspension was centrifuged at 1000xg for 10 minutes at 4°C to pellet nuclei, mitochondria, plasma membranes and unbroken cells. The supernatant was re-centrifuged at 17,000xg for 55 minutes at 4°C to pellet myelin, synaptosomes and mitochondria. That supernatant was re-centrifuged at 100,000xg for 60 minutes at 4°C to separate microsomes (pellet) from soluble proteins (supernatant).

Protein in the supernatant fraction was estimated by absorbance at 280 nm, using  $A_{280} = 1.0$  for 1 mg protein/ml. The 100,000xg supernatant was divided into 0.4 ml aliquots and stored at -70°C, along with the other sub-cellular fractions.

**2.6. Labeling with FP-biotin.** Mouse brain supernatant (1.25 mg protein/ml) was reacted with 2-40  $\mu$ M FP-biotin in 50 mM TrisCl buffer, pH 8.0, containing 5 mM EDTA and 2.4% methanol at 25°C for up to 450 minutes). The reaction was stopped by addition of 1/5 volume of 10% SDS, 30% glycerol, 0.6 M dithiothreitol, and 0.012% bromophenol blue in 0.2 M TrisCl buffer, pH 6.8; followed by heating at 80°C for 5 minutes.

A 10-20% gradient polyacrylamide gel with 4% stacking gel was used (overall dimensions 16x18x0.075 cm, with 20 lanes). Thirty micrograms of total protein were loaded per lane, and run for 3600 volt-hours in the cold room (4°C), with stirring. The bottom tank contained 60 mM TrisCl buffer, pH 8.1, plus 0.1% SDS. The top tank buffer contained 25 mM Tris, 192 mM glycine buffer, pH 8.2, plus 0.1% SDS. Protein was transferred from gel to PVDF membrane (ImmunBlot from BioRad) electrophoretically in a tank using plate electrodes (TransBlot from BioRad), at 0.5 amps, for 1 hour, in 25 mM Tris, 192 mM glycine buffer, pH 8.2, in the cold room (4°C), with stirring. The membrane was blocked with 3% gelatin (BioRad) in 20 mM TrisCl buffer, pH 7.5, containing 0.5 M NaCl for 1 hour at room temperature. Then it was washed twice with 20 mM TrisCl buffer, pH 7.5, containing 0.5 M NaCl and 0.05% Tween-20, for 5 minutes. Biotinylated proteins were labeled with 9.5 nM Streptavidin-Alexa 680 conjugate (Molecular Probes) in 20 mM TrisCl buffer, pH 7.5, containing 0.5 M NaCl and 1% gelatin, for 1 hour, at room temperature, while protected from light. Shorter reaction times resulted in less labeling. Then the membrane was washed twice with 20 mM TrisCl buffer, pH 7.5, containing 0.5 M NaCl and 0.05% Tween-20, and twice with 20 mM TrisCl buffer, pH 7.5, containing 0.5 M NaCl, for 20 minutes each. This is essentially the BioRad protocol (BioRad Lit 171 Rev D). Membranes were scanned with the Odyssey Flat Bed Fluorescence Scanner (LI-COR) at 42 microns per pixel. The intensity of the signal from each labeled protein was determined using a Gaussian deconvolution routine from the Kodak 1D Image Analysis program, v 3.5.3 (Kodak).

**2.7. Binding of OP to brain proteins.** Chlorpyrifos oxon, diazoxon, dichlorvos, or malaoxon were incubated with mouse brain extract at 25°C with concentrations of OP ranging from 0.1 to 500  $\mu$ M. At the end of the 30 min incubation period, excess OP

was separated from protein on a spin column. The protein was incubated with 10  $\mu$ M FP-biotin for 6 h at 25°C. The intensity of FP-biotin labeling was determined as described above. Proteins that had reacted with OP were identified by disappearance of a biotinylated band.

### 3. Results

**3.1. Phenotype of the adult AChE  $-/-$  mouse.** Adult AChE  $-/-$  mice are not normal in appearance. When they walk, the tail and abdomen drag on the ground. Their feet splay out and their gait is abnormal. They have no grip strength. By one year of age, AChE  $-/-$  mice never stand on their hind legs and they do not climb. They have a hump in their back, suggesting a deformed skeleton. They do not eat solid food, and cannot lift the head to drink from a suspended bottle. Body tremor is noticeable when they are moving about, but not when they are asleep. They have pinpoint pupils.

They are lethargic, spending most of the time hiding in a small dark box inside their cage. Another behavioral abnormality is their lack of housekeeping behavior; they defecate and urinate in their nest. They do not engage in mating behavior. AChE  $-/-$  mice have never become pregnant despite being housed all their life with male AChE  $-/-$  mice (n= 600).

About 25% of adult AChE  $-/-$  mice make a bird-like chattering sound when they are disturbed. This vocalization is a response to stress.

Adult female AChE  $-/-$  mice are small, averaging 18 g. In contrast, wild-type female littermates weigh 27-32 g. A few male AChE  $-/-$  mice reach a weight of 30-35 g, though the average male knockout mouse weighs 18 g. The surface body temperature of adult AChE  $-/-$  mice is 36.5°C, while that of AChE  $+/+$  mice is 37.1°C.

The average lifespan of AChE  $-/-$  mice is 120 days, though several have lived a normal lifespan of 2 years. In contrast, AChE  $+/+$  mice live for 2 years. AChE  $-/-$  mice die of seizures. A disproportionate number of AChE  $-/-$  mice die on postnatal days 25-35. More details on the phenotype of adult AChE  $-/-$  mice are in Duysen et al. (2002).

**3.2. Phenotype of AChE  $+/ -$  mice.** Heterozygous mice, carrying one deficient AChE allele, and expressing 50% of the normal AChE activity in tissues (Xie et al., 2000; Li et al., 2000), are indistinguishable from wild-type mice in appearance. They have a normal lifespan, are sexually active, and fertile. Their litter sizes are the normal 6-8 pups for strain 129Sv. A female AChE  $+/ -$  mouse has an average of 6-8 litters in her lifetime, similar to the number of litters produced by an AChE  $+/ +$  mouse of strain 129Sv. No health problems have been noticed in AChE  $+/ -$  mice. They do not have seizures. AChE  $+/ -$  mice have a reduced number of functional muscarinic receptors (Li et al., 2003), and are more sensitive to OP than wild-type mice.

**3.3. LD<sub>50</sub> of OP.** Strain 129Sv mice, differing only at the AChE gene locus, were tested with four organophosphorus toxicants (Table 1). Mice with no AChE were supersensitive to the lethal effects of DFP, chlorpyrifos oxon, VX, and iso-OMPA. Iso-OMPA discriminated between AChE  $-/-$  and  $+/ +$  mice more effectively than the other OP. A dose of 1 mg/kg was lethal to half of the AChE  $-/-$  mice but produced no toxic symptoms in AChE  $+/ +$  and

+/+ mice. The dose had to be increased 350-fold before iso-OMPA was lethal to AChE +/+ and +/- animals. The nerve agent VX is the most potent OP known. Microgram quantities are lethal. The finding that AChE -/- mice succumbed to VX shows that VX reacts with targets other than AChE and that reaction results in death.

**3.4. Symptoms of toxicity after OP treatment.** Untreated AChE -/- mice have cholinergic symptoms of OP toxicity even though they have never received any OP. Whole body tremor, pinpoint pupils, mucus on the eyes, and reduced body temperature are characteristic of untreated AChE -/- mice and are also cholinergic signs of toxicity attributed to excess acetylcholine.

Treatment with a nonlethal dose of VX caused a hypothermic response reminiscent of the response to oxotremorine (Li et al., 2003). AChE -/- mice were resistant to the hypothermic effects of VX, whereas AChE +/+ mice lost 8°C of surface body temperature and did not regain normal temperature for 24 hours (Duysen et al., 2001). The resistance of AChE -/- mice to the hypothermic effects of VX can be explained by a reduced number of functional M2 muscarinic receptors (Li et al., 2003). The receptors involved in thermal regulation are M2 (Gomeza et al., 1999).

Since the signs of OP toxicity are attributed to inhibition of AChE, it was of interest to determine whether mice with no AChE activity had different symptoms. Table 2 summarizes the symptoms observed in response to lethal injections of 4 different OP. AChE -/- mice exhibited the same symptoms as wild-type and heterozygous mice. Exceptions to this pattern are the salivation and defecation in iso-OMPA treated AChE -/- mice and the absence of hyperactivity in DFP treated AChE -/- mice. The lack of hyperactivity in DFP treated AChE -/- mice is explained by the fact that they died instantly, before movement could be observed.

The pattern of symptoms was different for each OP. This observation has been taken as evidence that OP react with several targets, and that the toxicity is not explained by inhibition of AChE alone (Pope et al., 1999; Moser 1995).

**3.5. Enzyme activity in tissues.** Tissues from VX (Duysen et al., 2001) and iso-OMPA treated animals have been tested. The results in Table 3 show that a lethal dose of VX inhibited AChE in brain 50%. BChE in brain was also inhibited about 50%. The extent of BChE inhibition in AChE -/- brain was no greater than in AChE +/+ and +/- brains. Similarly, AChE in muscle and serum was also inhibited about 50%, whereas AChE in intestine showed almost no inhibition. BChE activity was inhibited in all tissues tested.

A dose of 5 mg/kg iso-OMPA had no toxic effects on AChE +/+ and +/- mice, but was lethal to AChE -/- mice. Iso-OMPA is regarded as a specific inhibitor of BChE, however AChE activity in serum was inhibited 50% and AChE activity in liver was inhibited 95% in both AChE+/+ and +/- mice. AChE activity in brain was not inhibited by 5 mg/kg iso-OMPA. However, BChE activity in brain was inhibited 25% in both AChE+/+ and +/- brain. BChE activity in AChE-/- brain was inhibited 65% by 5 mg/kg iso-OMPA i.p. Serum and liver BChE activity were almost completely inhibited in all three genotypes. These results show that BChE is a significant target for inhibition by OP.

**3.6. Noncholinesterase targets of OP.** An assay to identify proteins inhibited by OP was developed. FP-biotin labeled at least 55 proteins in mouse brain 100,000xg supernatant (Fig. 1). When brain extract was preincubated with chlorpyrifos oxon, 3 of the FP-biotinylated protein bands disappeared (bands 12, 41, 45). Preincubation with diazoxon caused 4 bands to disappear (bands 9, 12, 41, 47), with dichlorvos 7 bands disappeared (bands 12, 23, 24, 32, 44, 45, 51), and with malaoxon 1 band disappeared (band 9). The set of bands that disappeared was unique for each OP, though there was overlap.

#### 4. Discussion

**Why is the acetylcholinesterase knockout mouse supersensitive to organophosphorus agent (OP) toxicity?** Since this mouse has zero AChE activity, it must be concluded that OP inhibited enzymes other than AChE and that the consequence of this inhibition was lethal to the AChE  $-/-$  mouse.

Our results suggest that inhibition of BChE is part of the explanation for the lethality of OP in AChE knockout mice. Evidence to support the idea that BChE inhibition is lethal to AChE  $-/-$  mice includes the following. 1) BChE was inhibited in OP treated AChE  $-/-$  mice. 2) AChE  $-/-$  mice had the same cholinergic signs of toxicity following treatment with OP, as AChE  $+/+$  mice. This means the mechanism of toxicity was the same, even though AChE  $-/-$  mice have no AChE. The common mechanism would be accumulation of excess acetylcholine, followed by overstimulation of acetylcholine receptors. Inhibition of BChE could lead to accumulation of excess acetylcholine, because BChE is capable of hydrolyzing acetylcholine. The implication in this conclusion is that BChE has a function in AChE  $-/-$  mice to hydrolyze the neurotransmitter acetylcholine at cholinergic synapses. Mesulam et al. (2002) proposed such a function for BChE in brain.

Binding of OP to noncholinesterase proteins may explain why each OP is associated with a distinct set of symptoms. Preliminary identification of a few of the FP-biotin labeled proteins can be made by comparing our results to the literature. Eight FP-biotin reactive proteins from rat testis supernatant have been identified by Kidd et al. (2001). Three, with molecular weights around 80 kDa, would be expected to travel in the vicinity of bands 9 to 17. They are acyl peptide hydrolase (82 kDa), prolyl oligopeptidase (80 kDa) and carboxylesterase 1 (80 kDa). One or more of these enzymes probably reacts with dichlorvos, chlorpyrifos oxon, malaoxon, and diazoxon. Long Chain acyl CoA hydrolase (48 kDa) and LDL-associated PLA2 (45 kDa) would appear in the region of bands 29 to 35, a region where reactivity was observed with dichlorvos.

**Implications for man.** Our finding that heterozygous mice who carry one deficient AChE allele are healthy, suggests that in the future we will find healthy humans who carry one deficient AChE allele. These humans will be more sensitive to OP toxicity than the average person. Noncholinesterase targets of OP binding may provide new biomarkers of OP exposure.

**Acknowledgement.** Supported by US Army Medical Research & Materiel Command Grants DAMD17-01-2-0036 and DAMD17-01-1-0776

## References

Duysen EG, Li B, Xie W, Schopfer LM, Anderson RS, Broomfield CA, Lockridge O. 2001. Evidence for non-acetylcholinesterase targets of organophosphorus nerve agent; supersensitivity of the acetylcholinesterase knockout mouse to VX lethality. *J. Pharmacol. Exp. Ther.* 299: 542-550

Duysen EG, Sibley JA, Fry DL, Hinrichs S, Lockridge O. 2002. Rescue of the acetylcholinesterase knockout mouse by feeding a liquid diet; phenotype of the adult acetylcholinesterase deficient mouse. *Brain Res Dev Brain Res* 137: 43-54

Ellman GL, Courtney KD, Andres V Jr, Featherstone RM. 1961. A new and rapid colorimetric determination of acetylcholinesterase activity. *Biochem Pharmacol* 7: 88-95

Gomez J, Shannon H, Kostenis E, Felder C, Zhang L, Brodin J, Grinberg A, Sheng H, Wess J. 1999. Pronounced pharmacologic deficits in M2 muscarinic acetylcholine receptor knockout mice. *Proc Natl Acad Sci USA* 96: 1692-1697

Gray EG, Whittaker VP. 1962. The isolation of nerve endings from brain: An electron-microscopic study of cell fragments derived by homogenization and centrifugation, *J Anat* 96: 79-88

Kidd D, Liu Y, Cravatt BF. 2001. Profiling serine hydrolase activities in complex proteomes, *Biochemistry* 40: 4005-4015

Li B, Sibley JA, Tieu A, Xie W, Schopfer LM, Hammond P, Brimijoin S, Hinrichs SH, Lockridge O. 2000. Abundant tissue butyrylcholinesterase and its possible function in the acetylcholinesterase knockout mouse, *J. Neurochem.* 75: 1320-1331

Li B, Duysen EG, Volpicelli-Daley LA, Levey AI, Lockridge O. 2003. Regulation of muscarinic acetylcholine receptor function in acetylcholinesterase knockout mice. *Pharmacol Biochem Behav* 74: 977-986

Liu Y, Patricelli MP, Cravatt BF. 1999. Activity-based protein profiling: The serine hydrolases, *Proc Natl Acad Sci USA* 96: 14694-14699

McDonough JH, Shih TM. 1997. Neuropharmacological mechanisms of nerve agent-induced seizure and neuropathology. *Neurosci Biobehav Rev* 21: 559-579

Mesulam MM, Guillozet A, Shaw P, Levey A, Duysen EG, Lockridge O. 2002. Acetylcholinesterase knockouts establish central cholinergic pathways and can use butyrylcholinesterase to hydrolyze acetylcholine *Neuroscience* 110: 627-639

Moser VC. 1995. Comparisons of the acute effects of cholinesterase inhibitors using a neurobehavioral screening battery in rats. *Neurotoxicol Teratol* 17: 617-625

Pope CN. 1999. Organophosphorus pesticides: do they all have the same mechanism of toxicity? *J Toxicol Environ Health B Crit Rev* 2: 161-181

Xie W, Sibley JA, Chatonnet A, Wilder PJ, Rizzino A, McComb RD, Taylor P, Hinrichs SH, Lockridge O. 2000. Postnatal developmental delay and supersensitivity to organophosphate in gene-targeted mice lacking acetylcholinesterase, *J. Pharmacol. Exp. Ther.* 293: 896-902

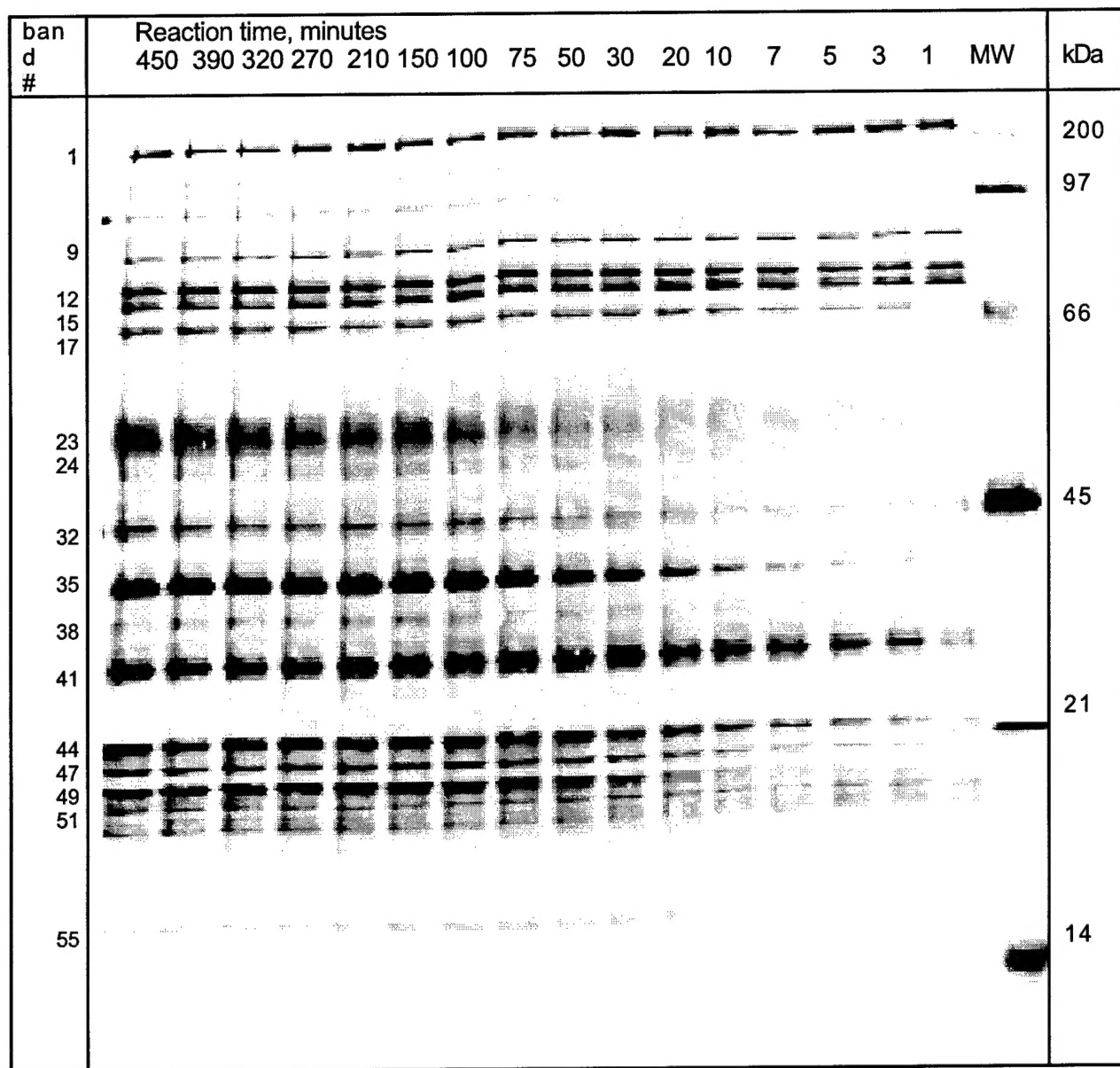


**Figure 1.** SDS-PAGE showing the time course for the reaction of FP-biotin with proteins extracted from mouse brain. The 10  $\mu$ M FP-biotin was reacted with 1.25 mg protein/ml of mouse brain supernatant in 50 mM Tris/Cl buffer, pH 8.0, containing 5 mM EDTA and 2.4% methanol, at 25°C, for selected times. The numbers above each lane indicate the reaction times in minutes. Biotinylated molecular weight markers were from BioRad. Endogenous biotinylated proteins are in bands 1, 14, and 15.

**Table 1.** LD<sub>50</sub> of organophosphorus toxicants (OP) in wild-type and AChE deficient mice, strain 129Sv. Doses are in mg/kg.

AChE Genotype	AChE activity	DFP LD <sub>50</sub>	Chlorpyrifos Oxon LD <sub>50</sub>	VX LD <sub>50</sub>	Iso-OMPA LD <sub>50</sub>
AChE +/+	100%	> 2.5	3.5	0.024	350
AChE +/-	50%	2.5	2.5	0.017	350
AChE -/-	0 %	< 2.5	0.5	0.011	1

**Table 2.** Toxic signs in OP treated AChE +/+, +/-, and -/- mice, following a lethal dose of OP.

OP	AChE genotype	Salivation	Mucus in eyes	Urination	Defecation	Reduced body temp	hyperactivity	tremor (clonic or tonic)	Convulsions	Vasodilation
CPO	+/+	no	yes	no	no	yes	no	yes	yes	yes
CPO	+/-	no	yes	no	no	yes	no	yes	yes	yes
CPO	-/-	no	yes	no	no	yes	no	yes	yes	yes
VX	+/+	yes	yes	no	no	yes	no	yes	yes	yes
VX	+/-	yes	yes	no	no	yes	no	yes	yes	yes
VX	-/-	yes	yes	no	no	yes	no	yes	yes	yes
iso-OMPA	+/+	no	yes	no	yes	yes	yes	yes	no	no
iso-OMPA	+/-	no	yes	no	yes	yes	yes	yes	no	no
iso-OMPA	-/-	yes	yes	no	no	yes	yes	yes	no	no
DFP	+/+	yes	-	yes	no	yes	yes	yes	-	-
DFP	+/-	yes	-	yes	no	yes	yes	yes	-	-
DFP	-/-	yes	-	yes	no	yes	no	yes	-	-

CPO is chlorpyrifos oxon. The dash indicates no data.

**Table 3.** AChE and BChE activity in tissues of mice treated with a lethal dose of VX. Units of enzyme activity are  $\mu$ moles substrate hydrolyzed per min per gram wet weight of tissue. The standard deviations were 3 to 30% of the average values shown.

Genotype	Tissue	AChE		BChE	
		Control	VX	Control	VX
+/+	brain	1.71	0.86 <sup>a</sup>	0.13	0.05 <sup>a</sup>
+/-	brain	0.91	0.53 <sup>a</sup>	0.11	0.05 <sup>a</sup>
-/-	brain	0	0	0.10	0.05 <sup>a</sup>
+/+	muscle	0.28	0.15 <sup>a</sup>	0.26	0.14
+/-	muscle	0.22	0.11 <sup>a</sup>	0.25	0.11 <sup>a</sup>
-/-	muscle	0	0	0.27	0.11 <sup>a</sup>
+/+	intestine	0.21	0.20	5.97	5.08
+/-	intestine	0.15	0.14	4.37	3.77
-/-	intestine	0	0	7.95	6.28
+/+	serum	0.54	0.31 <sup>a</sup>	2.79	1.64
+/-	serum	0.28	0.21	1.75	1.14 <sup>a</sup>
-/-	serum	0	0	1.88	1.48

<sup>a</sup> significantly different from control  $p \leq 0.025$  by ANOVA using Bonferroni correction to adjust for multiple comparisons.

<sup>b</sup>ND, not determined